UNIVERSITY *of* CALIFORNIA, MERCED

Radical Benzylic C–H Fluorination: The Use of Unprotected Amino Acids as Radical Precursors, Pyridines as Halogen Bond Acceptors, and The Development of a Novel Hydrogen Atom Transfer Agent

by,

Alyssa Minh Doan Hua

A dissertation submitted in partial fulfillment of the requirements for the degree of Doctor of Philosophy

in

Chemistry and Chemical Biology

Doctoral Committee:

Hrant P. Hratchian, Chair

Ryan D. Baxter, PI

David J. Russell

Benjamin J. Stokes

The Dissertation of Alyssa Minh Doan Hua is approved, and is acceptable in quality and form for publication on microfilm and electronically:

Ryan D. Baxter, PI

David J. Russell

Benjamin J. Stokes

Hrant P. Hratchian, Chair

University of California, Merced

2019

D E D I C A T I O N

To my parents, Diep N. Dinh and Binh P. Hua, for always pushing me to *do* better and *be* better.

To my sisters, Linda A. Farmer and Olivia M. Hua, for encouraging me to pursue this…I can print a copy of this thing for each of you as souvenirs.

To my cousins, Brian D. Lim, Brandon T. Lim, Trang Hua, Thanh Hua, and Nicole N. Nguyen, thank you for your endless love and support and all the pep talks.

To my PI, Ryan D. Baxter, your guidance has been inexpressibly priceless.

To Soy, Bean, and Churro…I love you 3000.

TABLE *of* CONTENT

LIST *of* ABBREVIATIONS

BDE	bond dissociation energy
Boc	*tert*-butyloxycarbonyl
BPin	boronic acid pinacol ester
DCM	dichloromethane
GC-MS	gas chromatography mass spectroscopy
h	hour
HAT	hydrogen atom transfer
HMBC	heteronuclear multiple bond correlation
HR-MS	high resolution mass spectroscopy
IR	infrared spectroscopy
equiv	equivalent
Me	methyl
mins	minutes
NMR	nuclear magnetic resonance
PET	positron emission tomography
Ph	phenyl
rt	room temperature
TBAF	tetrabutylammonium tetrafluoroborate
TEMPO	2, 2, 6, 6-Tetramethyl-1-piperidinyloxy
TLC	thin layer chromatography

LIST *of* FIGURES

LIST *of* SCHEMES

LIST *of* TABLES

A C K N O W L E D G E M E N T S

I would like to acknowledge Michael L. Sanfilippo for convincing me to apply to UC Merced even though I technically missed the application deadline by a month or two. I really would not be here, wrapping up this program had I not met you.

I would like to acknowledge the members of the Baxter Lab, past and current. Thank you for providing me a safe place to bounce ideas around and all the fruitful discussions about both personal life and chemistry things. Thank you for helping me better my presentations, and for letting me bore you guys with my practice presentations, especially this last one for my defense.

I would like to acknowledge the faculty and staff members who have helped me become a better chemist. Special thanks to those on my doctoral committee for believing in me, though my initial performances seemed dauntingly helpless. I am here today because you took the risk and continued to support me.

I would like to acknowledge Samantha I. Bidwell and Dr. Hrant P. Hratchian for working with us. I am quite proud of our publication together and am thankful for all the time you both spent writing the codes and checking the numbers and things, all of which I have not a single clue about. Thank you for the many tangent discussions at every meeting we have had, and for ping-ponging the manuscript back and forth until we got it just right.

I would like to acknowledge (now Dr.!) Amir Keshavarz for helping me since the day we started this program. You have undoubtedly been crucial to my growth as a scientist. I will be forever grateful.

Last, but not least, I would like to acknowledge my PI, Dr. Ryan D. Baxter. Thank you for being an exceptional mentor. I have learned so much from you…I have grown immensely both professionally and personally. It has truly been an honor to have had you guide me along this journey and to have worked with you. Deciding to join your lab has been one of the best decisions I have made in my life. I cannot thank you enough for your patience with me over the past few years. I am beyond honored to be your first graduate student.

CURRICULUM VITA

Education

Aug. 2014 – Aug. 2019	Ph.D. in Organic Chemistry University of California, Merced
Aug. 2009 – May 2013	B.S. in Chemistry Saint Mary's College of California

Publication(s)

1. **Hua, A. M.**; Bidwell, S. L.; Baker, S. I.; Hratchian, H. P.; Baxter, R. D. *ACS Catal.*, **2019**, *9*, 3322–3326. "Experimental and Theoretical Evidence for Nitrogen–Fluorine Halogen Bonding in Silver-Initiated Radical Fluorinations"
2. **Hua, A. M.**; Mai, D. N.; Martinez, R.; Baxter R. D. *Org. Lett.* **2017**, *19*, 2949–2952. "Radical C–H Fluorination Using Unprotected Amino Acids as Radical Precursors"

A B S T R A C T

Benzylic C–H bonds are ubiquitous in pharmaceutical and other biologically active compounds. The low BDE[1] of the benzylic C–H bond has made it a target for further functionalization, where the original bond may be replaced with a C–C bond,[2] C–O bond,[3] C–N bond,[3f,4] or C–X bond,[5] (where X = halogen). While the functionalization of benzylic C–H bonds to C–C/O/N bonds are relatively well established, selective halogenation proves to be more challenging. Halogenation typically refers to chlorination, bromination, and iodination, but has recently come to include fluorination. Achieving fluorination has traditionally been cumbersome. Classical methods of generating a C–F bond typically require harsh conditions with highly toxic reagents. C–F bond formation has increasingly become of interest primarily for its advantageous biological features. The focus of this dissertation will be method development and mechanistic investigation of silver(I)-catalyzed benzylic C–H fluorination via radical pathways.

Recent developments of new fluorinating reagents have afforded methods that no longer require highly toxic chemicals; however, current radical fluorination still require harsh reagents, (e.g. strong oxidants), or have a limited substrate scope. Utilizing the idea of radical decarboxylative fluorination, and the demonstrated utility of radical decarboxylation of unprotected amino acids,[6] a novel radical decarboxylative benzylic fluorination pathway was designed where unprotected amino acids were used as radical precursors to facilitate HAT at the benzylic site, and ultimately allow for subsequent fluorination.

Upon further mechanistic investigation of the unprotected amino acids system, it was found that radical benzylic fluorination was achievable in the absence of an amino acid, so long as a free nitrogen-bearing compound, such as pyridine, was present. Through experimental and theoretical investigations, it was proposed that halogen bonding between the pyridine and fluorinating agent was facilitating the more efficient radical benzylic fluorination pathway by producing a stronger HAT agent.

C H A P T E R 1

Benzylic C–H Fluorination using Unprotected Amino Acids as Radical Precursors

1.1 Introduction

1.1.1. Importance of Fluorinated Materials

Naturally, fluorine-containing molecules are found in a small number of plants.[7] Synthetically, organofluorine molecules can be found in many household items such as refrigerants, oil repellents, and water repellents.[8a] More importantly, organofluorine molecules are found in 20% of the top 200 pharmaceuticals and up to 40% of agrochemicals.[8] The physical and biological characteristics of carbon–fluorine bonds have made them highly desirable, thus, a vast chemical field devoted to forming fluorine bonds with carbon and other atoms has developed. The significant strength of a carbon–fluorine bond can be attributed to its polar covalent characteristics, which contributes to its metabolic and thermal stability, ultimately prolonging the lifetime of the molecule.[8c,9] From a pharmaceutical standpoint, these stabilities may translate to a more efficient medicine, as the molecule lasts longer. The presence of fluorines within a compound has also been shown to affect the lipophilicity of the molecule, increasing the bioavailability.[9] Additionally, the atomic size of a fluorine is similar to that of a hydrogen, making it a viable bioisostere to mimic enzyme substrates.[8c,9]

Fluorine is not only known for its medicinal applications, but also for its medical uses. The radioisotope of fluorine, ^{18}F, is used in positron emission tomography (PET) imaging, where the gamma radiation is detected and processed into an image, showing concentrations of ^{18}F in potential cancerous cells.[8-9] Classically, analogues of glucose are used as the radio tracer. However, the success of imaging potential cancerous cells lies in the assumption that the target cells uptake glucose and its various derivatives. Because some cancerous cells may not consume glucose, it is essential to find alternatives, which has led to the development and discoveries of late-stage fluorination.

1.1.1.1 Types of Fluorine Sources

Retro-synthetically, there are several ways to think about disconnecting a C–F bond. The fluorine may come as an electrophilic fluorine (F^+), a nucleophilic fluorine (F^-), or a radical fluorine ($F\cdot$) (Scheme 1-1). Classical electrophilic fluorine reagents include F_2, *N*-fluoropyridinium, perchlorofluoride ($FClO_3$), trifluoromethyl hypofluorite (CF_3OF), xenon difluoride (XeF_2), acyl and perfluoroacyl hypofluorites (RCOOF, RC_nOOF), and cesium fluoroxysulfate ($CsSO_4F$).[9c,10] However, these electrophilic fluorinating reagents are typically very strong oxidants, limiting successful fluorination of prefunctionalized molecules and are not ideal for late-stage fluorination. These reagents are also relatively unstable, and therefore difficult to handle, and considered highly hazardous.[10] The

instability of these electrophilic fluorine reagents contributes to their reactivity, making it difficult to perform site-selective fluorination. Modern electrophilic fluorine reagents have been developed to be less hazardous alternatives and include Selectfuor (1-chloromethyl-4-fluoro-1,4-diazoniabicyclo[2.2.2]octane bis(tetrafluoroborate)) and NFSI (N-fluorobenzensulfonimide). However, reacting with an electrophilic fluorine requires the substrate to be nucleophilic (C^-), which typically requires stabilizing functional groups to achieve and maintain the anionic characteristics of the carbon.[10f] As expected, fluorination of neutral substrates is achievable by electrophilic fluorination, but is not very efficient, while electrophilic substrates are not compatible.

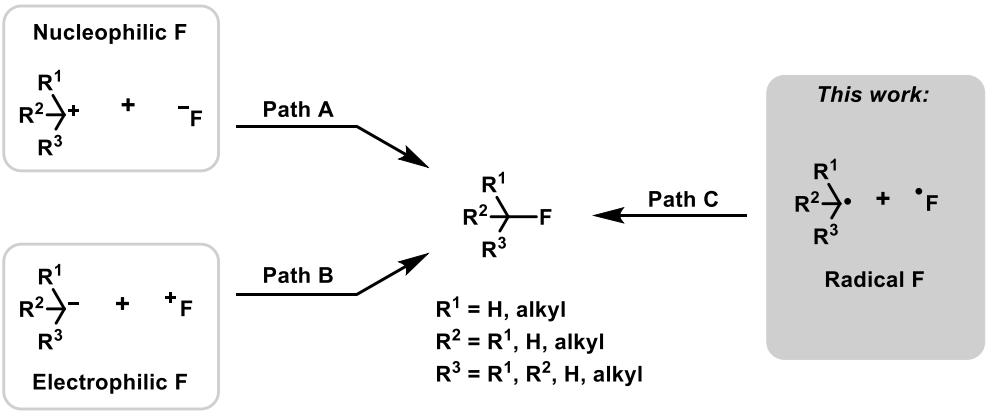

Scheme 1-1. Synthons of C–F Bonds.

Complimentary to electrophilic fluorination is nucleophilic fluorination, (Scheme 1-1, Path B). Hydrogen fluoride (HF) is the most commonly known nucleophilic reagent, but is sparingly used due to its high levels of toxicity and handling difficulties as it is in the gaseous phase at ambient conditions.[12] Olah's reagent (pyridine·9HF) and other amine-HF complex mixtures were designed to help aide in the handling of HF.[12] However, in the presence of an amine, the reactivity of HF is reduced. In attempts to circumvent the high toxicity levels of HF, alkali metal fluorides, (KF, NaF, CsF), were investigated as viable nucleophilic fluorine sources. While these alkali fluorides are easy to handle and have relatively low toxicity, their solubility often hinders their usage. Electrophilic fluorination is also inherently hindered because fluorine is highly electronegative, making it a poor nucleophile.

Alternatively, we can think of a C–F bond in terms of radicals, (Scheme 1-1, Path C). This route may prove to be far more synthetically useful than either of the previously mentioned ionic fluorine sources. Both the substrate radical and fluorine radical may be influenced to behave more nucleophilic- or electrophilic-like by simply altering the groups on their parent molecules. Typically, in this pathway, the substrate must first be transformed into an alkyl radical, which is then followed by fluorine atom transfer. Traditionally, CF_3OF, XeF_2, NFSI, Selectfluor are known to be electrophilic fluorine

sources, but in the presence of an alkyl radical, they may act as a electrophilic radical fluorine source as well.[9c,10] However, due to their high reactivity, generating radicals from CF_3OF, XeF_2 will likely lead to radical cascades and chain reaction that may lead to undesired byproducts and highly unstable conditions. Selectfluor and NFSI are less reactive, and more easily handled and controlled electrophilic fluorine sources.[10a] Thus generating an electrophilic fluorine radical from Selectfluor and NFSI is favored.

This dissertation will focus on radical fluorination with Selectfluor as the fluorine source.

1.1.2. α-Aminoalkyl Carbon-Centered Radicals

Oxidation of amines generate synthetically useful intermediates, especially α-aminoalkyl radicals. α-Aminoalkyl radicals can be directly accessed by single electron oxidation of an amine. However, due to their considerably lower oxidation potential as compared to their starting amines, the conditions they are generated in typically lead to over-oxidation, forming iminium ions.[13] In a recent publication, our lab demonstrated the use of readily available unprotected amino acids as radical precursors to alkylate heteroarenes with good yields and high selectivity.[14] In that work, it was proposed that Ag(I) oxidizes to Ag(II) in the presence of persulfate, heterolytically cleaving persulfate, and subsequent radical decarboxylation of the amino acid would occur, regenerating Ag(I) and producing an α-aminoalkyl radical. The α-aminoalkyl radical being particularly easily oxidized and in the presence of persulfate, a strong oxidant, would undergo rapid oxidation, generating an iminium ion that would ultimately lead to the desired heteroarene alkylation (Figure 1-1).

While iminium ions have been demonstrated as synthetically useful intermediates,[13] α-aminoalkyl radicals are more reactive and give access to a much broader scope of α-functionalized amines. Unlike iminium ions, α-aminoalkyl radicals do not necessarily rely on the presence of a nucleophile to afford α-substituted amines.[6a-f,14] α-Aminoalkyl radicals have been generated from radical decarboxylation or radical desilylation of the corresponding α-amino acid or α-silylamine. Minisci first demonstrated direct C–H alkylation of heteroarenes using carboxylic acids as a radical precursor.[15] Great advances have been made since, with alternative radical precursors now including boronic acids,[16] metal sulfinates,[17] *N*-protected amino acids,[6f] and unprotected amino acids.[14] It has been shown in earlier reports by Minisci[18] and Cowden[6f] that hydrogen atom abstraction was possible by the resulting alkyl and *N*-protected α-aminoalkyl radicals, in addition to the desired transformation. Particularly, Cowden and coworkers reported benzylic hydrogen atom abstraction leading to a competitive undesired α-aminoalkylation route.

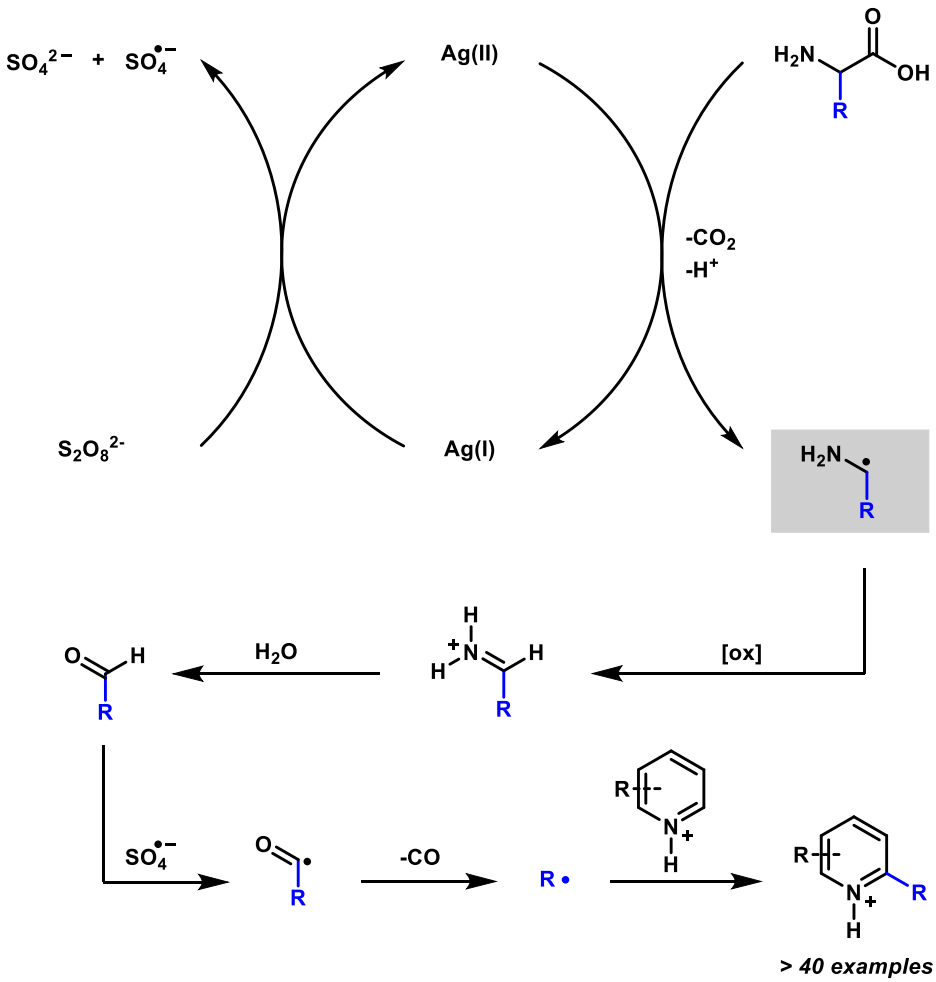

Figure 1-1. Proposed Mechanism Showing Oxidation of an α-Aminoalkyl Radical to an Iminium Ion.

In efforts to circumvent the issue of over-oxidation, recent developments in single electron reduction photocatalytic systems have been developed. Photoredox of amines entails a reaction between an excited photocatalyst and the α-amine substrate. MacMillan,[19] Pandaley and Reiser,[20] Nishibayashi,[21] Yoon,[22] have developed photocatalytic methods in which cyanoarenes and α,β-unsaturated systems were reacted with amines via an α-aminoalkyl radical intermediate. More recently, Yoshida,[23] Nagaoka,[24] and Mancheño[25] have reported α-aminoalkyl radicals adding into alkenes bearing electron withdrawing groups, radical hydroxyalkyaltion, and α-alkylation of olefins. However, all of these methods require some photocatalyst, or electrochemical conditions to generate the α-aminoalkyl radicals, and double bond systems bearing electron withdrawing groups as substrates.

1.2. Radical Decarboxylative Fluorination

In 2012, Chaozhong Li and coworkers reported successful radical decarboxylative fluorination.[26] Their method involved Ag(I) as the catalyst, Selectfluor, and the carboxylic acid in a 50/50 solvent mixture of acetone and water at temperatures varying from room temperature to reflux for a minimum of one hour up to 10 hours, (Scheme 1-2). Therein, they reported radical decarboxylative fluorination of primary, secondary, and tertiary alkanes starting from their respective carboxylic acid forms. Li and coworkers highlighted their work for being an efficient and general catalytic method that was chemoselective and tolerant of a broad range of functional groups.

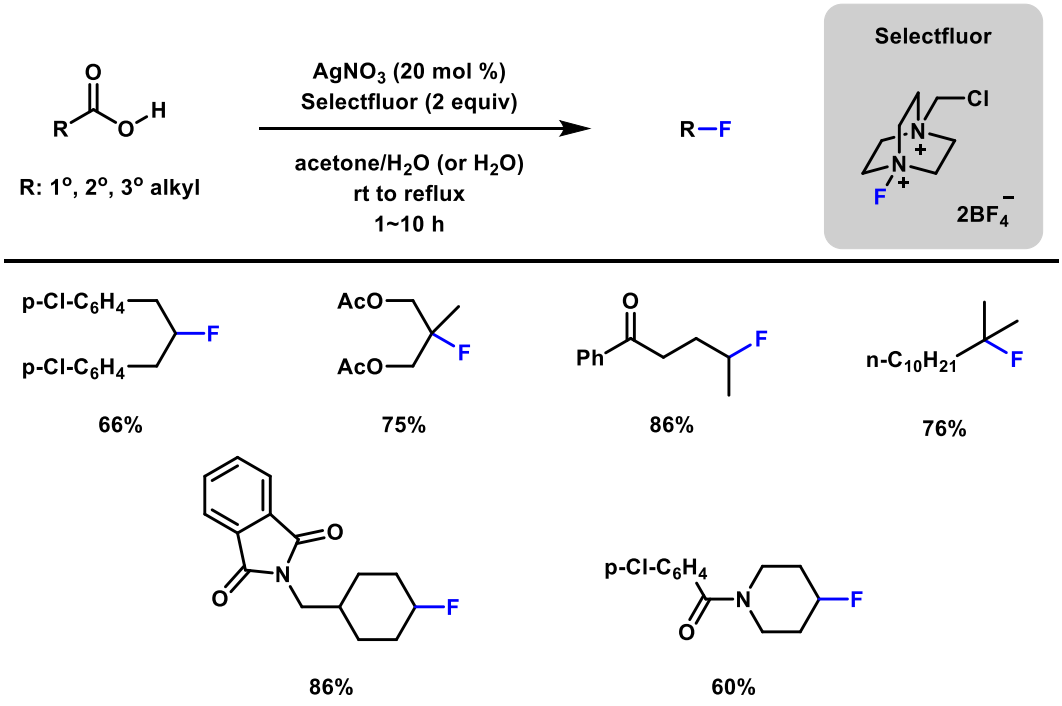

Scheme 1-2. Radical Decarboxylative Fluorination Reported by Chaozhong Li and Coworkers in 2012.

It was proposed that the reaction proceeded through a Ag(I)/Ag(III)/Ag(II) catalytic cycle wherein which oxidative addition occurs between Ag(I) and the fluorine from Selectfluor, generating Ag(III)–F (Figure 1-2). The Ag(III)–F species then undergoes single electron reduction upon radical decarboxylation of the substrate, releasing carbon dioxide gas as a byproduct, and generating the alkyl radical species. The alkyl radical takes F· from the Ag(II)–F species and regenerates Ag(I).

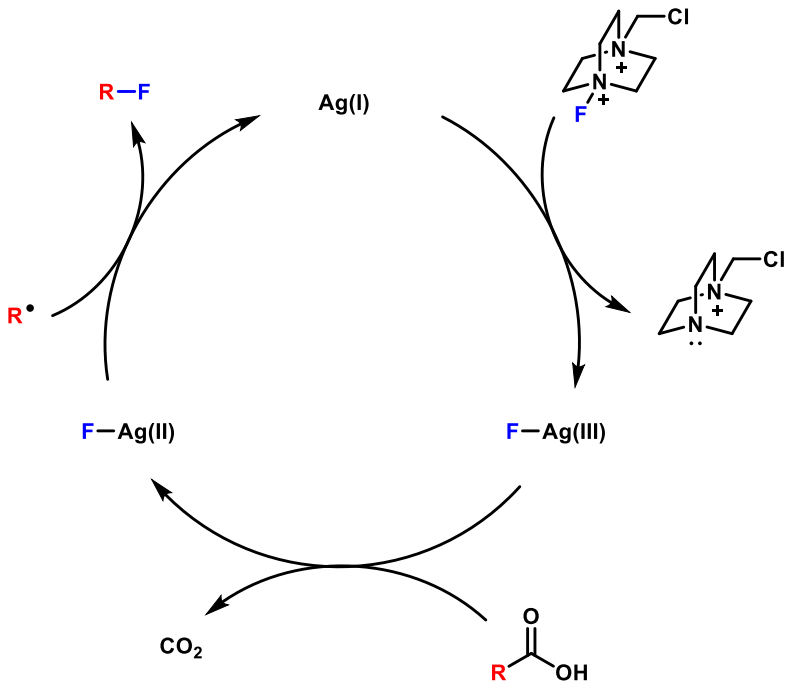

Figure 1-2. Proposed Mechanism by Li and Coworkers for Radical Decarboxylative Fluorination.

While this method can tolerate a range of functional groups, its substrate scope is limited to carboxylic acids. Arguably, there is a plethora of readily available carboxylic acids; however, for more complex and unique molecules, installation of a carboxylic group is necessary, and may not be practical. We were interested in utilizing this Ag(I)-radical decarboxylation process in a way that would allow for a different scope of substrates. Previously, our lab reported the use of unprotected amino acids as radical precursors for heterocyclic C–H functionalization, where persulfate undergoes heterolytic cleavage in the presence of Ag(I), (Figure 1-1).[14] The resulting Ag(II) species is then capable of performing radical decarboxylation of the unprotected amino acid, resulting in an α-aminoalkyl radical species. In the presence of persulfate, a strong oxidant, the α-aminoalkyl radical undergoes further oxidation, yielding an iminium species that is then hydrolyzed and undergoes hydrogen atom abstraction and radical decarbonylation before being trapped by the heterocyclic substrate. As mentioned, a side product found in reactions involving an α-aminoalkyl radical species was the hydrogenated α-aminoalkyl species which was suspected to have undergone hydrogen atom transfer.[6f,18] We contemplated the fate and capabilities of the α-aminoalkyl radical generated from the unprotected amino acid in less oxidizing conditions.

1.3. Use of Unprotected Amino Acids as Radical Precursors to Fluorination

Li and coworkers have established that radical decarboxylation of alkyl carboxylic acids was achievable in the presence of a Ag(I) catalyst and Selectfluor, and demonstrated tolerance of nitrogen-bearing substrates, (Scheme 1-2). Our lab has demonstrated the access to α-aminoalkyl radical species resulting from decarboxylation of unprotected amino acids, using persulfates as the oxidizing agent. We contemplated the decarboxylation of unprotected amino acids via Ag(I)/Selectfluor and the fate of the resulting α-aminoalkyl radical species. Being in less oxidizing conditions, the α-aminoalkyl radical is available to do other chemistry, specifically, hydrogen atom abstraction. We set out to find a suitable substrate from which the α-aminoalkyl radical would abstract a hydrogen atom. In comparison to α-aminoalkyl C–H bonds, benzylic C–H bonds have a lower BDE, suggesting that hydrogen atom abstraction would be thermodynamically favorable for benzylic C–H bonds, (Table 1-1).

Our preliminary reactions were run with glycine as the radical precursor and *p*-cymene as the benzylic substrate. Fluorination was completely selective for the primary benzylic site versus the secondary site (Scheme 1-3, b). Glycine was chosen as the radical precursor for its simplicity and neutrality in both sterics and electronics.

C—H Bond type	BDE (kJ/mol)
methane	431
alkane	427
alkene	523
alkyne	410
aromatic	431
cyclohexyl	400
benzylic	356

Table 1-1. BDE values for various C–H bonds.[1]

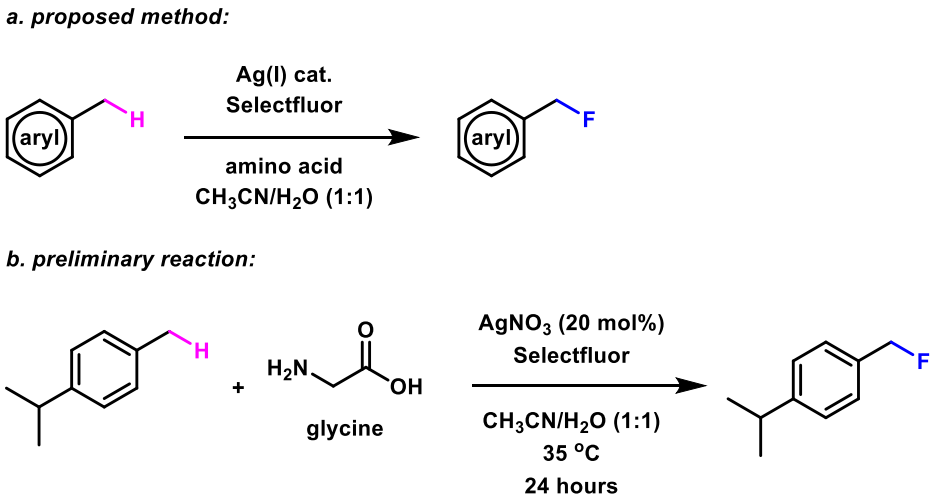

Scheme 1-3. Proposed Radical Fluorination and Preliminary Results.

1.3.1. Results and Discussion

For detailed information regarding experimental set-up, see Appendix A.

As we began further investigations, we considered two possible reaction initiation pathways, (Scheme 1-4). The Ag(I) catalyst could directly add into the N–F bond of Selectfluor, (eqn1), proceeding through a Ag(I)/Ag(III)/Ag(II) catalytic cycle, (Scheme 1-4, eqn1), as was proposed by Li and coworkers.[26] Alternatively, Ag(I) could undergo single electron oxidation by Selectfluor, (Scheme 1-4, eqn2), via a Ag(I)/Ag(II) catalytic cycle as proposed by Flowers and coworkers.[27] It was also demonstrated by Flowers that this Ag(I)/Ag(II) catalytic cycle is capable of radical decarboxylation. However, this second pathway is complicated by the generation of the iminium radical species **2** resulting from Selectfluor, as it is also a plausible HAT agent, making it difficult to identify the dominant HAT agent. Lectka and coworkers have also shown this iminium radical species from Selectfluor participating in HAT processes in a radical chain reaction for C–H fluorinations.[28] Our mechanistic studies using ReactIR, analytical electrochemistry, and deuterium labeling supports the Ag(I)/Ag(II) catalytic cycle with the α-aminoalkyl radical being the dominant HAT agent. A further discussion of our mechanistic studies can be found in the proceeding subsections.

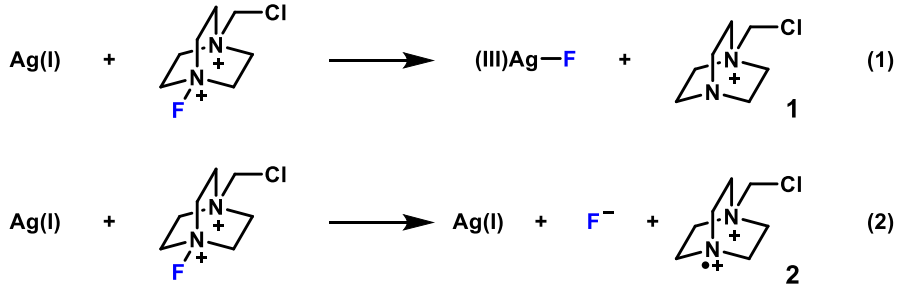

Scheme 1-4. Possible Pathways for Ag(I) Oxidation.

Originally, we had chosen *p*-cymene as the model substrate, but volatility issues led us to choose 4-methylbiphenyl **3**, a more benchtop-stable and easily isolable solid. As shown in Table 1-2, we found that catalytic $AgNO_3$, Selectfluor, and glycine in a 1:1 mixture of CH_3CN/H_2O, at 35 ^oC led to formation of **3a** in good yields. The reaction was ineffective at room temperature. At high temperatures, the reaction showed diminished yields (entry 2). While slightly higher yields were observed under inert atmosphere, the reaction gave moderate yields when open to air (entry 3). It was detected by GC-MS and NMR of the crude reaction mixture that oxidation of the substrate seemed to occur when run open to air, thus explaining the decrease in yield. Other unprotected amino acids also led to the formation of **3a** in good yields, with competing oxidation observed in some cases (entries 4–6). Among the unprotected amino acids tested, glycine proved to be the most effective in fluorination of all substrates examined. *N*-Boc-glycine proved to be detrimental to the formation of **3a**, (entry 7), and is rationalized upon further mechanistic investigations, (*vide infra*). Carboxylic acids did not lead to any formation of **3a**, suggesting the necessity and importance of nitrogen within the reaction system (entry 8). NFSI was ineffective as an electrophilic fluorine source (entry 9), likely due to its lower reduction potential ($E°$ = -0.78 V) compared to that of Selectfluor ($E°$ = -0.04 V).[29] Other solvents led to diminished yields (entries 10–11). Other Ag(I) catalysts, $Ag(Bpy)_2OTf$ and $Ag(Phen)_2OTf$, did not yield any fluorinated products (entries 12–13). Control reactions showed that both $AgNO_3$ and an unprotected amino acid were necessary for reaction (entries 14–15).

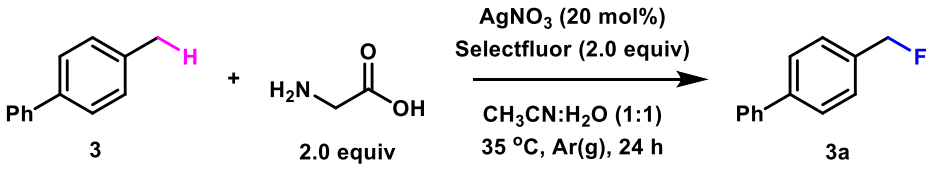

entry	deviation from standard conditions	yield (%)
1	none	76
2	50 °C	46
3	open to air	48
4	proline instead of glycine	62
5	valine instead of glycine	72
6	phenylalanine instead of glycine	59
7	*N*-Boc-glycine instead of glycine	0
8	mandelic acid instead of glycine	0
9	NFSI instead of Selectfluor	0
10	CH_2Cl_2/H_2O	0
11	acetone/H_2O	48
12	20 mol% $Ag(Bpy)_2OTf$	0
13	20 mol% $Ag(Phen)_2OTf$	0
14	no $AgNO_3$	0
15	no glycine	0

Table 1-2. Optimization of Benzylic Fluorination. Yields refer to chromatographically pure material. Reaction conditions: 4-methylbiphenyl **3** (0.2 mmol), glycine (0.4 mmol), Selectfluor (0.4 mmol), $AgNO_3$ (20 mol%), 2 mL of CH_3/H_2O (1:1).

With optimized conditions established, the scope of substrate was explored. As shown in Scheme 1-5, moderate yields were observed. Most functional groups were tolerated, except for free hydroxyl groups. Substrates with free hydroxyl groups resulted in diminished yields and increased amounts of varying byproducts. As a result, methylation or acylation was done to protect any free hydroxyl groups present (**12**). Carboxylic groups, as expected, were also not tolerated by this method. Competing radical decarboxylation occurred, leading to uncontrollable fluorination at both the benzylic site and carboxylate site. For substrates containing carboxylic groups, methylation was done

to prevent decarboxylation (**18**). Among the functional groups that were tolerated, we want to highlight the boronic acid pinacol esters (**13**, **14**). Boronic acid pinacol esters are typically sensitive to oxidative cleavage, but our method is mild enough to leave them intact. It is also noteworthy that these products did not require further purification following reaction quenching and extraction work-up. We are also excited that these boronic acid pinacol esters were tolerated because the products may be subjected to cross-coupling reactions to form more complex molecules that may be advantageous for pharmaceuticals.

In most cases, unreacted substrate accounted for mass balance of incomplete reactions. Mono- or difluorinated products were accessible for select electron-rich substrates by changing the stoichiometric amounts of Selectfluor and glycine (**3a**, **3b** from 4-methylbiphenyl; **4a**, **4b** from 4-ethylbiphenyl). Tertiary benzylic sites were unreactive, yielding trace amounts of fluorinated product (**7a**), while secondary sites were suitably fluorinated. Primary benzylic sites were shown to be the most reactive. Analogous selectivity (1° > 2° > 3°) has been previously observed in other reports of radical fluorination and is likely due to the stereoelectronic sensitivity of the proton-coupled electron transfer mechanism. Both electron-rich (**3a–9a**) and electron-poor (**10a**, **11a**) substrates were tolerated, albeit electron-rich substrates showed more efficient fluorination which is consistent with fluorination from a nucleophilic benzylic radical. Although direct fluorination of heterobenzylic substrates was challenging, nitrogen-bearing substrates were successfully fluorinated (**15a–17a**), supporting feasibility of late-stage fluorination of pharmaceutical scaffolds. The failure of heterobenzyllic substrates may be explained by the nucleophilicity of the heteroatom (typically oxygen or nitrogen). The nucleophilic heteroatom, as shown by Rios and coworkers, would react directly with the electrophilic fluorine in an S_N2-type fashion, rather than at the benzylic site.[30]

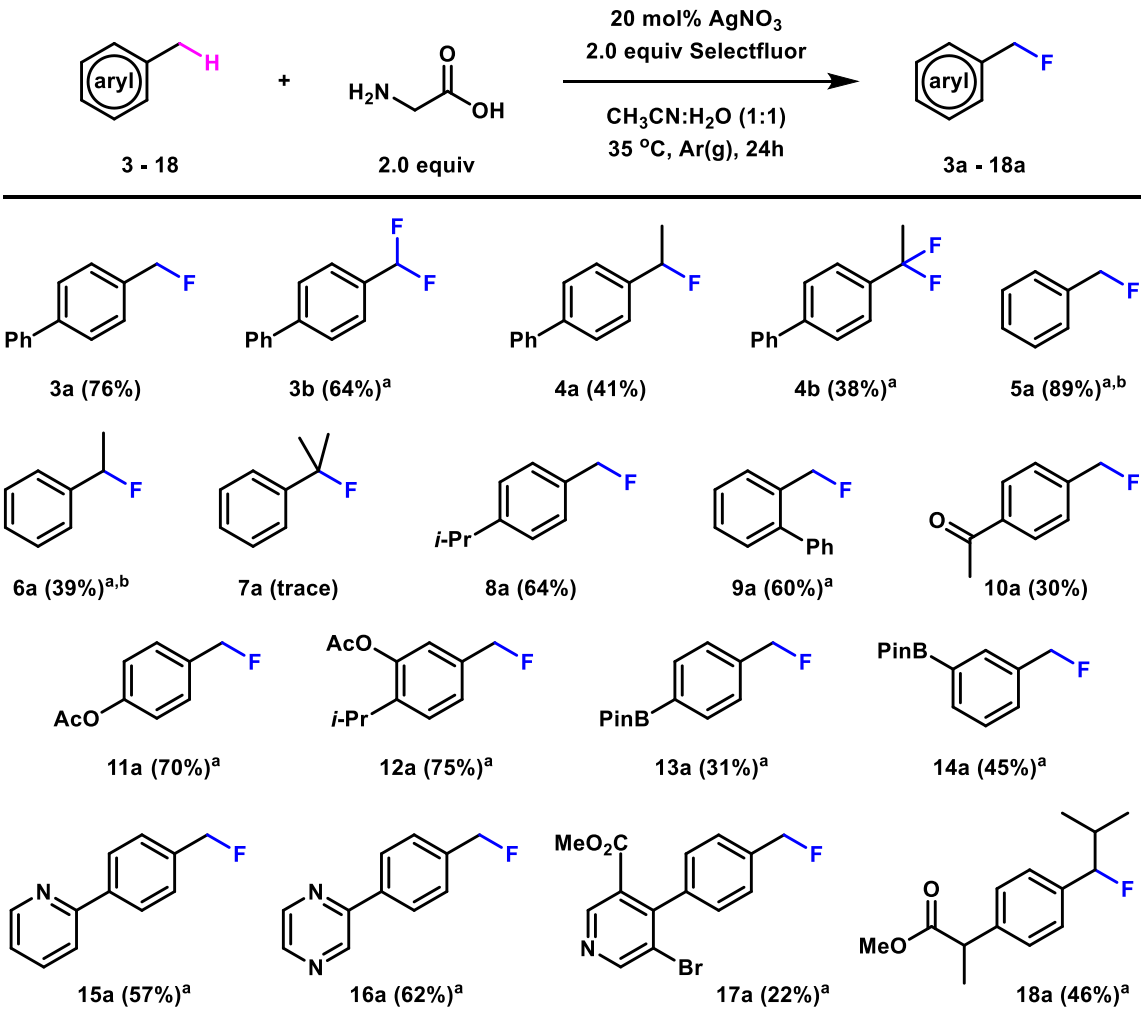

Scheme 1-5. Scope of Benzylic Fluorination. Yields refer to chromatographically pure material unless otherwise noted. Reaction conditions: arene (0.2 mmol), glycine (0.4 mmol), 2 mL CH_3CN/H_2O (1:1). [a]5.0 equiv of Selectluor (1.0 mmol) and glycine (1.0 mmol). [b]NMR yield compared to benzotrifluoride as an internal standard.

1.3.1.1. Mechanistic Investigation

As previously stated, there are two plausible initiation pathways (Scheme 1-4). We set out to determine which of the two pathways was more likely to occur. We also wanted to understand why glycine is the best performing amino acid among the others. ReactIR was used to track the reaction progress under standard reaction conditions and the fate of Selectfluor in the presence of the different unprotected amino acids. The onset oxidation potentials of Ag(I) in the presence of the varying amino acids were also determined by cyclic voltammetry. NMR investigations included deuterium labeling experiments to identify the HAT agent and if the HAT event was a rate determining step. ^{19}F NMR was also used to determine the fate of Selectfluor in standard reaction conditions and in the

presence of varying amino acids. ^{13}C NMR was also done under optimized reaction conditions with toluene-d8 to track the fate of the decarboxylated amino acid.

Based on the reduction potential of Selectfluor alone, it should not be capable of generating Ag(II) from Ag(I) via single electron transfer. Therefore, we first considered the Ag(I)/Ag(III)/Ag(II) cycle. We used *in situ* ReactIR to probe for Ag(III)–F in a reaction where the substrate was *p*-tolyl acetate **11**. We deviated from our model substrate, 4-methylbiphenyl **3**, due to solubility issues. As the reaction progressed and product formation increased, it appeared that a secondary oily layer would form at the top of the reaction mixture. The biphasic nature of our model substrate reaction made it difficult to get an accurate IR representation of the reaction mixture. For all ReactIR studies, assume *p*-tolyl acetate is the substrate unless otherwise stated.

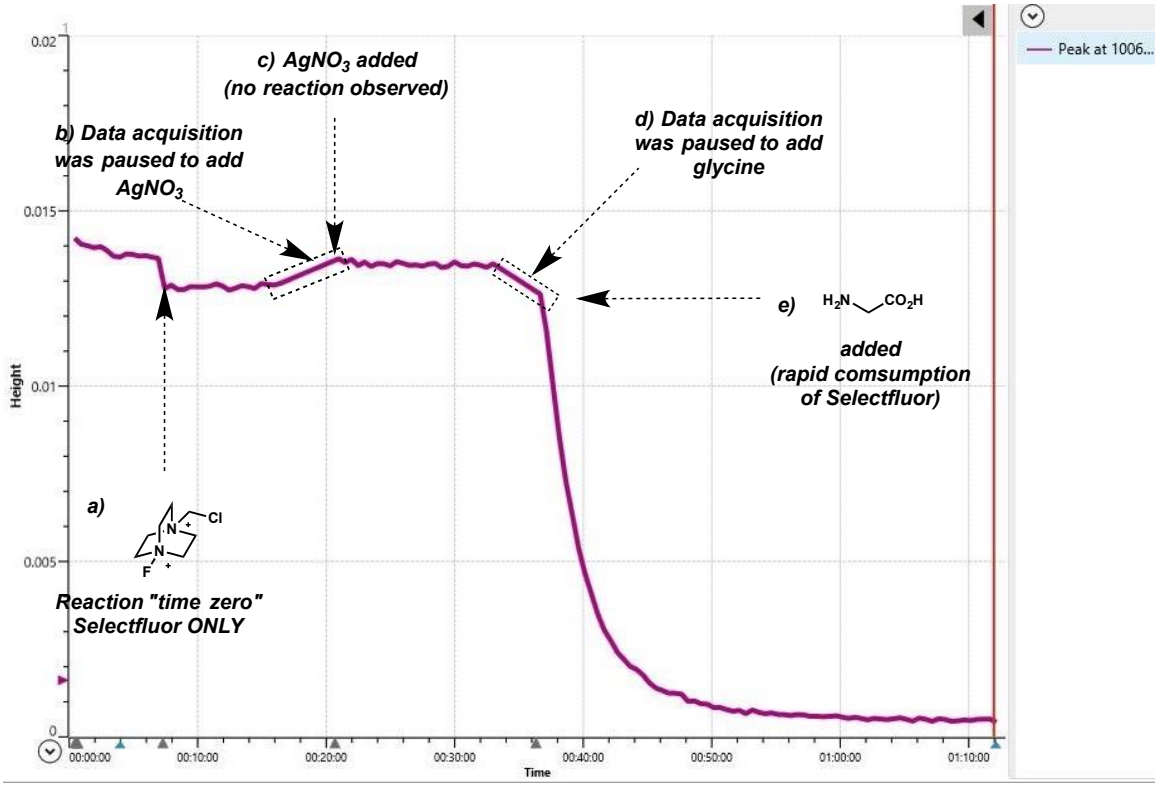

Figure 1-3. ReactIR Monitoring of Selectfluor Concentration. Reaction conditions: **11** (0.2 mmol), glycine (0.4 mmol), Selectfluor (0.4 mmol), $AgNO_3$ (0.4 mmol), 2 mL of CH_3CN/H_2O (1:1). 25% reaction conversion observed by GC-MS.

We investigated the fate of Selectfluor in presence of stoichiometric amounts of $AgNO_3$ and observed no significant change in the concentration of Selectfluor. No indication of Ag(III)–F within the reaction was observed, suggesting that the Ag(I)/Ag(III)/Ag(II) cycle was not the likely initiation pathway. To this reaction mixture, stoichiometric amounts of glycine was added. A rapid decrease in Selectfluor

concentration was observed upon addition of glycine, indicating a significant role of glycine in the reaction of $AgNO_3$ and Selectfluor, (Figure 1-3).

We began investigating the onset oxidation potentials of $AgNO_3$ in the presence of different unprotected amino acids to rationalize the plausibility of the Ag(I)/Ag(II) initiation pathway. In the presence of glycine, alanine, and valine, the onset oxidation potential of $AgNO_3$ decreased (Table 1-3). Oxidized substrate was observed in small amounts via GC-MS analysis of the crude reaction mixture for alanine, which was reasonable. Valine did not decrease the oxidation potential of $AgNO_3$ to the extent that glycine did, which may explain the slight decrease in yield of **3a** (Table 1-2). *N*-Boc-glycine did not seem to have any effect on the onset oxidation potential of $AgNO_3$, which may explain why no reaction was observed. These analytical electrochemical data suggest that the amino acids must have some ligation interaction with $AgNO_3$, and that this event is necessary for radical decarboxylation to occur. These studies also suggested that the free Lewis basic nitrogen of the unprotected amino acid must be the point of ligation to the Ag(I) catalyst. We ran a reaction with *N*-Boc-glycine in the presence of a free Lewis basic nitrogen, pyridine, and observed 67% yield of benzylic fluorination, confirming the importance of Lewis basic additives (Scheme 1-6).

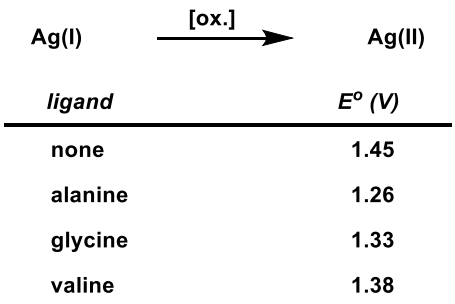

ligand	E^o *(V)*
none	1.45
alanine	1.26
glycine	1.33
valine	1.38

Table 1-3. Experimentally Determined Onset Oxidation Potential of Ag(I) in the Presence of Amino Acids. Electrical conditions: $AgNO_3$ (0.4 mmol), in 5 mL of CH_3CN, tetrabutylammonium tetrafluoroborate supporting electrolyte (0.1 M), amino acid (0.4 mmol). The reverse waveform of Ag(II) to Ag(I) was not observed under these conditions due to instability of aqueous Ag(II).

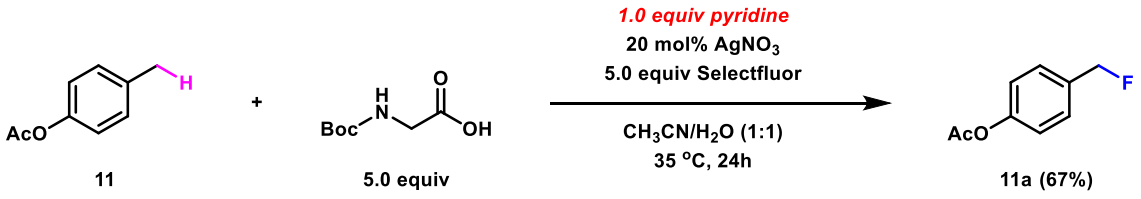

Scheme 1-6. Catalyst Activation via Pyridine Additive. Yield refers to chromatographically pure material. Reaction conditions: **11** (0.2 mmol), *N*-Boc-glycine (1.0 mmol), Selectfluor (1.0 mmol), pyridine (0.2 mmol), $AgNO_3$ (0.04 mmol), 2 mL of CH_3CN/H_2O (1:1).

Because we have rationalized the reaction initiation pathway to be a Ag(I)/Ag(II) cycle, we needed to determine the dominant HAT agent. *In situ* carbon NMR was conducted with a deuterium-labeled substrate (toluene-d8) to track the fate of the hydrogen/deuterium being abstracted from the substrate, and ultimately determine the HAT agent responsible for the benzylic fluorination. Deuterated methylamine resulting from HAT by the decarboxylated glycine was observed in ^{13}C NMR. Attempts of *in situ* protection of the methylamine for isolation proved to be challenging and unfortunately failed. Because the methylamine was only clearly observed in the ^{13}C NMR and isolation was not feasible, quantitative analysis of deuterium incorporation was not possible. The deuterium-labeled ^{1}H NMR studies also showed that fluorination of toluene-d8 occurred at a slower rate than toluene, indicating that the hydrogen/deteurium atom transfer is a rate determining step.

We contemplated the role of glycine and wondered if it was only necessary in catalytic amounts to promote a radical chain reaction process, or if it was participating beyond initiation, and therefore was required in stoichiometric amounts. At catalytic amounts of glycine, (20–40 mol%), only trace fluorination was observed. Fluorine NMR of fluorination under standard reaction conditions was taken as the reaction progressed to track the fate of the fluorine from Selectfluor after single electron oxidation of the Ag(I) catalyst occurred. Fluorine NMR showed the formation of fluoride anion as we had originally proposed. As the reaction progressed, the relative concentration of fluoride anion increased in a directly proportional manner to that of product formation, (Figure 1-4).

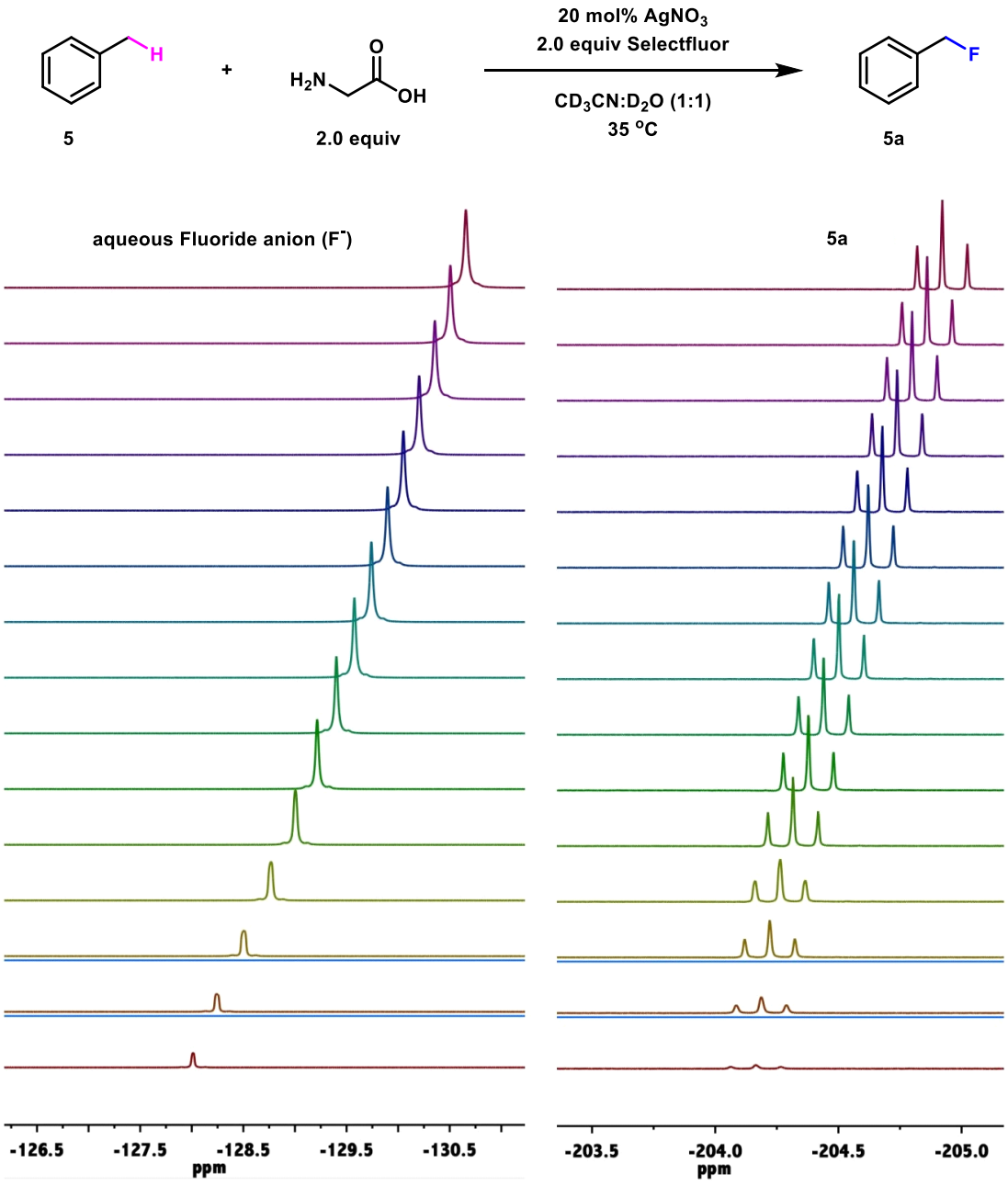

Figure 1-4. ^{19}F NMR and ^{1}H NMR of Reaction Progress. Reaction conditions: toluene (0.1 mmol), glycine (0.5 mmol), Selectfluor (0.5 mmol), $AgNO_3$ (0.02 mmol) in 1 mL of CD_3CN/D_2O (1:1) at 35 ^{o}C.

1.3.1.1.1. Proposed Mechanism

Based on our mechanistic investigations, we have proposed that our reaction starts with the pre-coordination of Ag(I) to one or more unprotected glycine molecules, (Figure 1-5). This is important to note, as the glycine interaction with the Ag(I) catalyst is what allows for the reaction to occur at all, lowering the oxidation potential of Ag(I) to allow for single electron oxidation to Ag(II). The glycine-ligated Ag(I) catalyst then undergoes single electron oxidation by Selectfluor, generating Ag(II) and the iminium radical **2** and releasing aqueous fluoride anion. A molecule of glycine then undergoes radical decarboxylation by Ag(II), resulting in the regeneration of Ag(I) and the α-aminoalkyl radical. Because the oxidation of glycine by Ag(II) is believed to occur rapidly, Ag(II) is expected to exist in low concentrations throughout the duration of the reaction. It is significant to note the low concentration of Ag(II) in the reaction mixture because α-aminoalkyl radicals are typically easily oxidized by Ag(II). With minimal concentration of Ag(II) in the reaction mixture at any given time suggests that the α-aminoalkyl radical is able to survive long enough to perform HAT. The α-aminoalkyl radical then abstracts a benzylic hydrogen from the substrate, forming methylamine and the corresponding benzylic radical. Subsequent radical fluorination occurs, yielding the desired product.

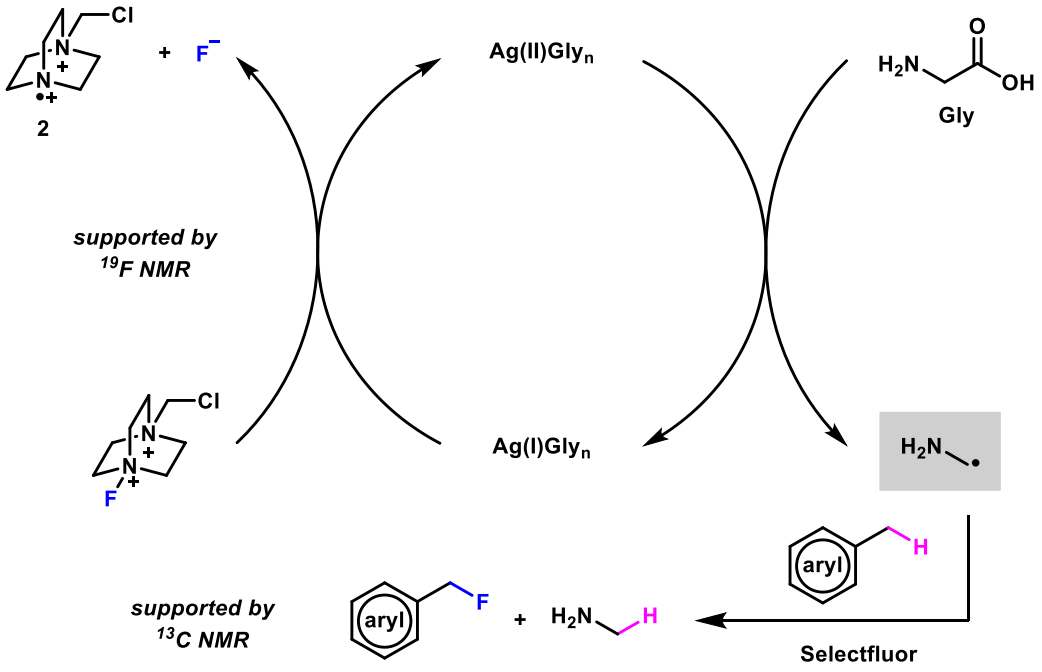

Figure 1-5. Proposed Mechanism for Benzylic Fluorination.

1.4. Summary of Unprotected Amino Acids as Radical Precursors that Facilitate Benzylic C–H Fluorination

We have developed a novel method for benzylic C–H radical fluorination using unprotected amino acids as radical precursors and as ligands that lower the oxidation potential of the Ag(I) catalyst. With a lower oxidation potential, Ag(I) can participate in the oxidative radical decarboxylation of the amino acid while in mildly oxidizing conditions. The mildly oxidizing condition is critical in the survival of the α-aminoalkyl radical, allowing it to abstract a benzylic hydrogen atom from the substrate. Our method features mild conditions that effectively fluorinates both electron-rich and electron-poor benzylic substrates using biologically available amino acids as radical precursors.

This work has led our lab to explore Minisci-type reactions using Selectfluor and Ag(I)/Ag(II) as a single electron mild oxidizing system.[31] A variety of carboxylic acids and boronic acids were demonstrated to be viable radical precursors that afforded C–H alkylation and arylation of heteroarenes and quinones. Transformations that have otherwise been difficult through classical Minisci-type reactions are now accessible through this Selectfluor-Ag(I)/Ag(II) method.

C H A P T E R 2

Benzylic C–H Radical Fluorination Facilitated by Halogen Bonding

2.1. Introduction

2.1.1. Hydrogen Bonding: Descriptions and Uses

Hydrogen bonding is a form of an electrostatic noncovalent bonding interaction that is capable of altering the local electron density, and ultimately, altering the physical and/or chemical properties of a molecule.[32] In a review by Doyle and Jacobsen, hydrogen bonding was demonstrated to be critical in the development of organocatalysis, in which the interaction enhances the reactivity or promotes asymmetric transformations.[33] Among the plethora of asymmetric transformations that benefit from hydrogen-bound intermediates are the Aldol reaction, Diels-Alder cycloaddition, Baylis-Hillman reaction, and Friedel-Crafts addition.[33] For example, while enantioselective aldol cyclization of triketones and terpenoids were shown to be catalyzed by proline, it was not until decades later that hydrogen bonding was realized as a significant role towards the success and selectivity of the transformation.[34] With a new appreciation for the impact of hydrogen bonding in asymmetric catalysis, previously reported transformations have been revisited and theoretical explorations and overall understanding of hydrogen bonding has expanded

greatly. With a better understanding of the influence of hydrogen bonding and hydrogen bonding networks, new catalysts have been designed.[35]

While a hydrogen bond acceptor may be any Lewis basic atom, it is limited in that the hydrogen donor is limited to a hydrogen atom.

2.1.2. Halogen Bonding: Early Descriptions and Uses

Halogen bonding can be thought of analogously to hydrogen bonding, where the halogen atom interacts electrostatically with a Lewis basic atom (Figure 2-1). Unlike hydrogen bonding, halogen bonding is not limited to one type of atom to which the electron density is being donated. Typically chlorine, bromine, and iodine are the halogens that are seen participating in a halogen-bond.[36b] These halogens may provide varying physical and chemical properties based on their size and electronegativity.[36] Because of this, halogen bonding has gained much attention as a surrogate for hydrogen bonding and has been shown to promote organic transformations.[37]

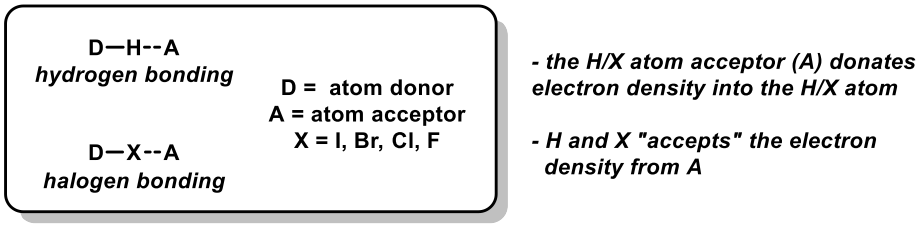

Figure 2-1. Analogous Behavior of Hydrogen and Halogen Bonding.

In their recent work demonstrating heterobenzylic radical fluorination, van Humbeck and coworkers briefly suggested a halogen bonding interaction between the nitrogen of electron-rich pyridines and the fluorine of Selectfluor (Scheme 2-1, A).[38] Our concurrent work in radical fluorination has led us to explore the electronically diverse scope of pyridines as additives that halogen bond to the fluorine of Selectfluor, generating a $[N–F–N]^+$ complex **19** responsible for the facilitation of the fluorination (Scheme 2-1, B).

A) Heterobenzylic Radical Fluorination (Van Humbeck)

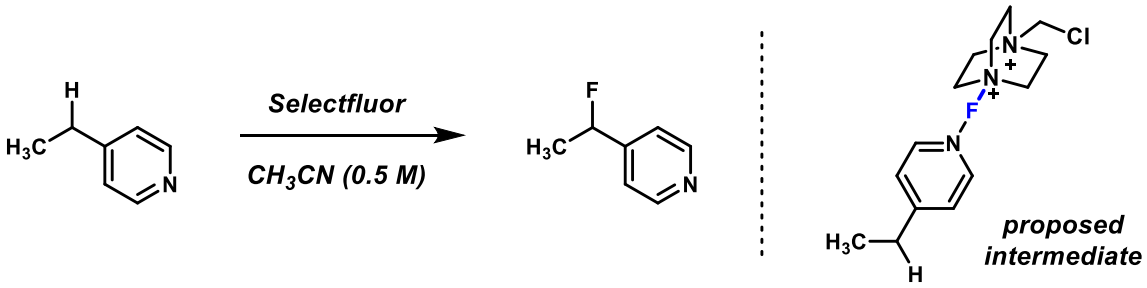

B) Benzylic Radical Fluorination Facilitated by Halogen Bonding (this work)

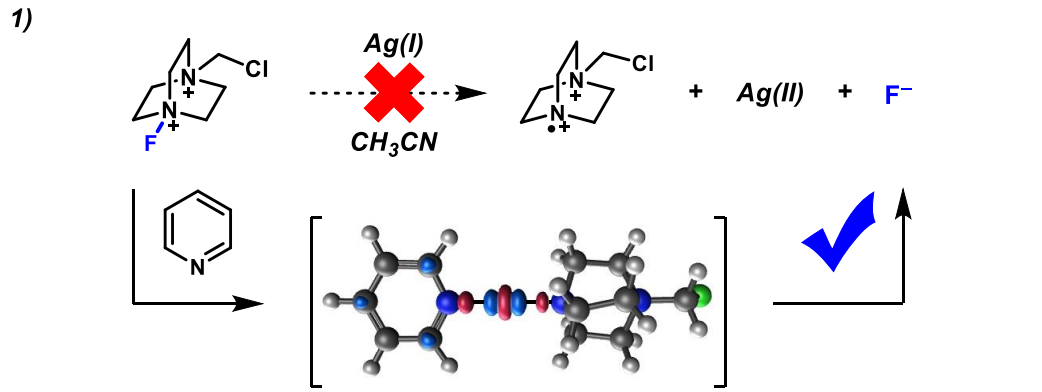

Scheme 2-1. Radical Fluorination via Halogen Bonding.

2.2. Pyridine-Mediated Benzylic Fluorination

2.2.1. Results and Discussion

For detailed information regarding experimental set-up, see Appendix B.

From our previous work with the unprotected amino acid and Ag(I)/Ag(II) system, we suspected that a free Lewis basic nitrogen was necessary to promote the radical fluorination when *N*-Boc-glycine was used instead of glycine and no fluorinated product was afforded (Table 1-2, entry 7). We ran a reaction with *N*-Boc-glycine in the presence of a simple Lewis basic additive, pyridine. As expected, the reaction yielded high quantities of **3a** (Table 2-1, entry 1). Before we continued with further investigations, we ran control reactions to ascertain that all components of the reaction were necessary to afford fluorination, (Table 2-1). As expected, no fluorination was observed in the absence of $AgNO_3$, or pyridine additive (entries 2–3). However, it was to our surprise that a 51% yield of **3a** was observed in the absence of *N*-Boc-glycine (entry 4).

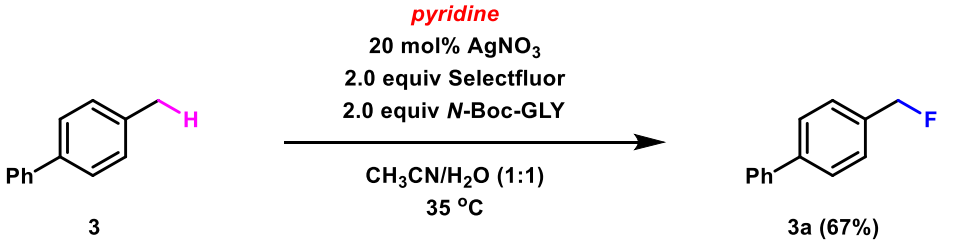

entry	deviation from standard conditions	yield (5%)
1	none	88
2	no $AgNO_3$	00
3	no pyridine	00
4	no *N*-Boc-GLY	51
5	no *N*-Boc-GLY, TEMPO added	*trace*

Table 2-1. Discovery of Pyridine Mediated Fluorination.

Before delving into mechanistic investigations, the optimum reaction conditions were determined (Table 2-2). At ambient temperatures, lower conversion was observed (entry 2), while no significant change was observed at elevated temperatures (entry 3). Other pyridines with varying range of electronics also led to fluorinated products, with the electron-rich pyridines yielding lower conversions (entries 4–5), and electron-poor

pyridines affording moderate to good conversions (entries 6–7). Sterically hindered electron-poor pyridines proved to be problematic, yielding no product (entry 8). Increasing the amount of the pyridine additive lead to decreased conversions, while reducing the concentration gave comparable conversions (entries 9–10). Changing the global concentration of the reaction allowed for the manipulation of product distribution, where a more dilute reaction favored **3a** and a more concentrated reaction gave preference to **3b** (entries 11–12). Other solvents led to significantly lower conversions (entries 13–14). Both $AgNO_3$ and a pyridine additive is necessary for fluorination (entries 14–15). As identified, entry 6 is optimal for efficient fluorination.

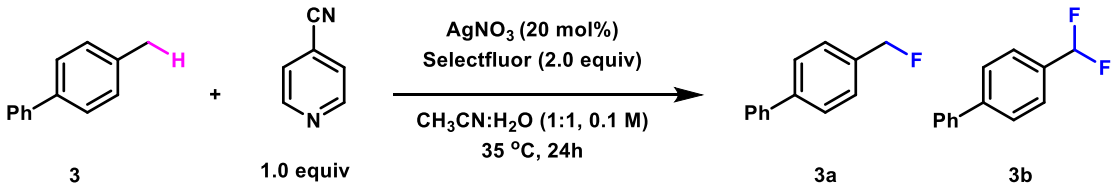

3 1.0 equiv 3a 3b

entry	deviation from standard conditions	NMR yield (%)	
1	none	28	70
2	25 °C	37	49
3	50 °C	9	68
4	pyridine instead of 4-cyanopyridine	52	trace
5	4-methoxypyridine instead of 4-cyanopyridine	35	0
6	4-(trifluoromethyl)pyridine instead of 4-cyanopyridine	12	85
7	ethyl isonicotinate instead of 4-cyanopyridine	25	49
8	ethyl 2,6-diisopropylnicotinate	0	0
9	2.0 equiv 4-cyanopyridine	23	31
10	0.5 equiv 4-cyanopyridine	7	76
11	$CH_3CN:H_2O$ (1:1, 0.05 M)	70	30
12	$CH_3CN:H_2O$ (1:1, 0.2 M)	15	77
13	$CH_2Cl_2:H_2O$ (1:1)	50	0
14	acetone:H_2O (1:1)	54	0
15	no $AgNO_3$	0	0
16	no 4-cyanopyridine	0	0

Table 2-2. Optimization of Pyridine-Mediated Benzylic Fluorination.

As we contemplated the role of the pyridine additive, we sought to explore the electronics of the additive. We suspected that the pyridine additive would interact with the Ag(I) catalyst as ligands, as it is known that Ag(I) has an affinity to nitrogen-containing ligands, especially pyridyl ligands.[39] It was anticipated that the pyridine additives would lower the onset oxidation potential of Ag(I), resulting in moderate fluorination as was seen with the unprotected amino acids. More precisely, we had expected that an electron-rich pyridine additive would significantly lower the oxidation potential of the Ag(I) and behave analogous to the amino acid system, yielding greater conversions than that of an electron-poor pyridine. While the oxidation potential of Ag(I) was decreased in the presence of the pyridine additives (Table 2-3), fluorination proved to be more efficient with electron-poor pyridine additives (Scheme 2-2). This was counterintuitive and further suggested that this was a vastly different reaction mechanism from that of the unprotected amino acids system.

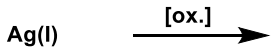

ligand	E^o *(V)*
none	1.45
alanine	1.26
glycine	1.33
valine	1.38
4-R-pyridine	--------
R = OCH_3	1.24
R = H	1.31
R = CO_2Et	1.54
R = CF_3	1.60

Table 2-3. Oxidation Potentials of $AgNO_3$ in the Presence of Amino Acids and Pyridine Additives.

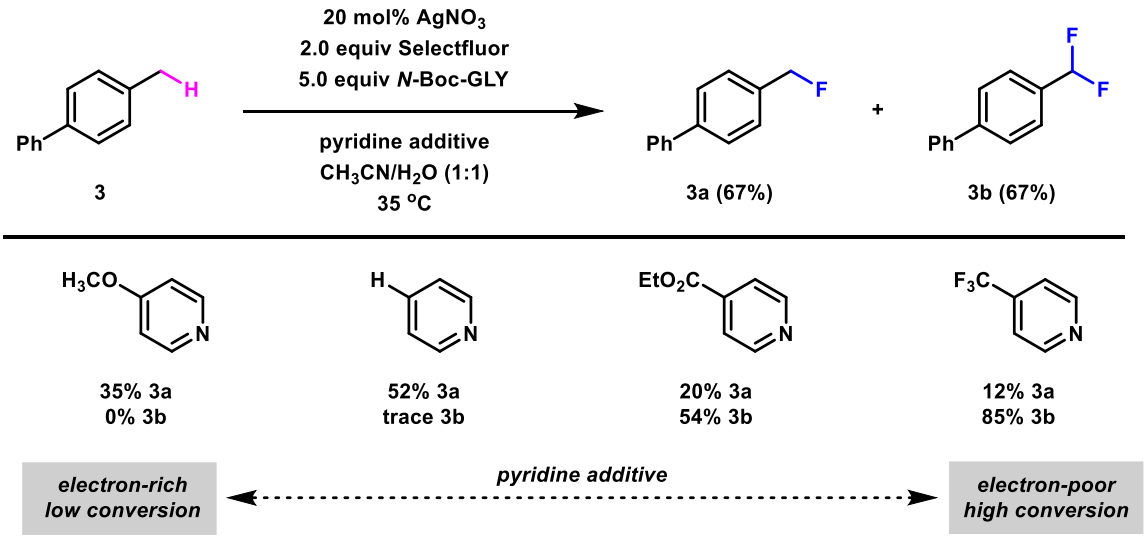

Scheme 2-2. Pyridine-Dependent Product Distribution.

As shown in Table 2-5, the addition of TEMPO was detrimental to the fluorination (entry 5), suggesting, but is not conclusive, of a radical pathway. In the presence of water and oxidants, TEMPO can be oxidized to its oxoammonium derivative, (Table 2-5), which may be reactively competitive with the fluorination pathway, giving a false indication for a radical pathway. A reaction was run under standard conditions *without* TEMPO and was quenched after 24 hours to give product yield of an unaltered reaction (Table 2-4, entry 1). Another reaction was run under standard conditions and globally quenched after five hours to determine the progress of a productive reaction up to that time point, (entry 2). In a separate reaction run under standard conditions, TEMPO was added after five hours of productive reaction time and was stirred and heated for a total reaction time of 22 hours, (entry 3).

Table 2-4, entry 1 shows that a reaction run to completion under standard conditions yields 12% mono-fluorinated product and 85% di-fluorinated product. Entry 2 shows that a reaction run under standard conditions and stopped after five hours yielded 37% mono-fluorination without any di-fluorination observed. If the fluorination does not occur radically, then the reaction shown in entry 3 should give yields that are comparable to what is shown in entry 1, despite the addition of TEMPO after five hours. Conversely, if the fluorination does occur radically, then we would expect the addition of TEMPO at hour five would stop further productive reaction and give yields closer to what is shown in entry 2. To our pleasure, entry 3 yielded very similar results as entry 2, indicating that the reaction is likely to occur radically. Further HR-MS analysis determined that our reaction occurs radically as we were able to find evidence for TEMPO trapping the substrate benzylic radical, (Table 2-5).

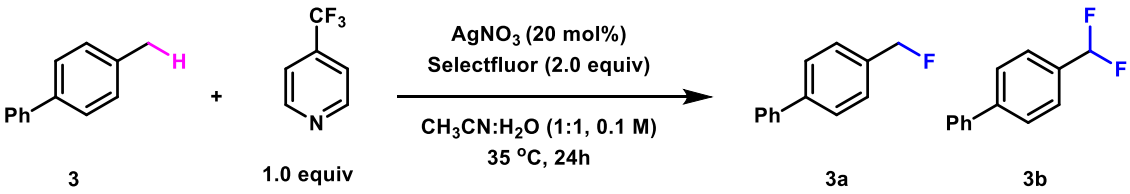

3 1.0 equiv 3a 3b

entry	deviation from standard conditions	time (h)	NMR yield (%)	
1	none	24	12	85
2	globally quenched after 5 hours	5	37	00
3	TEMPO (1.0 equiv) added after 5 hours	22	34	00

Table 2-4. NMR Yields of TEMPO Radical Trapping Experiments.

Compound	Structure	Calculated (m/z)	Found (m/z)
oxoammonium derivative of TEMPO	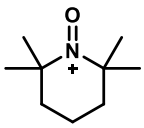	156.1383	156.1379
4-methylbiphenyl radical trapped by TEMPO	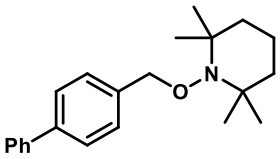	[M]+1 324.2322	[M]+1 324.2311
Diazobicyclo radical derivative of Selectfluor trapped by TEMPO	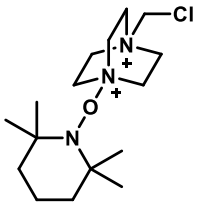	158.6111	not found

Table 2-5. HR-MS Analysis of TEMPO Radical Trapping.

2.2.2. Experimental Investigation of the Role of Pyridine Additives

2.2.2.1. Electronic Influence

The cyclic voltammetry data and the counterintuitive pyridine-dependent product distribution led us to believe that the role of the pyridine additives with the Ag(I) catalyst was not its dominant role. To ensure that the pyridine additives were not simply contributing to the reaction via an acid/base mechanism, we ran a reaction where Hünig's base (diisopropylethylamine) was used as the Lewis basic free nitrogen additive instead of a pyridine. No fluorinated product was observed. We then contemplated the fate of Selectfluor in the presence of the pyridine additives. Using *in situ* ReactIR, the consumption of Selectfluor in the presence of each of the pyridine additives was monitored. The concentration of Selectfluor was determined by the relative intensity of the N–F bond of Selectfluor. Upon addition of the 4-R-pyridine additives, the concentration of Selectfluor decreased when R = H and OCH_3, with the latter consuming Selectfluor more rapidly. However, when R = CO_2Et and CF_3, no significant consumption, if any, of Selectfluor was observed. This may be a suitable explanation as to why the yield of fluorinated products is much lower when in the presence of a more electron-rich pyridine. The electron-rich pyridines unproductively consume Selectfluor, which was also supported by the formation of fluoride anion seen in the ^{19}F NMR for those experiments. A direct correlation between the electronics of the pyridine additives and the initial rate of consumption of Selectfluor was observed, where that of 4-methoxypyridne was the greatest, followed by pyridine, ethyl isonicotinate, and then 4-trifluoromethylpyridine. Under standard reaction conditions, the initial rate of consumption of Selectfluor for ethyl isonicotinate and 4-trifluoromethylpyridine was notably slower than that of either 4-methoxypyridine and pyridine, but their global consumption of Selectfluor proved to be greater, explaining the higher yields observed (Figure 2-2). It was evident that the pyridine additives played a significant role in its interaction with Selectfluor, contributing to the breaking of the N–F bond.

The onset reduction potential of Selectfluor was then investigated. It was found that in the presence of the pyridine additives, the reduction potential of Selectfluor was decreased (Table 2-6). A general trend was observed across the pyridines, where the more electron-poor pyridines seem to perturb the reduction potential of Selectfluor more significantly, leading to a more facile cleavage of the N–F bond. We began contemplating the idea of halogen bonding between the nitrogen of the pyridine additives and the fluorine of Selectfluor, in such a way that it generated an $[N–F–N]^+$ complex (**19**). There was a possibility that an *N*-fluoropyridinium intermediate may have been formed and was the species that performed the fluorination. However, no fluorinated product was observed from a reaction using *N*-fluoropyridinium as the fluorine source instead of Selectfluor, suggesting the unlikelihood of the *N*-fluoropyridinium intermediate behaving as the fluorinating agent. It should be noted that while the *N*-fluoropyridinium species is not likely the fluorinating agent, it does not rule out the possibility of the formation of such species as a byproduct.

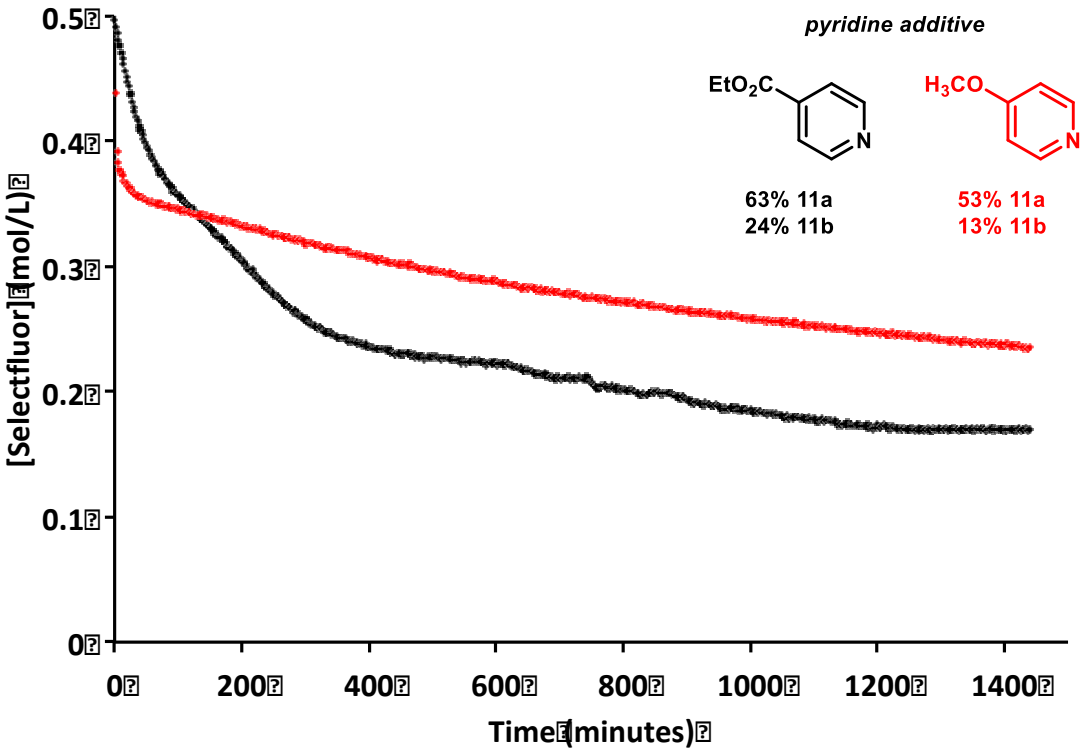

Figure 2-2. ReactIR Spectra of Selectfluor Consumption in the Presence of Pyridine Additives. ReactIR trend plot for N–F bond of Selectfluor at ~1008 cm^{-1}. Standard reaction conditions were used. Yields reflect NMR yields.

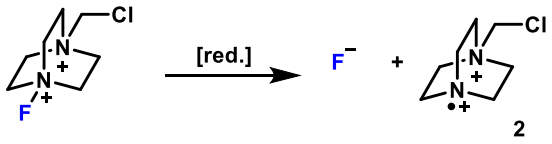

pyridine additive	*E^o (V)*
none	-1.49
4-R-pyridine	----------
R = OCH_3	-1.32
R = H	-1.29
R = CO_2Et	-1.40
R = CF_3	-1.33

Table 2-6. Experimentally Determined Reduction Potentials of Selectfluor in the Presence of Pyridine Additives.

In efforts to obtain more direct evidence of the proposed $[N–F–N]^+$ halogen-bound complex, ^{19}F NMR spectroscopy was considered. However, spectroscopic and theoretical work done by Erdelyi, indicate that ^{19}F NMR spectroscopy was not a good method due to the lack of significant differences in chemical shifts between unbound fluorines and pyridine halogen-bound fluorines.[40] In that work, Erdelyi also established pyridines as halogen bond acceptors, and showed the effects of the pyridine electronics on the halogen bonding event through ^{15}N NMR spectroscopy. Our *in situ* NMR spectroscopic studies under synthetic conditions aligned with Erdelyi's findings where ^{19}F NMR chemical signals for Selectfluor's $[F–N]^+$, *N*-fluoropyridinium, and Selectfluor in the presence of the different pyridine additives showed negligible differences (Table 2-7). We were able to observe significant changes in pyridine ^{15}N chemical shifts through $^{1}H/^{15}N$ HMBC. For all pyridines studied, the ^{15}N signal shifted to more negative values in the presence of Selectfluor, which is consistent to the generation of "pyridinium-like" intermediates. When in the presence of Selectfluor, 4-methoxypyridine exhibited a chemical shift of greater than 50 ppm along the ^{15}N axis, appearing as a series of broad signals correlated to the line broadening of the C-2 ^{1}H NMR signal (Figure 2-3). Additionally, the ^{1}H NMR spectra for 4-methoxypyridine in the presence of Selectfluor shows signals that suggests the presence of trace amounts of an *N*-fluoro-4-methoxypyridinium species, further supporting the idea of direct interaction between pyridine nitrogen and fluorine of Selectfluor.

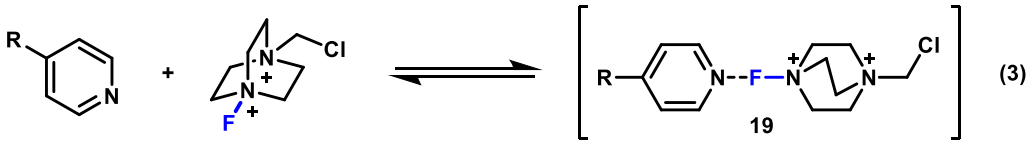

(3)

R	^{15}N	^{1}H (C–2)	^{15}N	^{1}H (C–2)	^{19}F
CF_3	-52.98	8.34	-55.34	8.31	50.43
CO_2Et	-52.16	8.26	-54.04	8.21	50.46
H	-64.29	8.09	-68.01	8.05	50.44
OCH_3	-86.89	7.88	-136.87*	7.85	50.40

Table 2-7. $^{1}H/^{19}F/^{15}N$ NMR Chemical Shifts of Pyridines and Selectfluor Independently and as Halogen Bound Complexes.

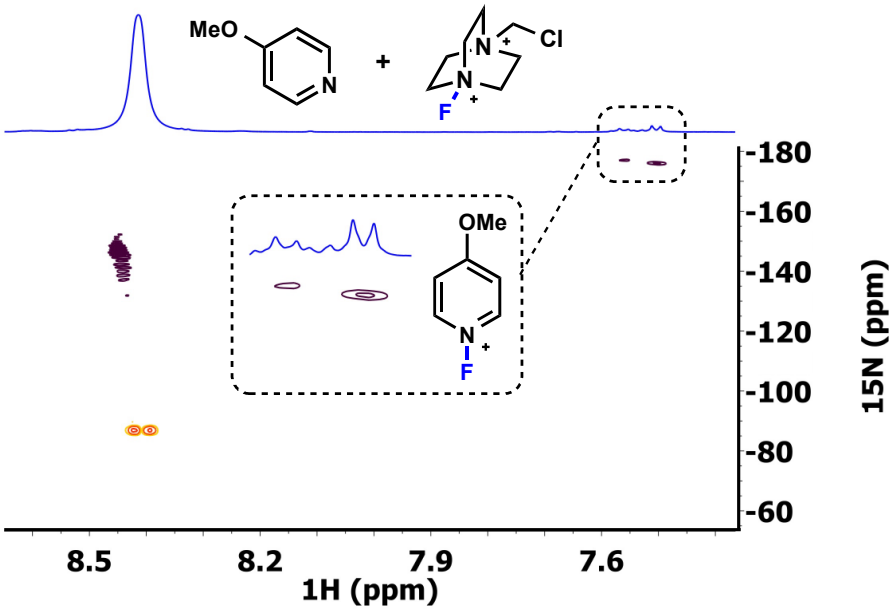

Figure 2-3. $^{1}H/^{15}N$ Coupled HMBC Spectra of Selectlfuor with and without 4-Methoxypyridine. 4-methoxypyridine alone (orange) and with Selectfluor (purple). Conditions: 4-methoxypyridine (0.1 mmol,) Selectfluor (0.1 mmol), in 700 uL CD_3CN at 25 °C.

2.2.2.2. Steric Influence

A brief investigation into steric hinderances of the pyridine additive was conducted. As shown in Scheme 2-3, looking specifically at **20** and **21**, adding a simple methyl group adjacent to the nitrogen atom, the yield of fluorinated product decreases. When two methyl groups are on either adjacent positions to the nitrogen atom, no fluorinated product is observed (**22**). A drastic decrease in fluorination is observed between **23** and **24**. Again, no product is observed when both sites adjacent to the nitrogen atom is substituted (**25**). It is possible that the steric hinderance may be affecting the ligation of the pyridine derivatives to the Ag(I). However, Ag(I) is known to coordinate well with ligands such as 2,2-bipyridyl and phenanthroline, which arguably are more hindered and provide a small pocket for the Ag(I). The steric hinderances of the pyridines disrupts the halogen bonding with the fluorine of the Selectfluor. Halogen bonding events are known to occur at bond angles of 180°.[36b] The substituents disrupts this linearity of the electrostatic interaction, justifying the trends observed in Scheme 2-3. While a single adjacent substituent can still afford fluorinated products, it does so at significantly decreased efficiency. The addition of a second substituent to the remaining adjacent site distances the pyridine enough so that is unable to participate in halogen bonding, and therefore no fluorinated product is observed. Further analytical and computational studies are necessary to understand the extent of steric effects of pyridine additives towards halogen bonding.

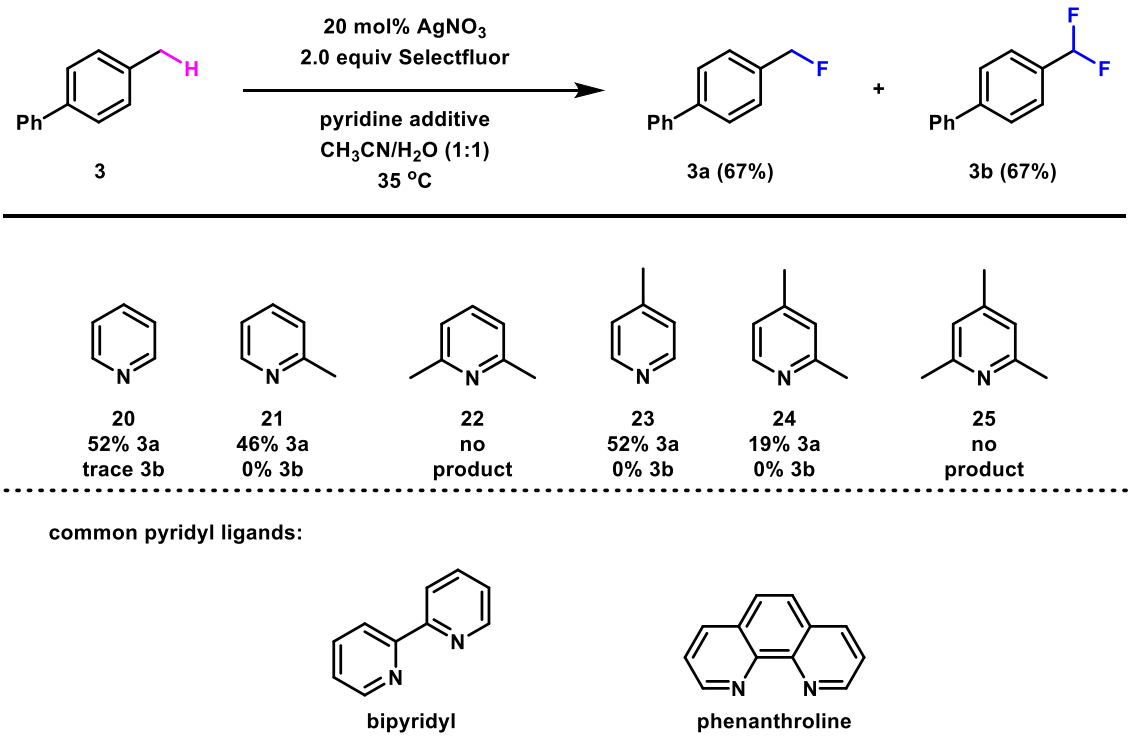

Scheme 2-3. Exploring the Steric Effects of the Pyridine Additives.

2.2.3. Computational Investigation

Our colleagues in the Hratchian Lab carried out theoretical investigations to determine the ligation of the pyridines to Ag(I) and the likelihood of halogen bonding between the nitrogen atom of the pyridines and the fluorine of Selectfluor. Calculations were done with B3PW91/6-311+G(d) model that accounted for implicit solvation by acetonitrile using a local development of Gaussian.[41] The oxidation potentials calculated for Ag(I) indicated that bis-pyridine Ag(I) species is the likely reductant that initiates the radical fluorination. The theoretical values were generally consistent with those obtained experimentally through cyclic voltammetry, confirming that the onset oxidation potential of Ag(I) is lower in the presence of electron rich pyridines (Table 2-8).

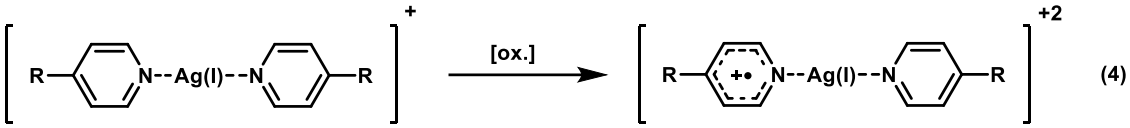

(4)

R Group	E^o experimental (V)	E^o calculated (V)
OCH_3	1.24	2.04
H	1.31	2.08
CO_2Et	1.54	2.20
CF_3	1.60	2.27

Table 2-8. Experimental and Computational Oxidation Potential of Ag in the Presence of Pyridines.

In modelling the halogen bonding event, preliminary data suggested the density functional theory (DFT) calculations both with and without empirical dispersion corrections were unable to treat the physics of the $[N–F–N]^+$ halogen bound complex (**19**). Benchmark reports by Martin and Wong[42] indicate that only a limited set of approximate functionals can predict halogen bonding strengths. It was suspected that the DFT calculations failed because of the exceptionally electron deficient characteristics of the $[N–F–N]^+$ motif. Alternatively, correlated wave function methods were assessed. The geometries of the halogen bound species candidates were optimized using MP2/6-311+G(d) theory. Single-point energies were evaluated with CCSD(T)/6-311+G(d) model including implicit solvation. The calculations indicated that the halogen bound complex are slightly higher in energy than the unbound species (<1–4 kcal/mol) (Table 2-9, eqn 1). However, calculations did show that the subsequent reduction from **2** to be favorable (Table 2-9, eqn 2).

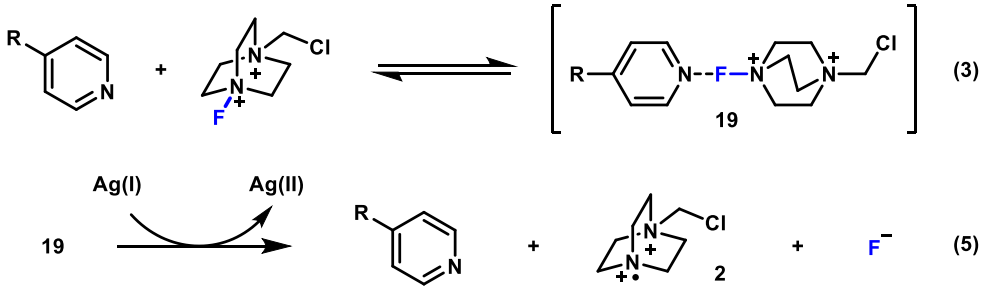

R Group	ΔH1 (kcal/mol)	ΔH2 (kcal/mol)
OCH_3	0.34	-31.42
H	0.74	-31.82
CO_2Et	3.63	-33.66
CF_3	2.57	-34.71

Table 2-9. Computational Data Trends for Selectfluor-Pyridine Halogen Bond.

Computational data indicated that electron rich pyridines were more effective halogen bond acceptors than the electron poor pyridines. This is in agreement with our NMR spectral data in Table 2-7. Interestingly, there were no significant differences in calculated bond lengths for either of the N–F bonds (1.84 Å) when bound in the complex. The complexes with the different pyridines each exhibited a linear bond angle. To our delight, the calculated reduction potential of the $[N–F–N]^+$ complex was shown to be most favorable when the pyridine is most electron poor, which correlates with and rationalizes our experimental reactivity trends shown in Scheme 2-2. Calculations were also done to explore other possible binding interactions. It was determined that no other suitable geometry existed other than the proposed $[N–F–N]^+$ linear complex. The chlorine of Selectfluor does not participate in halogen bonding with the pyridines. Additional calculations were done with water to mimic synthetic conditions and to determine if there were any mixed hydrogen/halogen bonding network. The inclusion of discrete water molecules into the $[N–F–N]^+$ complexes did not result in any meaningful structures, suggesting that the reactivity trends in Scheme X are a result of the pyridine nitrogen directly interacting with the fluorine of Selectfluor.

2.2.4. Proposed Mechanism

As we began contemplating about the mechanism of our system, we recognized the possibility that the reduction of Selectfluor could occur independently of the halogen bonding effect with the pyridine additive. As shown, the pyridine additive is necessary for the reaction to occur (Table 2-2, entry 16). And as previously discussed, the pyridine additive has two roles in which it facilitates the reaction: (1) ligation to the Ag(I) catalyst, and (2) halogen bonding to Selectfluor. In the first case, as supported by experimental cyclic voltammetry and theoretical calculations, the pyridine additive ligates to Ag(I), lowering the oxidation potential of Ag(I). It is believed that this decrease in oxidation potential of Ag(I) is what leads to the initiation of the radical fluorination. The pyridine-ligated Ag(I) catalyst would more easily give an electron into the N–F bond of Selectfluor, releasing a fluorine and generating **2**. **2** should then be able to abstract the benzylic hydrogen atom from the substrate, and subsequent fluorination would occur. Theoretically, the fluorination could occur without any halogen bonding interaction between Selectfluor and the pyridine additive (highlighted in Scheme 2-4).

To probe this, we first ran reactions in which the pyridines were added in catalytic amounts, at twice the loading of $AgNO_3$. We thought that the bis-pyridine ligated Ag(I) catalyst would form *in situ* and initiate the reaction. However, no reaction was observed. We wondered if the concentrations of the pyridine and $AgNO_3$ was in such low concentrations as compared to the global reaction concentration that the pyridines were unable to ligate with the Ag(I) in sufficient amounts or even at all. We then synthesized the precoordinated bis-pyridine Ag(I) catalysts, following the literature preparation reported by Hii and coworkers.[43] Because the oxidation potential of Ag(I) was most affectively lowered by 4-methoxypyridine, and therefore should be the best precoordinated catalyst to reduce the Selectfluor N–F bond, we started with the $Ag(I)[4\text{-OMePyr}]_2$

catalyst. The Ag(I)[4-OMePyr]$_2$ catalyst was subjected to our reaction conditions in the absence of additional pyridine additives. No reaction was observed. We contemplated the fate of the 4-methoxypyridine ligands and explored the possibility of dissociation. If dissociation of the pyridine ligands was occurring in solution, then it would provide some explanation as to why no reaction was observed. HMBC of the Ag(I)[4-OMePyr]$_2$ catalyst was taken immediately upon introduction to solvent. The same sample was left to stand for a week before another HMBC was taken. No significant changes were observed in the chemical shifts, indicating that dissociation was not likely occurring. These results indicated that the reaction was driven by the pyridine additives via halogen bonding with Selectfluor. However, this does not discredit the role that the pyridine additive has with the Ag(I) catalyst. We believe that while the pyridine ligands lowered the oxidation of the Ag(I) catalyst, it simply was not enough to reduce the Selectfluor N–F bond without the assistance of halogen bonding.

As shown in Scheme 2-4, we have proposed that the pyridine additive participates in both the halogen bonding with the Selectfluor, forming a [N–F–N]$^+$ complex, and as ligands for Ag(I). The pyridine-ligated Ag(I) catalyst participates in the single electron reduction of the halogen bound Selectfluor N–F bond, releasing a fluoride and generating **2**. **2** abstracts a benzylic C–H hydrogen atom from the substrate, generating a benzylic radical. The benzylic radical then takes a fluorine atom from another molecule of Selectfluor, regenerating **2** as the catalytic HAT species.

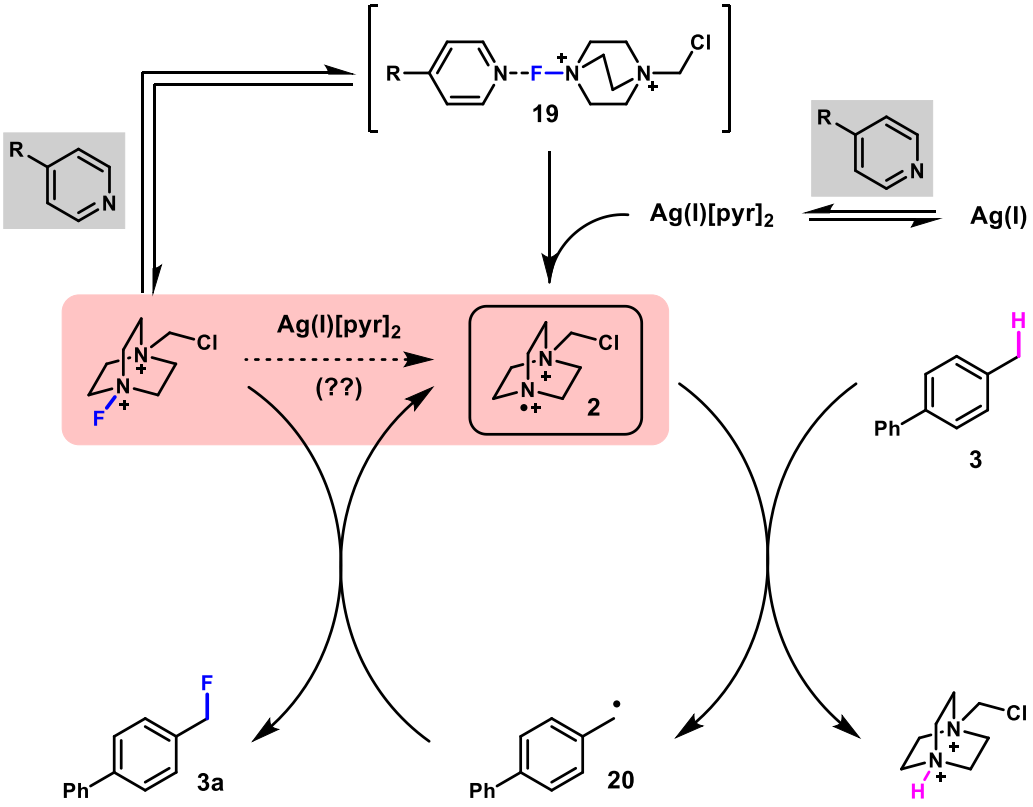

Figure 2-4. Proposed Mechanism for Pyridine-Mediated Halogen Bonding Radical Fluorination.

2.3. Summary of [N–F–N]$^+$ Halogen Bonding between Pyridines and Selectfluor

In summary, we have developed a method in which radical benzylic fluorination is facilitated by a halogen bonding event between the nitrogen of a pyridine additive and the fluorine–nitrogen of Selectfluor. The electronic characteristics of the pyridine contributes immensely to the product distribution, where mono- or di-fluorinated products can be favored as the major product. We have experimental and computational data to support the idea of halogen bonding and rationalize the proposed mechanism by which this reaction occurs. While we are not the first to propose such an interaction between pyridine and Selectfluor, our work does represent the most direct experimental and analytical evidence for a transient halogen bond between Selectfluor and pyridines, which would have the potential for modulating other single electron events. Our lab has developed a metal-free Minisci reaction which is thought to rely on a transient halogen bound intermediate. Additionally, our lab has been able to observe both bromination and chlorination which also relies on the transient halogen bound intermediate. The electronic characteristics of the pyridine additives seem to behave analogously to what was observed for this radical fluorination work. This is significant to note because the successful installation of halogens onto aryl molecules have potential significance in organic chemistry, where there are possibilities of cross-coupling transformations, among others, between molecules that may have not existed before.

This work has also inspired us to seek a better *N*-centered HAT agent to allow for hydrogen abstraction from bonds where their BDE was likely an enthalpic barrier that **2** was unable to overcome, limiting our fluorination to benzylic sites. Our goals and preliminary data on this topic are discussed in Chapter 3 of this dissertation.

C H A P T E R 3

Novel Nitrogen-Centered Radicals as Hydrogen Atom Transfer Agents

3.1. Introduction

3.1.1. Hydrogen Atom Transfer

By definition, HAT is a concerted movement of a hydrogen and a single electron between two substrates in a similar fashion that S_N2-type reactions occur (Scheme 3-1, eqn 6).[44] Two general considerations should be made when thinking of HAT: (1) the BDE of the Y–H bond of the hydrogen atom donor, (Y = any reasonable atom); (2) the polarity match of both the hydrogen atom donor and acceptor (also known as a hydrogen abstractor). As previously discussed in Chapter 1 of this dissertation, BDE is an enthalpic barrier. In efforts to conceptualize HAT barriers, Mayer established a systematic

evaluation method using both experimentally observed and theoretically calculated BDEs in a Marcus Theory approach.[45] Additionally, the polarity of the hydrogen atom donor should be considered in relation to the proposed hydrogen acceptor. Like an S_N2 reaction, if the hydrogen atom donor is more nucleophilic-like, then the hydrogen acceptor should be more electrophilic-like, and vice versa (eqn 7–8). If the polarity of the hydrogen atom donor and acceptor are "mismatched," then HAT would likely not occur, regardless of the BDE of the donor (eqn 9–10). Likewise, if the BDE is too high, HAT will likely not be observed despite a polarity match between the hydrogen donor and acceptor.

However, hydrogen donors with higher BDEs may still be accessible by HAT by choosing a hydrogen acceptor that is very strongly polar from the donor. For example, in equation **7**, if the BDE of electrophilic hydrogen donor was high, it may undergo HAT in the presence of an acceptor that is far more nucleophilic than the donor is electrophilic. In the case of polarity mismatch, there are catalysts that can be used to "reverse" the polarity. Polarity reversal catalysts (PRCs) do not actually affect the polarity of either the hydrogen donor or acceptor.[46] PRCs serve as a "middleman" between a nucleophilic hydrogen donor and a nucleophilic acceptor, being just more electrophilic than both the donor and acceptor (eqn 11–13).

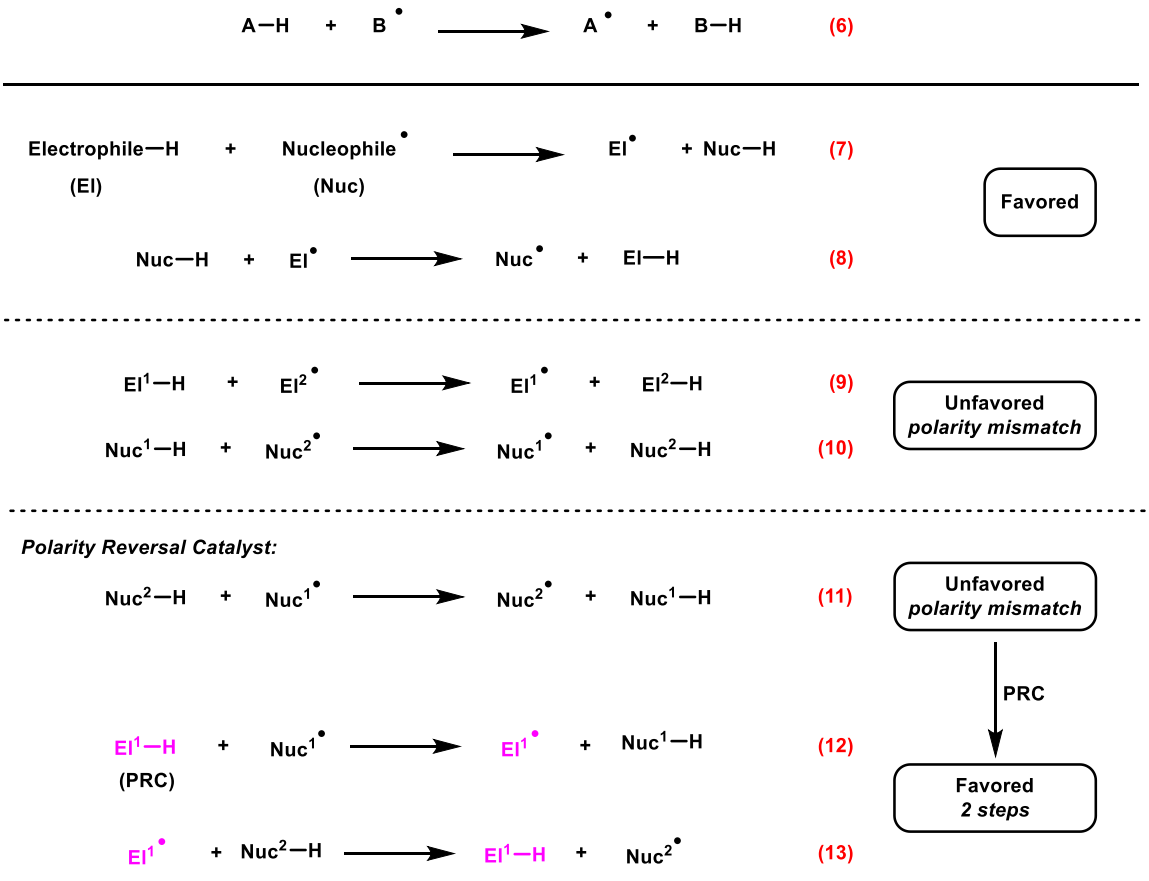

Scheme 3-1. General Hydrogen Atom Transfer Concept.

The issue we faced in both of our radical fluorination methods does not have to do with the hydricity of the transferring hydrogen atom, but the strength of the hydrogen abstractor. We were limited to benzylic substrates. In hopes to overcome this limitation, we sought to identify other HAT agents that may allow us to expand our substrate scopes. In the unprotected amino acids Ag(I)/Ag(II) system (Chapter 1), there were two viable hydrogen abstractors: **2** and the α-aminoalkyl radical. In the pyridine-Selectfluor halogen bonding system, **2** was the hydrogen atom abstractor. Neither **2** nor the α-aminoalkyl radical were nucleophilic enough to break C–H bonds other than benzylic ones. While there are several different types of hydrogen atom abstractors, this chapter will focus on nitrogen-centered radicals as hydrogen atom abstractors.

3.1.2. Nitrogen-Centered Radicals

It should be noted that nitrogen-centered (*N*-centered) radicals, as with any other products of organic chemistry bond cleavage, comes in two categories: neutral and ionic. The electronic characteristics alter the physical and chemical properties of the *N*-centered radicals, facilitating a wide variety of transformations.

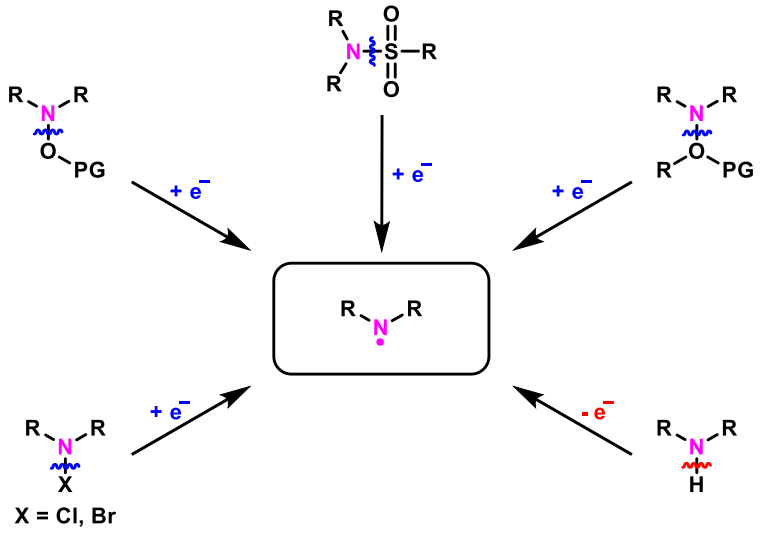

Scheme 3-2. General Methods to Access Neutral *N*-Centered Radical.

Neutral *N*-centered radicals are typically accessed via reductive cleavage of bonds such as N–O, N–N, N–S, N–X (Scheme 3-2).[47] However, the typical conditions for achieving neutral *N*-centered radicals are not compatible with functional groups and require installation of protecting groups (Scheme 3-3, a-c). As shown in Scheme 3-3, neutral *N*-centered radicals achieved via single electron reduction include acidic conditions (a), very low temperatures and specialized catalysts (b), precious metal catalysts (c-d), and even activating groups and leaving groups installed on the nitrogen atom (d). Neutral *N*-centered radicals may also be achieved by oxidative cleavage of an

N–H bond at elevated temperatures and under stoichiometric amounts of strong oxidants such as Dess-Marin periodinane, 2-iodoxybenzoic acid, and di-*tert*-butyl peroxide. Again, the tolerance of functional groups is vastly hindered by these conditions.

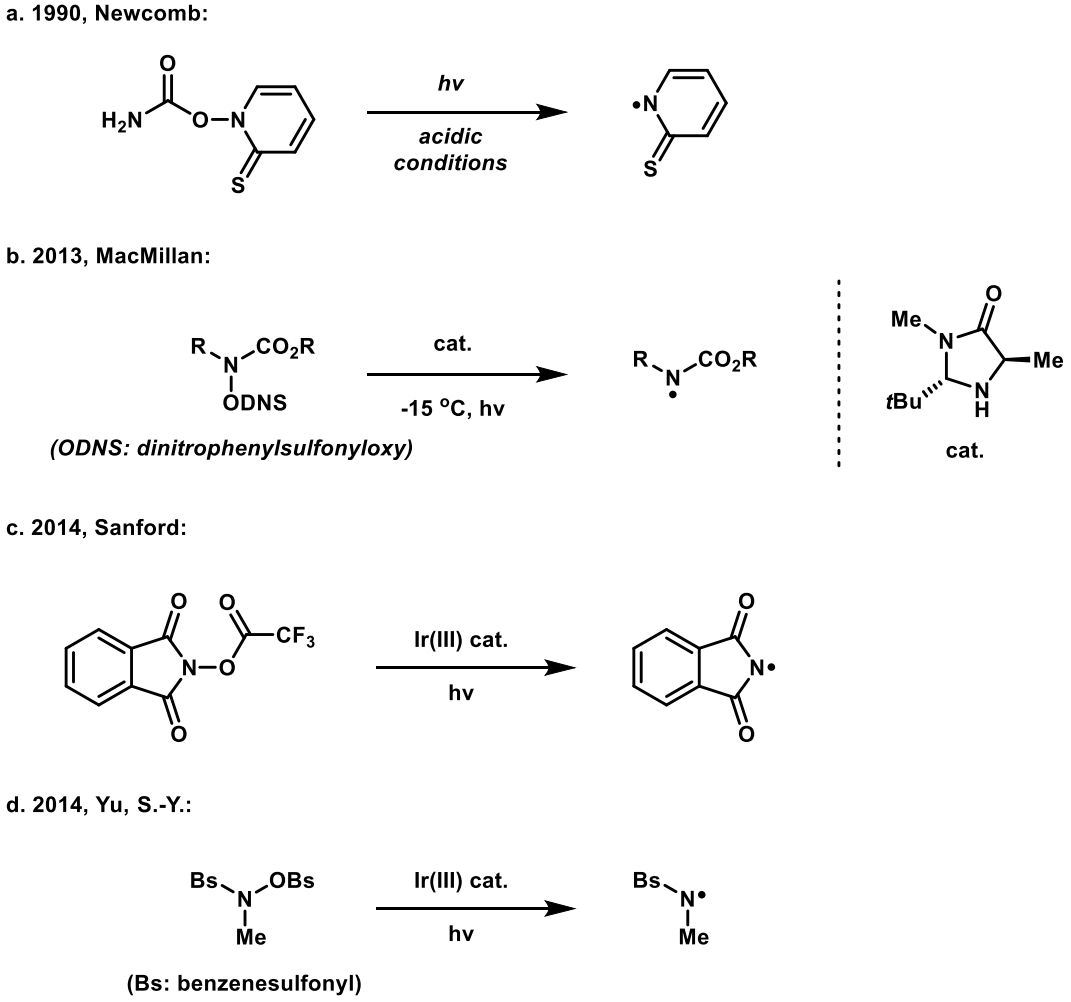

Scheme 3-3. Examples of Neutral *N*-Centered Radicals Derived from N–O Bonds.[48]

As previously mentioned, *N*-centered radicals can also be ionic, typically possessing a positive charge. These cationic *N*-centered radicals are commonly known for their wide application in forming C–N bonds.[47,48] There are two common modes of accessing cationic *N*-centered radicals: (1) via a radical initiator; (2) via a photocatalytic initiator. Photocatalytically generated cationic *N*-centered radicals has been prevalent in much of recent literature; however, the photocatalysts typically used are of precious metals, such as Ir(III), Ru(II), and in some methods a catalytic couple between Ru(II) and Pd(II) (Scheme 3-4, a).[48] While they are commonly used in organic chemistry, and are used in amounts as low as 2 mol%, the use of precious metals is costly due to their low abundance, and are relatively toxic.[49] Inspired by the current work of a colleague within our lab, who is developing a method to access *N*-centered radicals through photolytic cleavage in the

absence of precious metal catalysts, we sought out to design a cationic *N*-centered hydrogen atom abstractor that could be similarly accessed (Scheme 3-4, b). Of the cationic *N*-centered radicals shown in Scheme 3-4, c, **25** and **2** have been demonstrated as HAT agents, while the others typically perform amination either in the form of cyclization, or addition into olefins or aromatic rings (**21**–**24**).[28] **2** was the HAT agent within our previously discussed system. Because it was a well-behaved HAT agent, we wanted to electronically modify **2** in hopes of expanding the scope of hydrogen atom donors. We also had interests in accessing **24** via photolytic cleavage of *N*-nitrosopyridinium type species, which we also hope to be able to modify the electronic characteristics of by using readily available 4-R-pyridines.

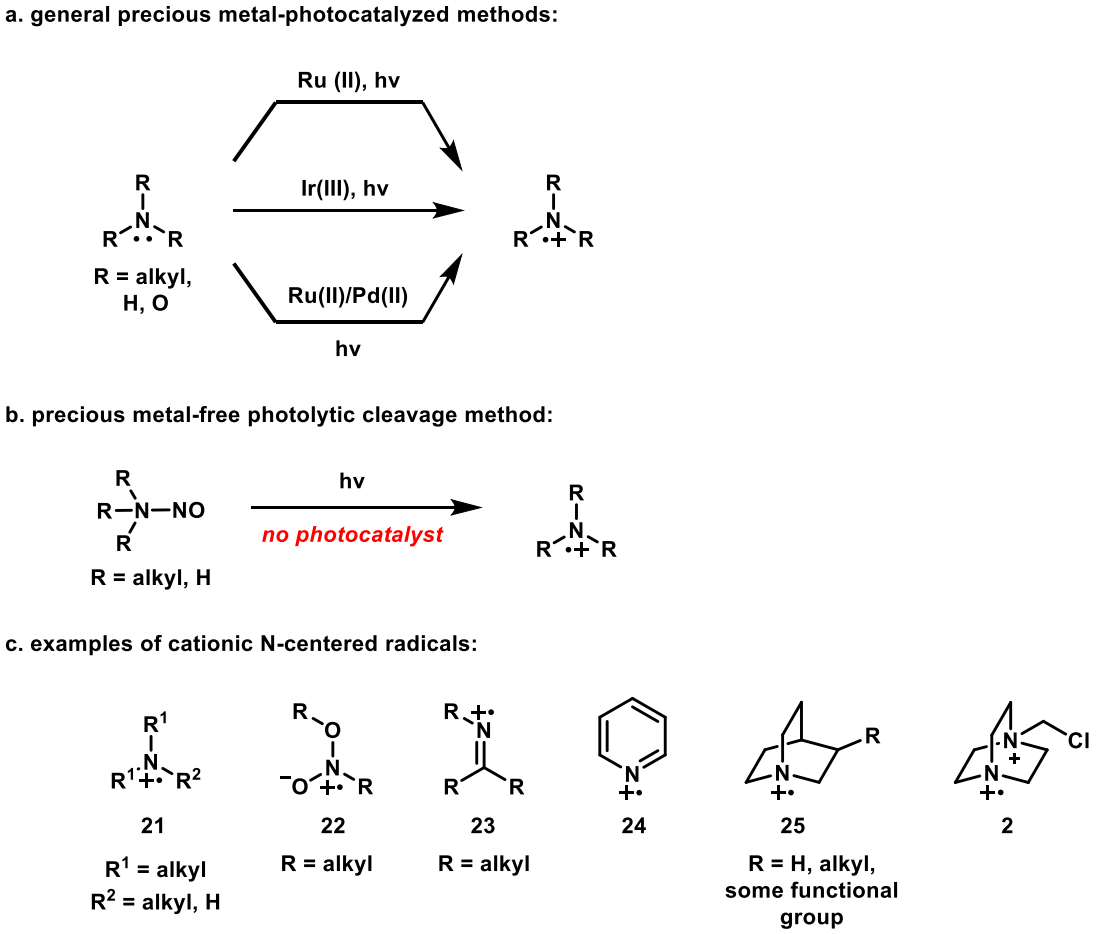

Scheme 3-4. Examples and Methods to Iminium Cation Radical Species.

3.2. Proposed Study

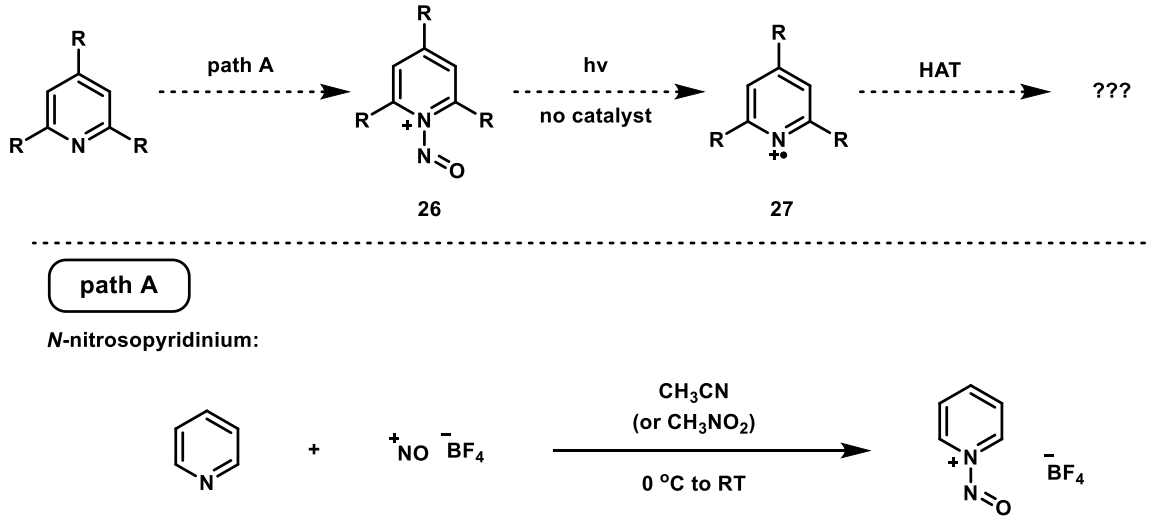

Scheme 3-5. Proposed Pyridinium Cationic *N*-Centered Radical as HAT Agent.

Despite it being known for aryl amination, we had contemplated the possibilities of using a pyridinium *N*-centered radical as a possible HAT agent because the work done by Kochi and coworker in 1992 demonstrated the utility of sterically hindered pyridinium (2,6-dimethyl-*N*-nitropyridinium) as a nitration agent rather than an aryl amination agent.[51] We contemplated the fate of the sterically hindered pyridinium radical (**27**) and wondered if we could tune it both electronically and sterically to perform HAT rather than aryl amination, or nitration. As shown in Scheme 3-5, we propose the transformation of a pyridinium into an *N*-nitrosopyridinium, using the method presented by Overchuk and coworkers in 1965.[50]

2 has been proven to be a viable HAT agent in our previous work and the work of others.[28] We wanted to explore electronic diversity of **2** as we contemplated the design of a more electrophilic novel HAT agent. As shown in Figure 3-3, the electron affinity of **2** would suggest that it is a better hydrogen atom abstractor in relative comparison to others. We wanted to design a hydrogen atom abstractor that would have a stronger electron affinity and have proposed to functionalize 1,4-diazabicyclo[2.2.2]octane (**2**) at both nitrogen sites, similarly to Selectfluor. To make a more electrophilic HAT agent, one of the nitrogen atoms (N^1) will be functionalized with some electron withdrawing group (EWG) (Scheme 3-6, Path A). As previously stated, we wanted to nitrosylate the nitrogen that would become the cationic *N*-centered radical (the hydrogen atom acceptor, N^2) (Scheme 3-6, Path B). Because the stability and tolerance of a quaternary nitrosaminium species in the conditions required to functionalize the N^1 is uncertain, we decided to proceed with Path A first. We contemplated the possibility of installing an EWG such as 2,4-dinitrobenzene via nucleophilic aromatic substitution (S_NAr). We also looked into different methods by which we could install an EWG to tertiary amines, and came across

the Menshutkin reaction.[53] While it was our hope to have the EWG be directly alpha to the N^1-nitrogen atom to give the strongest electronic effect, literature regarding the Menshutkin reaction only demonstrated installation in the beta position and further from nitrogen atom. A couple of other methods to install an EWG involved brute force, such as high pressure and elevated temperatures.

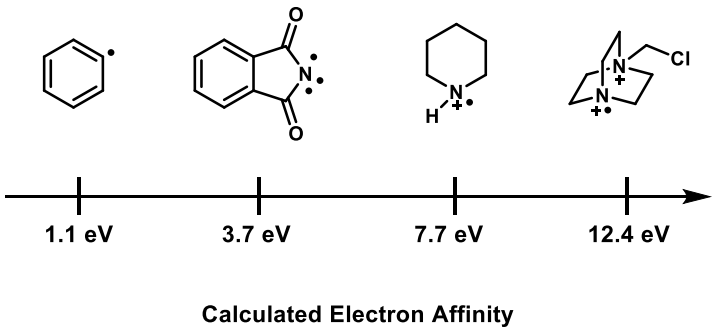

Figure 3-1. Relative Electron Affinity as Calculated by Ritter.[52]

We then assessed the possibilities of nitrosylation of the N^2 of DABCO. While reports in literature do not show successful nitrosylation of tertiary amines, we contemplated the possibilities of applying those methods to our tertiary amine substrate with plans to adjust conditions as necessary. As shown for Path B, there are a few possible routes to achieve nitrosylation. The last method shown requires $SnCl_4$, which fumes at ambient atmosphere and is highly toxic, thus, will be left as a last resort attempt for those reasons. We plan to approach this design in two ways: (1) by first installing the EWG and then nitrosylate (Path A followed by Path C); (2) nitrosylate and then installing the EWG (Path B followed by Path D, where Path D). Once we have achieved the di-functionalization of DABCO, it is our hope that *in situ* photolytic cleavage of the nitroso group is successful, generating our desired cationic *N*-centered radical. Our plan is to take a UV-vis spectrum of **29** to determine the wavelength at which the N–NO bond should cleave. Once a narrow range of wavelength has been determined, we would irradiate **30** and probe the resulting reaction mixture for **31**, nitrate and nitrite. The presence of these species would suggest the photolytic cleavage of the nitroso group is possible. This will help us determine if the photolytic cleavage is even possible before we try to put **30** into a system where there are too many variables to understand how/why the reaction works or fails.

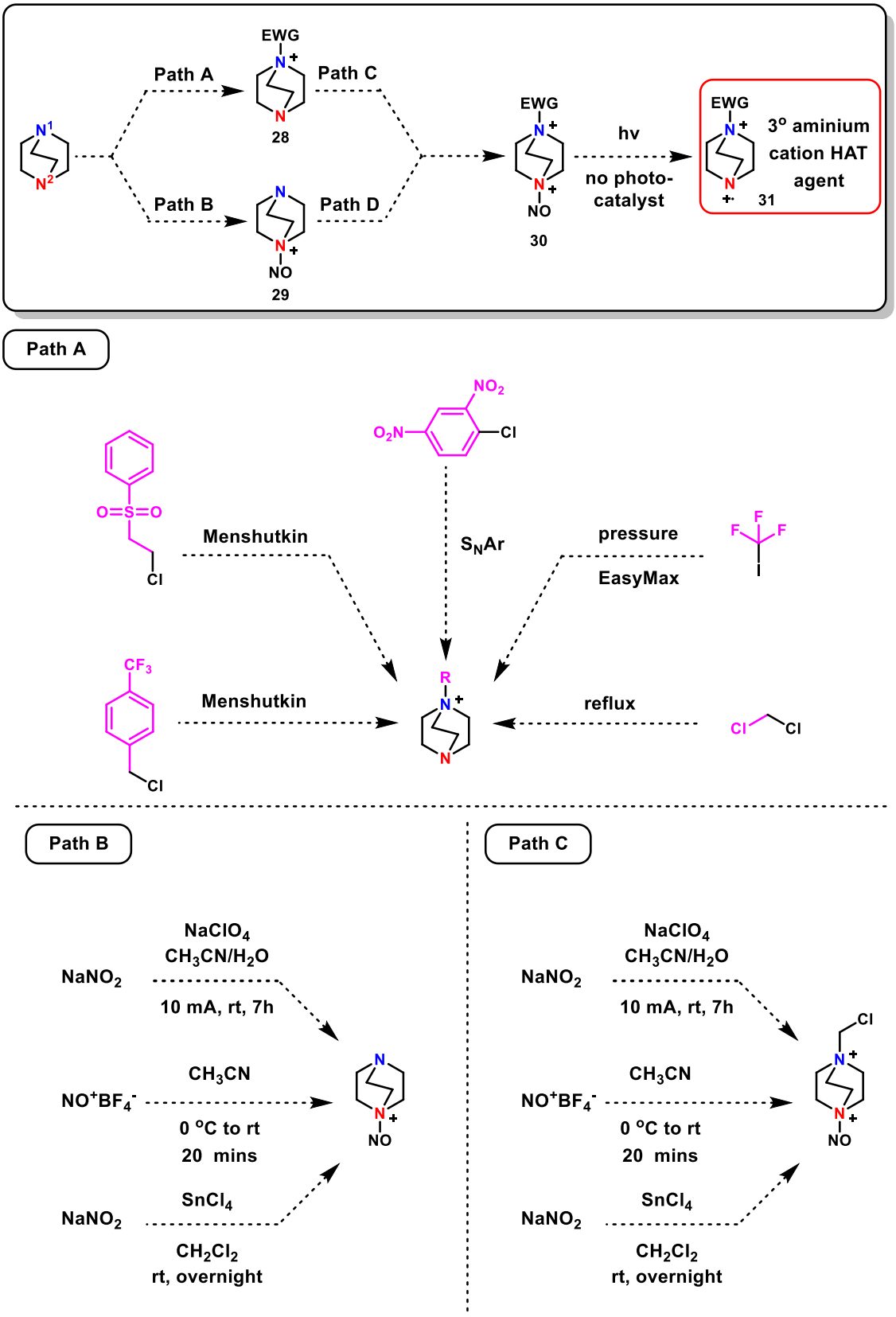

Scheme 3-6. Proposed Work: Development of a Novel HAT Agent.

3.3. Results and Discussion

3.3.1. Preliminary Results of Novel Nitrogen-Centered Radical Precursors

Based on the physical observations and descriptions given by Overchuk and coworkers regarding the reaction progress, we have reasons to believe the nitrosylation of the pyridine was successful under inert atmosphere. However, upon subjecting the reaction mixture to work-up, the reaction solution changed colors drastically, which we suspect may be due to the product's sensitivity to both air and moisture, like the nitrosylating reagent. ^{1}H and ^{13}C NMR analysis of the crude reaction mixture taken after reaction work-up were inconclusive, showing no signals for the desired product. We then decided to rerun the reaction under a Schlenk line. However, upon quenching and work-up, it seemed that the reaction mixture was susceptible to air and/or moisture. While the color change was noticeably more gradual this time, we still observed the same drastic color change. HR-MS was quickly taken to see if we could find any traces if desired product. Trace amounts of the desired product mass was detected. However, subsequent NMR analysis showed no signs of desired product. This affirmed the instability of our desired *N*-nitrosopyridinium species. Alternatively, the reaction could be run under a Schlenk line and then transferred to a glovebox for inert handling during the reaction quenching and work up, or the reaction can be set up, ran, and worked up all within the glove box. Additionally, our solvents were not rigorously dried, as only activated mole sieves were used to remove moisture. Freeze-pump-thaw may be better alternative to prepare our solvents and rigorously remove both air and moisture. While these are all possible "fixes" for our reaction to obtain the *N*-nitrosospyridinium, it also diminishes the ease of our proposed work.

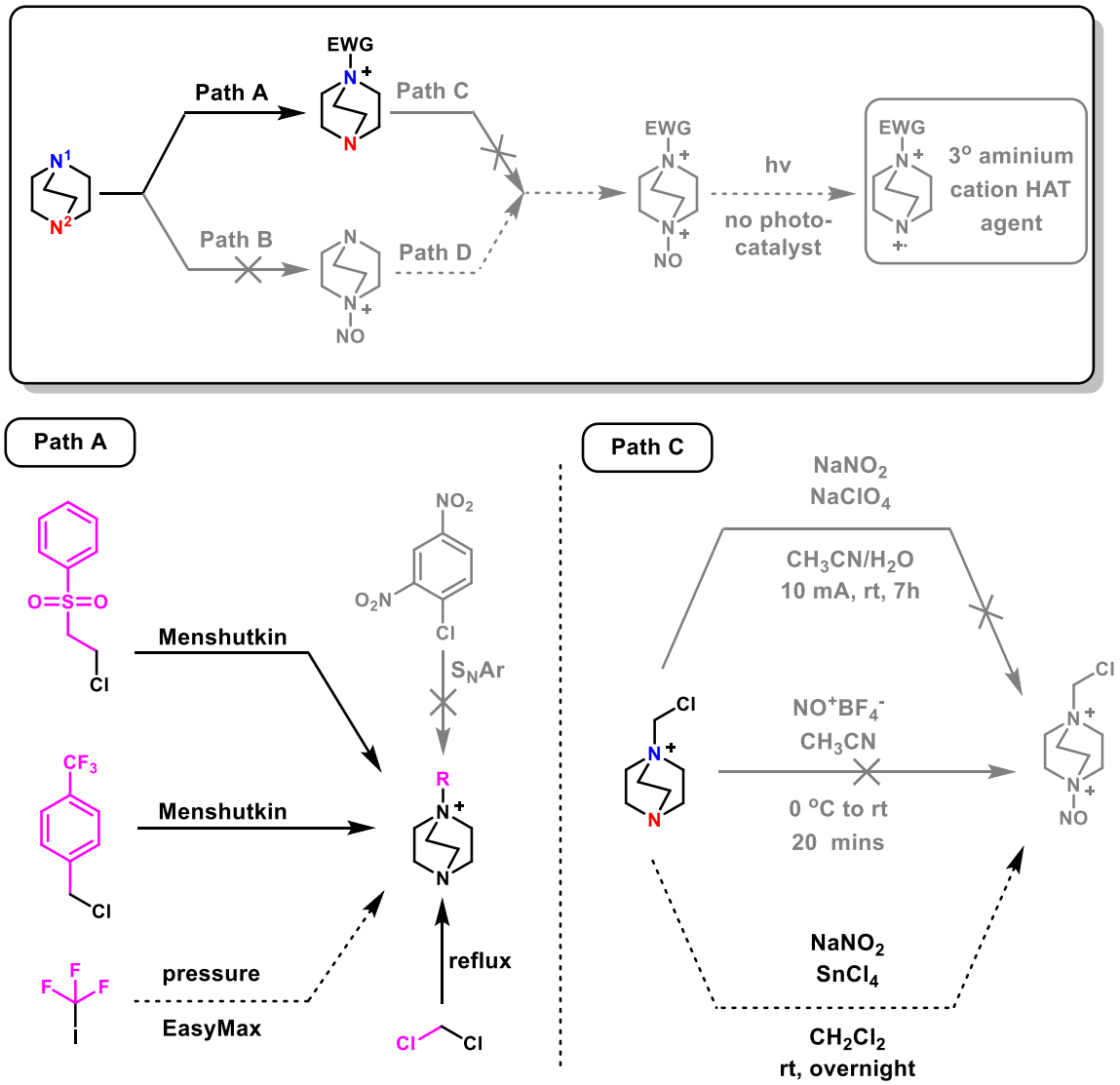

Scheme 3-7. Preliminary Results in the Development of a Novel HAT Agent.

We were able to functionalize DABCO at the N^1 site with EWG, using the Menshutkin reaction, and refluxing. Unfortunately, S_NAr did not yield any desired product. We have not yet carried out the functionalization under high pressure, due to its impracticality for our purposes, and cumbersome handling of the trifluoromethyl iodide gas, but are reserving it as a last resort option. We proceeded with nitrsoylation of **28**. Unfortunately, we have not had success in nitrosylating **28**. We have only tried two of the three possible routes to access the desired nitrosylated EWG-functionalized DABCO. As shown in Scheme 3-7, the last possible route uses $SnCl_4$, which, as previously mentioned is not an ideal chemical to handle, and therefore is not the route we would like to proceed with at this time.

3.3.2. Other Possible Routes to Nitrogen-Centered Radicals

Given the instability of the *N*-nitrosopyridinium species, we suspect that the nitrosylation of a tertiary amine may be hindered/unfavored and likely impossible due to its stability. Instead of installing a nitroso group onto the N^2 site of DABCO, we have decided that some other functional group should be used. Inspired by our earlier work and knowledge of radical decarboxylation, we contemplated the possibilities of installing a carboxylic group at the N^2 site (Scheme 3-8). However, current literature search does not seem very promising, as it seems no one has installed a carboxylic group directly on a nitrogen atom. Further literature search and exploration is needed to be done. It is our hope to be able to install some functional group that may be radically cleaved photochemically without the use of additional catalysts, or under chemical conditions that will not require additional catalysts outside of the $AgNO_3$ that is necessary to afford fluorination.

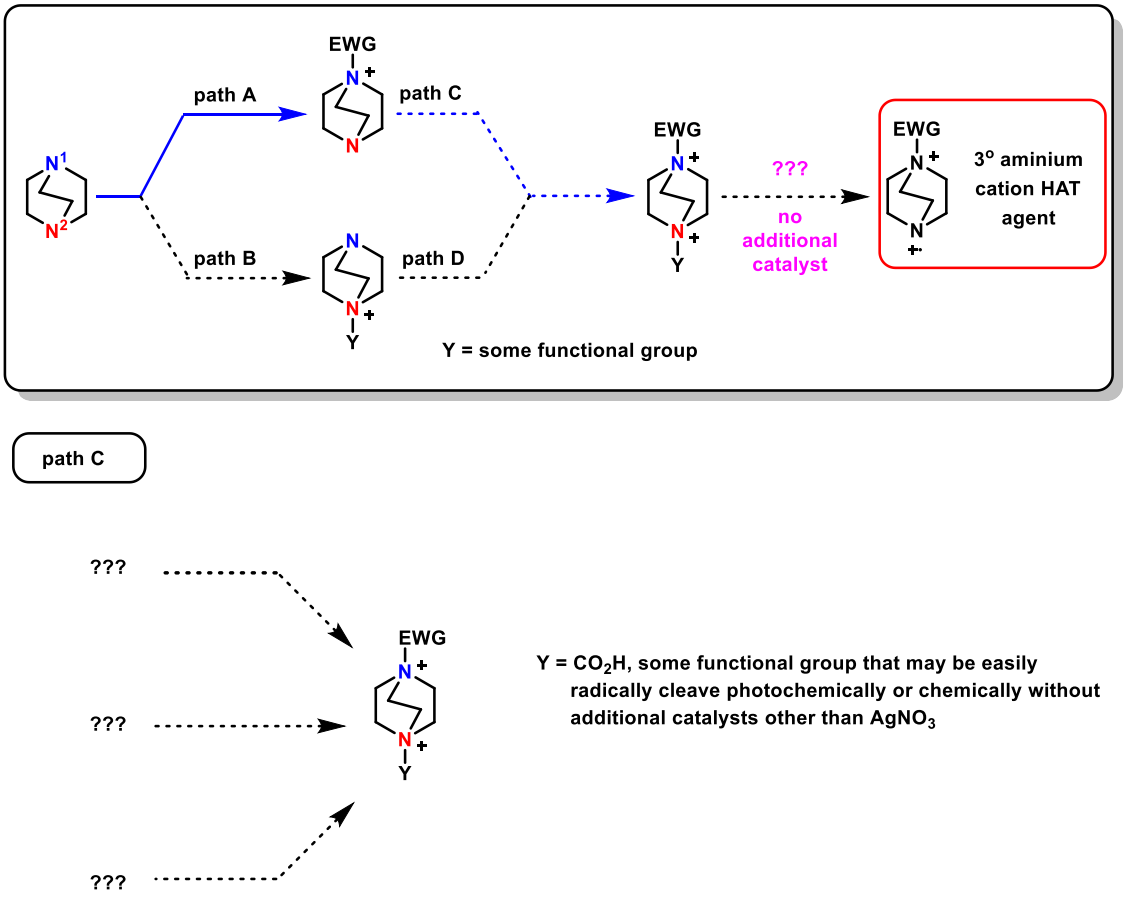

Scheme 3-8. Proposed Future Work and Development of a Novel HAT Agent.

3.4. Summary on Novel Nitrogen-Centered Radical Precursors

In summary, we have preliminary data to suggest that a quaternary nitrosoaminium is not a practical *N*-centered radical precursor likely due to stability issues. Because we have successfully installed a few electron withdrawing groups onto the N^1 of DABCO, it is our hope to further the exploration of installing some other group on the N^2 that is ideally cleavable by some light source. However, we are also concurrently exploring the possibilities of installing some groups that have been shown to be cleavable by a simple catalyst such as $AgNO_3$. It is our goal to design and HAT agent that is (1) capable of abstracting hydrogens from C–H bonds that may be stronger than that of a benzylic one, (2) can be initiated without specialized or additional catalysts.

R E F E R E N C E S

1. (a) Benson, S. W. Bond Energies. *J. Chem. Educ.* **1965**, *42*, 502–518. (b) Kerr, J. A. Bond Dissociation Energies by Kinetic Methods. *Chem. Rev.* **1966**, *66*, 465–500. (c) Bond Dissociation Energies in Small Molecules. *National Standard Reference Data Series*, National Bureau of Standards, no. 31, Washington, **1970**. (d) Cottrell, T. L. *The Strengths of Chemical Bonds*, Buttersworth, London, **1958**.
2. (a) Dohi, T.; Ueda, S.; Iwasaki, K.; Morimoto, K.; Kita, Y. Selective carboxylation of reactive benzylic C–H bonds by a hypervalent iodine(III)/inorganic bromide oxidation system. *Belstein J. Org. Chem.* **2018**, *14*, 1087–1094. (b) Deng, G.-J.; Xiao, F.; Yang, L.; in *From C–H to C–C Bonds: Cross-Dehydrogenative-Coupling*; Li, C.-J., Ed.; RSC Green Chemistry Series, **2015**, vol. 26, pp 93–113. (c) Pandey, G.; Laha, R.; Singh, D. *J. Org. Chem.* ***2016****, 81*, 7161. (d) He, Y.; Cai, Y.; Zhu, S. Mild and Regioselective Benzylic C–H Functionalization: Ni-Catalyzed Reductive Arylation of Remote and Proximal Olefins. *J. Am. Chem. Soc.* **2017**, *139*, 1061–1064. (e) Guo, S.; AbuSalim, D. I.; Cook, S. P. Aqueous Benzylic C–H Trifluoromethylation for Late-Stage Functionalization. *J. Am. Chem. Soc.* **2018**, *140*, 12378–12382.
3. (a) Ziegler, D. T.; Fu, G. C. Catalytic Enantioselective Carbon-Oxygen Bond Formation: Pjosphine-Catalyzed Synthesis of Benzylic Ethers via the Oxidation of Benzylic C–H Bonds. *J. Am. Chem. Soc,* **2016**, *138*, 12069–12072. (b) Andrus, M. B.; in *Sciences of Synthesis, Stereoselective Synthesis*; DeVries, J. G.; Molander, G. A.; Evans, P. A., Eds.; Georg Theime Verlog: Stuttgart, **2011**, vol. 3, pp 469–482. (c) Sheldon, R. A.; in *Fine Chemicals through Heterogeneous Catalysis*; Sheldon, R. A.; van Bekkum, H., Eds.; Wiley-VHC: Weinheim, **2001**, pp 519–526. (d) Liu, J.; Hu, K.-F.; Qu, J.-P.; Kang, Y.-B. Organopromoted Selectivity-Switchable Synthesis of Polyketones. *Org. Lett.* **2017**, *19*, 5593. (e) Chen, K.; Zhang, P.; Wang, Y.; Li, H. Metal-free allylic/benzylic oxidation strategies with molecular oxygen: recent advances and future prospects. *Green Chem.* **2014**, *16*, 2344–2374. (f) Shimojo, H.; Moriyama, K.; Togo, H. A One-Pot, Transition-Metal-Free Procedure for C–O, C–S, C–N Bond Formation at the Benzylic Position of Methylarenes. *Synthesis* **2015**, *47*, 1280–1290. (g) Batista, V. S.; Crabtree, R. H.; Konezny, S. J.; Luca, O. R.; Praetorius, J. M. Oxidative functionalization of benzylic C–H bonds by DDQ. *New J. Chem.* **2012**, *36*, 1141–1144. (h) Fan, L.; Zhang, Z.; Wang, T.; Liang, Q.; Zhao, J. Copper-catalyzed oxidative functionalization of benzylic C–H bonds with quinazoline 3-oxides. *Org. Chem. Front.* **2018**, *5*, 2492–2495.
4. (a) Ramesh, D.; Ramulu, U.; Mukkanti, K.; Venkateswarlu, Y. DDQ-mediated direct oxidative coupling of amides with benzylic and allylic sp^3 C–H bonds under metal-free conditions. *Tetrahedron Lett.* **2012**, *53*, 2904. (b) Liu, W.; Liu, C.; Zhang, Y.; Sun, Y.; Abdukader, A.; Wang, B.; Li, H.; Ma, X.; Zhang, Z. Reusable ionic liquid-catalyzed oxidative coupling of azoles and benzylic compounds via sp^3 C–N bond formation under metal-free conditions. *Org. Biomol. Chem.* **2015**, *13*, 7154–7158. (c) Clark, J.

R.; Feng, K.; Sookezian, A.; White, M. C. Manganese-catalysed benzylic C(sp^3)–H amination for late-stage functionalization. *Nature Chem.* **2018**, *10*, 583–591.

5. (a) Pierce, O. R.; McBee, E. T. Halogenation. *Ind. Eng. Chem.* **1952**, *44*, 2015–2020. (b) Pierce, O. R.; McBee, E. T. Halogenation. *Ind. Eng. Chem.* **1953**, *45*, 1969–1975. (c) McBee, E. T.; Pierce, O. R. Halogenation. *Ind. Eng. Chem.* **1954**, *46*, 1835–1841. (d) Weiss, H. M.; Granz, L. A Safe Simple Halogenation Experiment. *J. Chem. Ed.* **1999**, *76*, 534. (e) Wan, X.; Ma, Z.; Li, B.; Zhang, K.; Cao, S.; Zhang, S.; Shi, Z. Highly Selective C–H Functionalization/Halogenation of Acetanilide. *J. Am. Chem. Soc.* **2006**, *128*, 7416–7417. (f) Cristiano, R.; Ma, K.; Pottanat, G.; Weiss, R. G. Tetraalkylphosphonium Trihalides. Room Temperature Ionic Liquids as Halogenation Reagents. *J. Org. Chem.* **2009**, *74*, 9024–9033. (g) Xu, T.; Yu, Z.; Wang, L. Iron-Promoted Cyclization/Halogenation of Alkyl Diethyl Acetals. *Org. Lett.* **2009**¸*11*, 2113–2116. (h) Pouloit, M.-F.; Mahe, O.; Hamel, J.-D.; Desroches, J.; Paquin, J.-F. *Org. Lett*. **2012**, *14*, 5428–5431.
6. (a) Noble, A.; MacMillan, D. W. C. Photoredox α-Vinylation of α-Amino Acids and *N*-Aryl Amines. *J. Am. Chem. Soc.* **2014**, *136*, 11602−11605. (b) McCarver, S. J.; Qiao, J. X.; Carpenter, J.; Borzilleri, R. M.; Poss, M. A.; Eastgate, M. D.; Miller, M.; MacMillan, D. W. C. Decarboxylative Peptide Macrocyclization through Photoredox Catalysis. *Angew. Chem., Int. Ed*. **2017**, *56*, 728−732. (c) Zuo, Z.; MacMillan, D. W. C. Decarboxylative Arylation of α-Amino Acids via Photoredox Catalysis: A One-Step Conversion of Biomass to Drug Pharmacophore. *J. Am. Chem. Soc*. **2014**, *136*, 5257−5260. (d) Zuo, Z.; Ahneman, D. T.; Chu, L.; Terrett, J. A.; Doyle, A. G.; MacMillan, D. W. C. Merging photoredox with nickel catalysis: Coupling of α-carboxyl sp^3-carbons with aryl halides. *Science* **2014**, *345*, 437−440. (e) Zuo, Z.; Cong, H.; Li, W.; Choi, J.; Fu, G. C.; MacMillan, D. W. C. Enantioselective Decarboxylative Arylation of α-Amino Acids via the Merger of Photoredox and Nickel Catalysis. *J. Am. Chem. Soc*. **2016**, *138*, 1832−1835. (f) Cowden, C. J. Use of *N*-Protected Amino Acids in the Minisci Radical Alkylation. *Org. Lett*. **2003**, *5*, 4497−4499. (g) Shore, D. G. M.; Wasik, K. A.; Lyssikatos, J. P.; Estrada, A. A. Minisci alkylations of electron-deficient pyrimidines with alkyl carboxylic acids. *Tetrahedron Lett***. 2015**, *56*, 4063−4066.
7. (a) Murphy, C. D.; Schaffrath, C.; O'Hagan, D. Fluorinated natural products: the biosynthesis of fluoroacetate and 4-fluorothreonine in streptomyces cattleya. *Chemsphere* **2003**, *52*, 455–461. (b) Proudfoot, A. T.; Bradberry, S. M.; Vale, J. A. Sodium Fluoroacetate Poisoning. *Toxicol. Rev.* **2006**, *25*, 213–219.
8. (a) Thayer, A. M. Fabulous Fluorine. *Chem. Eng. News* **2006**, *84*, 15–24. (b) McGrath, N. A. A graphical journey of innovative organic architectures that have improved our lives. *J. Chem. Educ.* **2010**, *87*, 1349 –1349. (c) Purser, S.; Moore, P. R.; Swallow, S.; Governeur, V. Fluorine in medicinal chemistry. *Chem. Soc. Rev.* **2008**, *37*, 320–330.
9. (a) Müller, K.; Faeh, C.; Diederich, F. Fluorine in Pharmaceutical: Looking Beyond Institution. *Science* **2007**, *317*, 1881–1886. (b) Hagmann, W. K. The Many Roles for Fluorine in Medicinal Chemistry. *J. Med. Chem.* **2008**, *51*, 4359–4369. (c) Kirk, K. L. Fluorination in Medicinal Chemistry: Methods, Strategies, and Recent Developments. *Org. Process Res. Dev.* **2008**, *12*, 305–321. (d) Isanbor, C.; O'Hagan, D. J. Fluorine in medicinal chemistry: A review of anti-cancer agents. *J. Fluorine Chem*. **2006**, *127*,

303–319. (e) Kirk, K. L. Fluorine in medicinal chemistry: Recent therapeutic applications of fluorinated small molecules. *J. Fluorine Chem.* **2006**, *127*, 1013–1029.
10. (a) Rueda-Becerril, M.; Sazepin, C. C.; Leung, J. C. T.; Okbinoglu, T.; Kennepohl, P.; Paquin, J.-F.; Sammis, G. M. Fluorine Transfer to Alkylradicals. *J. Am. Chem. Soc.* **2012**, *134*, 4026–2029. (b) Hiyama, T. *Organofluorine Compounds: Chemistry and Applications;* Yamamoto, H., Ed.; Springer: Berlin, **2000**. (c) Tius, M. A. Xenon difluoride synthesis. *Tetrahedron* **1995**, *51*, 6605–6634. (d) Yamada, S.; Gavryushin, A.; Knochel, P. Convenient Electrophilic Fluorination of Functionalized Aryl and Heteroaryl Magnesium Reagents. *Angew. Chem., Int. Ed.* **2010**, *49*, 2215–2218. (e) Döbele, M.; Vanderheiden, S.; Jung, N.; Bräse, S. Synthesis of Aryl Fluorides on a Solid Support and in Solution by Utilizing a Fluorinated Solvent. *Angew. Chem., Int. Ed.* **2010**, *49*, 5986–5988. (f) Lal, G. S.; Pez, G. P.; Syvret, R. G. Electrophilic NF Fluorinating Agents. *Chem. Rev.* **1996**, 1737–1755.
11. Pattison, G. *'Green' and Sustainable Halogenation Processes* in *Green and Sustainable Medicinal Chemistry: Methods, Tools and Strategies for the 21st Century Pharmaceutical Industry*; Royal Society of Chemistry: SI, **2016**, pp 203–216.
12. (a) Olah, G. A.; Nojima, M.; Keresh, I. Synthetic Methods and Reactions II. Hyrdofluorination of Alkenes, Cyclopropane and Alkynes with Poly-Hydrogen Fluoride/Pyridine (Trialkyamine) Reagents. *Synthesis* **1973**, *12*, 779–780. (b) Olah, G. A.; Shih, J. G.; Prakash, J. K. S. Fluorine-containing reagents in organic synthesis. *J. Fluorine Chem.* **1986**, *33*, 377–396.
13. (a) Schonnerg, A.; Moubacher, R. The Strecker Degradation of α-Amino Acids. *Chem. Rev.* **1952**, *50*, 261–277. (b) Zelechonok, Y.; Silverman, R. B. Silver(I)/peroxdisulfate-induced oxidative decarboxylation of amino acids. A chemical model for a possible intermediate in the monoamine oxidase-catalyzed oxidation of amines. *J. Org. Chem.* **1992**, *57*, 5787–5790. (c) Rizzi, G. P. The Strecker degradation of amino acids: Newer avenues for flavor formation. *Food Rev. Int.* **2008**, *24*, 416–435. (d) Nashalian, O.; Yaylayan, V. A. Thermally Induced Oxidative Decarboxylation of Copper Complexes of Amino Acids and Formation of Strecker Aldehyde. *J. Agric. Food Chem.* **2014**, *62*, 8518–8523.
14. Mai, D. N.; Baxter, R. D. Unprotected Amino Acids as Stable Radical Precursors for Heterocycle C–H Functionalization. *Org. Lett.* **2016**, *18*, 3738–3741.
15. (a) Minisci, F.; Bernardi, R.; Bertini, F.; Galli, R.; Perchinummo, M. Nucleophilic character of alkyl radicals—VI: A new convenient selective alkylation of heteroaromatic bases. *Tetrahedron* **1971**, *27*, 3575−3579. (b) Minisci, F. Novel Applications of Free-Radical Reactions in Preparative Organic Chemistry. *Synthesis* **1973**, *1973*, 1−24. (c) Minisci, F.; Vismara, E.; Fontana, F. Recent Developments of Free-Radical Substitutions pf Heteroaromatic Bases. *Heterocycles* **1989**, *28*, 489−519. (d) Minisci, F.; Fontana, F.; Vismara, E. J. Substitutions by nucleophilic free radicals: A new general reaction of heteroaromatic bases. *Heterocycl. Chem.* **1990**, *27*, 79−96.
16. Seiple, I. B.; Su, S.; Rodriguez, R. A.; Gianatassio, R.; Fujiwara, Y.; Sobel, A. L.; Baran, P. S. Direct C−H Arylation of Electron-Deficient Heterocycles with Arylboronic Acids. *J. Am. Chem. Soc.* **2010**, *132*, 13194−13196.

17. (a) Langlois, B. R.; Laurent, E.; Roidot, N. Trifluoromethylation of aromatic compounds with sodium trifluoromethanesulfinate under oxidative conditions. *Tetrahedron Lett*. **1991**, *32*, 7525−7528. (b) Ji, Y.; Brückl, T.; Baxter, R. D.; Fujiwara, Y.; Seiple, I. B.; Su, S.; Blackmond, D. G.; Baran, P. S. Innate C-H trifluoromethylation of heterocycles. *Proc. Natl. Acad. Sci. U. S. A.* **2011**, *108*, 14411−14415. (c) Fujiwara, Y.; Dixon, J. A.; Rodriguez, R. A.; Baxter, R. D.; Dixon, D. D.; Collins, M. R.; Blackmond, D. G.; Baran, P. S. A New Reagent for Direct Difluoromethylation. *J. Am. Chem. Soc.* **2012**, *134*, 1494−1497. (e) Fujiwara, Y.; Dixon, J. A.; O'Hara, F.; Funder, E. D.; Dixon, D. D.; Rodriguez, R. A.; Baxter, R. D.; Herle, B.; Sach, N.; Collins, M. R.; Ishihara, Y.; Baran, P. S. Practical and innate carbon–hydrogen functionalization of heterocycles *Nature* **2012**, *492*, 95−99.
18. Gardini, G. P.; Minisci, F.; Palla, G.; Galli, A. R. Homolytic amidation of heteroaromatic bases: New selective process. *Tetrahedron Lett.* **1971**, *12*, 59–62.
19. McNally, A.; Prier, C. K.; MacMillan, D. W. C. Discovery of an α-Amino C–H Arylation Reaction Using the Strategy of Accelerated Serendipity. *Science* **2011**, *334*, 1114–1117.
20. Kohls, P; Jadhav, D.; Pandey, G.; Reiser, O. Visible Light Photoredox Catalysis: Generation and Addition of N-Aryltetrahydroisoquinoline-Derived α-Amino Radicals to Michael Acceptors. *Org. Lett.* **2012**, *14*, 672–675.
21. (a) Nakajima, K.; Miyake, Y.; Nishibayashi, Y. Synthetic Utilization of α-Aminoalkyl Radicals and Related Species in Visible Light Photoredox Catalysis. *Acc. Chem. Res.* **2016**, *49*, 1946–1956. (b) Miyake, Y.; Nakajima, K.; Nishibayashi, Y. Visible-Light-Mediated Utilization of α-Aminoalkyl Radicals: Addition to Electron-Deficient Alkenes Using Photoredox Catalysts. *J. Am. Chem. Soc.* **2012**, *134*, 3338–3341.
22. Ruiz Espelt, L.; McPherson, I. S.; Wiensch, E. M.; Yoon, T. P. Enantioselective Conjugate Additions of α-Amino Radicals via Cooperative Photoredox and Lewis Acid Catalysis. *J. Am. Chem. Soc*. **2015**, *137*, 2452−2455.
23. (a) Yoshida, J.; Suga, S.; Suzuki, S.; Kinomura, N.; Yamamoto, A.; Fu-jiwara, K. *J. Am. Chem. Soc.* **1999**, *121*, 9546–9549. (b) Suga, S.; Suzuki, S.; Yoshida, J. *J. Am. Chem. Soc*. **2002**, *124*, 30–31.
24. Yoshi-mitsu, T.; Arano, Y.;Nagaoka, H. *J. Am. Chem. Soc*. **2005**, *127*, 11610–11611.
25. (a) Richter, H.; Frçhlich, R,; Dani-liuc, C.-G.; Mancheño, O. G. *Angew. Chem.* **2012**, *124*, 8784–8788. (b) Richter, H.; Frçhlich, R,; Dani-liuc, C.-G.; Mancheño, O. G. *Angew.Chem. Int. Ed.* **2012**, *51*, 8656–8660.
26. Yin, F.; Wang, Z.; Li, Z,; Li, C. Silver-Catalyzed Decarboxylative Fluorination of Aliphatic Carboxylic Acids. *J. Am. Chem. Soc.* **2012**, *134*, 25, 10401–10404.
27. Patel, N. R.; Flowers, R. A. Mechanistic Study of Silver-Catalyzed Decarboxylative Fluorination. *J. Org. Chem.* **2015**, *80*, 5834–5841.
28. (a) Pitts, C. R.; Bloom, S.; Woltornist, R.; Auvenshine, D. J.; Ryzhkov, L. R.; Siegler, M. A.; Lectka, T. Direct, Catalytic Monofluorination of sp3 C–H Bonds: A Radical-Based Mechanism with Ionic Selectivity. *J. Am. Chem. Soc.* **2014**, *136*, 9780–9791. (b) Pitts, C. R.: Ling, B.; Woltornist, R.; Liu, R.; Lectka, T. Triethylborane-Initiated Radical Chain Fluorination: A Synthetic Method Derived from Mechanistic Insight. *J. Org. Chem.* **2014**, *79*, 8895–8899.

29. Liang, T.; Neumann, C. N.; Ritter, T. Introduction of Fluorine and Fluorine-Containing Functional Groups. *Angew. Chem., Int. Ed.* **2013**, *52*, 8214–8264.
30. Antelo, J. M.; Crugeira, J.; Leis, J. R.; Rios, A. Nucleophilic reactivity towards electrophilic fluorinating agents: Reaction with fluorobenzenesulfonimide ($(PhSO_2)_2NF$). *J. Chem. Soc., Perkin Trans. 2*, **2000**, 2071–2076.
31. Galloway, J. D.; Mai, D. N.; Baxter, R. D. Silver-Catalyzed Minisci Reactions Using Selectfluor as a Mild Oxidant. *Org. Lett.* **2017**, *19*, 5772–5775.
32. (a) Grabowski, S. J. What Is the Covalency of Hydrogen Bonding? *Chem. Rev.* **2011**, *111*, 2597–2625. (b) Arunan, E.; Desiraju, G. R.; Klein, R. A.; Sadlej, J.; Scheiner, S.; Alkorta, I.; Clary, D. C.; Crabtree, R. H.; Dannenberg, J. J.; Hobza, P.; Kjaergaard, G. H.; Legon, A. C.; Mennucci, B.; Nesbitt. D. J. Definition of the hydrogen bond (IUPAC Recommendations 2011). *Pure Appl. Chem.* **2011**, *83*, 1637–1641.
33. (a)Doyle, A. G.; Jacobsen, E. N. Small Molecule H-Bond Donors in Asymmetric Catalysis. *Chem. Rev.* **2007**, *107*, 5713–5743. (b) Carreira, E. M. In *Comprehensive Asymmetric Catalysis*; Jacobsen, E. N.; Pfaltz, A.; Yamamoto, H., Eds.; Springer: Berlin, Germany, **1999**, vol 3, Chapter 29.1. (c) Shibasaki, M.; Yoshikawa, N.; Matsunaga, S. In *Comprehensive Asymmetric Catalysis*; Jacobsen, E. N.; Pfaltz, A.; Yamamoto, H., Eds.; Springer: Berlin, Germany, **1999**, vol 3, Chapter 29.4. (d) Ooi, T.; Maruoka, K. In *Comprehensive Asymmetric Catalysis*; Jacobsen, E. N.; Pfaltz, A.; Yamamoto, H., Eds.; Springer: Berlin, Germany, **1999**, vol 3, Chapter 33.2. (e) Basavaiah, D.; Rao, A. J.; Satyanarayan, T. Recent Advances in the Baylis−Hillman Reaction and Applications. *Chem. Rev.* **2003**, *103*, 811–892. (f) Masson, G.; Housseman, C.; Zhu, J. The enantioselective Morita-Baylis-Hillman reaction and its aza counterpart. *Angew. Chem., Int. Ed.* **2007**, *46*, 4614–4628. (g) Jørgensen, K. A. Asymmetric Friedel-Crafts Reactions: Catalytic Enantioselective Addition of Aromatic and Heteroaromatic C-H Bonds to Activated Alkenes, Carbonyl Compounds, and Imines. *Synthesis* **2003**, *7*, 1117–1125. (h) Bandini, M.; Melloni, A.; Umani-Ronchi, A. New Catalytic Approaches in the Stereoselective Friedel–Crafts Alkylation Reaction. *Angew. Chem., Int. Ed.* **2004**, *43*, 550–556.
34. (a) Hajos, Z. G.; Parrish, D. R.; Hoffman-La-Roche. German Patent DE 2102623, 1971*; Chem. Abstr*. **1972**, *76*, 59072. (b) Eder, U.; Sauer, G.; Wiechert, R.; Schering AG. German Patent DE 2014757, 1971; *Chem. Abstr*. **1972**, *76*, 59072. (c) Eder, U.; Sauer, G.; Wiechert, R. New Type of Asymmetric Cyclization to Optically Active Steroid CD Partial Structures. *Angew. Chem., Int. Ed. Engl.* **1971**, *10*, 496–497. (d) Hajos, Z. G.; Parrish, D. R. Asymmetric synthesis of bicyclic intermediates of natural product chemistry. *J. Org. Chem*. **1974**, *39*, 1615–1621. (e) Danishefsky, S.; Cain, P. Optically specific synthesis of estrone and 19-norsteroids from 2,6-lutidine. *J. Am. Chem. Soc*. **1976**, *98*, 4975–4983. (f) Cohen, N. Asymmetric induction in 19-norsteroid total synthesis. *Acc. Chem. Res*. **1976**, *9*, 412. (g) Woodward, R. B.; Logusch, E.; Nambiar, K. P.; Sakan, K.; Ward, D. E.; Au-Yeung, B. W.; Balaram, P.; Browne, L. J.; Card, P. J.; Chen, C. H. Asymmetric total synthesis of erythromycin. 1. Synthesis of an erythonolidine A secoacid derivative via asymmetric induction. *J. Am. Chem. Soc.* **1981**, *103*, 3210–3213. (h) Smith, A. B., III; Kingery-Wood, J.; Leenay, T. L.; Nolen, E. G.; Sunazuka, T. Indole diterpene synthetic studies. 8. The total synthesis of (+)-paspalicine and (+)-paspalinine. *J. Am. Chem. Soc*. **1992**, *114*, 1438–1449. (i) Isaacs,

R. C. A.; Di Grandi, M. J.; Danishefsky, S. J. Synthesis of an enantiomerically pure intermediate containing the CD sunstructure of taxol. *J. Org. Chem*. **1993**, *58*, 3938–3944.

35. (a) Klare, H.; Neudörfl, J. M.; Goldfuss, B. New hydrogen-bonding organcatalysts: Chiral cyclophosphazanes and phosphorous amides as catalysts fo asymmetric Michael additions. *Beilstein J. Org. Chem.* **2014**, *10*, 224–236. (b) Nishikawa, Y. Recent topics in dual hydrogen bonding catalysis. *Tetrahedron Lett.* **2018**, *59*, 216–223. (c) Hamza, A.; Schubert, G.; Soos, T.; Papai, I. Theoretical Studies on the Bifunctionality of Chiral Thiourea-Based Organocatalysts: Competing Routes to C−C Bond Formation. *J. Am. Chem. Soc*. **2006**, *128*, 13151−13160. (d) Armstrong, A.; Boto, R. A.; Dingwall, P.; Contreras-Garcia, J.; Harvey, M. J.; Mason, N. J.; Rzepa, H. S. The Houk-List Transition States for Organocatalytic Mechanisms Revisited. *Chem. Sci*. **2014**, 5, 2057−2071. (e) Zabka, M.; Sebesta, R. Experimental and Theoretical Studies of Hydrogen-Bonding in Organocatalysis. Molecules **2015**, *20*, 15500−15524. (f) Grayson, M. N. Mechanism and Origins of Stereoselectivity in the Cinchona Thiourea- and Squaramide-Catalyzed Asymmetric Michael Addition of Nitroalkanes to Enones. *J. Org. Chem*. **2017**, *82*, 4396−4401.
36. (a) Desiraju, G. R.; Ho, P. S.; Kloo, L.; Legon, A. C.; Marquardt, R.; Metrangolo, P.; Politzer, P.; Resnati, G.; Rissanen, K. Definition of the halogen bond (IUPAC Recommendations 2013). *Pure Appl. Chem*. **2013**, *85*, 1711−1713. (b) Politzer, P.; Lane, P.; Concha, M. C.; Ma, Y.; Murray, J. S. An overview of halogen bonding. *J. Mol. Model* **2007**, *13*, 305–311. (c) Wolters, L. P.; Bickelhaupt, F. M. Halogen Bonding versus Hydrogen Bonding: A Molecular Orbital Perspective. *ChemistryOpen* **2012**, *1*, 96–105.
37. (a) Nagorny, P.; Sun, Z. New approaches to organocatalysis based on C−H and C−X bonding for electrophilic substrate activation. *Beilstein J. Org. Chem*. **2016**, *12*, 2834−2848. (b) Guha, S.; Kazi, I.; Nandy, A.; Sekar, G. Role of Lewis-Base-Coordinated Halogen(I) Intermediates in Organic Synthesis: The Journey from Unstable Intermediates to Versatile Reagents. *Eur. J. Org. Chem*. **2017**, *2017*, 5497−5518. (c) Chen, M.-W.; Ji, Y.; Wang, J.; Chen, Q.-A.; Shi, L.; Zhou, Y.-G. Asymmetric Hydrogenation of Isoquinolines and Pyridines Using Hydrogen Halide Generated in Situ as Activator. *Org. Lett*. **2017**, *19*, 4988−4991. (d) Ma, R.; He, L.-N.; Liu, X.-F.; Liu, X.; Wang, M.-Y. DBU as Activator for the N-iodosuccinimide Promoted Chemical Fixation of Carbon Dioxide with Epoxides. *Journal of CO2 Utilization* **2017**, *19*, 28−32. (e) Kobayashi, Y.; Nakatsuji, Y.; Li, S.; Tsuzuki, S.; Takemoto, Y. Direct N-Glycofunctionalization of Amides with Glycosyl Trichloroacetimidate by Thiourea/Halogen Bond Donor Co-Catalysis. *Angew. Chem., Int. Ed*. **2018**, *57*, 3646−3650. (f) Lu, Y.; Nakatsuji, H.; Okumura, Y.; Yao, L.; Ishihara, K. Enantioselective Halo-oxy- and Halo-azacyclizations Induced by Chiral Amidophosphate Catalysts and Halo-Lewis Acids. *J. Am. Chem. Soc*. **2018**, *140*, 6039−6043. (g) Brückner, R.; Haller, H.; Steinhauer, S.; Müller, C.; Riedel, S. A 2D Polychloride Network Held Together by Halogen-Halogen Interactions. *Angew. Chem., Int. Ed.* **2015**, *54*, 15579−15583. (h) Riedel, S.; Köchner, T.; Wang, X.; Andrews, L. Polyfluoride Anions, a MatrixIsolation and Quantum-Chemical Investigation. *Inorg. Chem*. **2010**, *49*, 7156−7164. (i) Gliese, J.; Jungbauer, S. H.; Huber, S. M. A HalogenBonding-Catalyzed Michael Addition Reaction. *Chem.*

Commun. **2017**, *53*, 12052−12055. (j) Heinen, F.; Engelage, E.; Dreger, A.; Weiss, R.; Huber, S. M. Iodine(III) Derivatives as Halogen Bonding Organocatalysts. *Angew. Chem., Int. Ed*. **2018**, *57*, 3830−3833. (k) Schindler, S.; Huber, S. M. Halogen Bonds in Organic Synthesis and Organocatalysis. In *Halogen Bonding II: Impact on Materials Chemistry and Life Sciences*; Metrangolo, P., Resnati, G., Eds.; Springer International Publishing: Cham, **2015**; Vol. 359, pp 167−204. (l) Breugst, M.; von der Heiden, D. Mechanisms in Iodine Catalysis. *Chem. - Eur. J.* **2018**, *24*, 9187. (m) von der Heiden, D.; Detmar, E.; Kuchta, R.; Breugst, M. Activation of Michael Acceptors by Halogen-Bond Donors. *Synlett* **2018**, *29*, 1307−1313. (n) Breugst, M.; von der Heiden, D.; Schmauck, J. Novel Noncovalent Interactions in Catalysis: A Focus on Halogen, Chalcogen, and Anion-n Bonding. *Synthesis* **2017**, *49*, 3224−3236.

38. Danahy, K. E.; Cooper, J. C.; Van Humbeck, J. F. Benzylic Fluorination of Aza-Heterocycles Induced by Single-Electron Transfer to Selectfluor. *Angew. Chem., Int. Ed*. **2018**, *57*, 5134−5138.
39. (a) Del Piero, S.; Fedele, R.; Melchior, A.; Portanova, R.; Tolazzi, M.; Zangrando, E. Solvation Effects on the Stability of Silver(I) Complexes with Pyridine-Containing Ligands Studied by Thermodynamic and DFT Methods. *Inorg. Chem.* **2007**, *46*, 4693–4691. (b) Thaler, A.; Cox, B. G.; Schneider, H. Stability constants of aza-oxa-crown ether complexes with silver(I) in nonaqueous polar solvents. *Inorg. Chim. Acta.* **2003**, *351*, 123–132.
40. (a) Carlsson, A.-C. C.; Veiga, A. X.; Erdelyi, M. Halogen Bonding´ in Solution. In *Halogen Bonding II: Impact on Materials Chemistry and Life Sciences*; Metrangolo, P., Resnati, G., Eds.; Springer International Publishing: Cham, **2015**; Vol. 359, pp 49−76. (b) Bedin, M.; Karim, A.; Reitti, M.; Carlsson, A.-C. C.; Topic, F.; Cetina, M.; Pan, F.; Havel, V.; Al-Ameri, F.; Sindelar, V.; Rissanen, K.; Grafenstein, J.; Erdelyi, M. Counterion Influence on the N−I−N Halogen Bond. *Chem. Sci*. **2015**, *6*, 3746−3756. (c) Carlsson, A.-C. C.; Mehmeti, K.; Uhrbom, M.; Karim, A.; Bedin, M.; Puttreddy, R.; Kleinmaier, R.; Neverov, A. A.; Nekoueishahraki, B.; Gräfenstein, J.; Rissanen, K.; Erdelyi, M.´ Substituent Effects on the [N−I−N]+ Halogen Bond. *J. Am. Chem. Soc.* **2016**, *138*, 9853−9863.
41. (a) Becke, A. Density-functional thermochemistry. III. The role of exact exchange. *J. Chem. Phys*. **1993**, *98*, 5648. (b) Wang, Y.; Perdew J. P. Spin Scaling of the electron-gas correlation energy in highdensity limit. *Phys. Rev. B*. **1991**, *43*, 8911. (c) Marenich, A.V.; Cramer, C.J.; Truhlar, D.G. Universal solvation model based on solute electron density and on a continuum model of the solvent defined by the bulk dielectric constant and atomic surface tensions. *J. Phys. Chem. B.* **2009**, *113* (18), 6378–6396. (d) Hratchian, H.P.; Schlegel, H. B. Finding Minima, Transition States, and Following Reaction Pathways on Ab Initio Potential Energy Surfaces. In *Theory and applications of computational chemistry: The first forty years*, Dykstra, C. E.; Frenking, G.; Kin, K. S.; Scuseria, G. E., Eds. Elsevier: Amsterdam, **2005**, 95. (5) Baik M.; Friesner, R. A. Computing redox potentials in solution: density functional theory as a tool for rational design of redox agents. *J. Phys. Chem. A*, **2002**, *106*(32), 7407–7412.
42. (a) Kozuch, S.; Martin, J. M. L. Halogen Bonds: Benchmarks and Theoretical Analysis. *J. Chem. Theory Comput.* **2013**, *9*, 1918−1931. (b) Anderson, L. N.; Aquino, F. W.; Raeber, A. E.; Chen, X.; Wong, B. M. Halogen Bonding Interactions: Revised

Benchmarks and a New Assessment of Exchange vs Dispersion. *J. Chem. Theory Comput*. **2018**, *14*, 180−190.
43. Wong, V. H. L.; White, A. J. P.; Hor, T. S. A.; Hii, K. K. Ligand Effect and Control of E- and Z-Selectivity in the Silver-Catalyzed Synthesis of 4-Bromoxazolines. *Adv. Synth. Catal.* **2015**, *357*, 2485–2491.
44. (a) Ludwig, R. *Hydrogen-transfer reactions*; Wiley-VCH: Weinheim, 2007; Vol. 4. (b) Chatgilialoglu, C.; Struder, A. *Encyclopedia of radicals in chemistry, biology, and materials*; Wiley: Chichester, 2012. (c) Cole, S. J.; Kirwan, N.; Roberts, B. P.; Willis, C. R. Radical chain reduction of alkyl halides, dialkyl sulphides and O-alkyl S-methyl dithiocarbonates to alkanes by trialkylsilanes. *J. Chem. Soc.*, Perkin Trans. 1, 1991, 103–112. (d) Cai, Y.; Roberts, B. P. Formation of silanethiols by reaction of silanes with carbonyl sulfide: Implications for radical-chain reduction of thiocarbonyl compounds by silanes. *Tetrahedron Lett.* **2001**, *42*, 763–766.
45. (a) Mayer, J. M. Understanding Hydrogen Atom Transfer: From Bond Strength to Marcus Theory. *Acc. Chem. Res.* **2011**, *44*, 36–46. (b) Lai, W.; Li, C.; Chen, H.; Shaik, S. Hydrogen-Abstraction Reactivity Patterns from A to Y: The Valence Bond Way. *Angew. Chem., Int. Ed.* **2012**, *51*, 5556–5578.
46. (a) Hays, D. S.; Scholl, M.; Fu, G. C. Organotin Hydride-Catalyzed Conjugate Reduction of α,β-Unsaturated Ketones. *J. Org. Chem.* **1996**, *61*, 6751–6752. (b) Baguley, P. A.; Walton, J. C. Flight from the Tyranny of Tin: The Quest for Practical Radical Sources Free from Metal Encumbrances. *Angew, Chem., Int. Ed.* **1998**, *37*, 3072–3082. (c) Struder, A.; Amrein, S. Tin Hydride Substitutes in Reductive Radical Chain Reactions. *Synthesis* **2002**, *7*, 835–849. (d) Chatgilialagon, C. (Me3Si)3SiH: Twenty Years After Its Discovery as a Radical-Based Reducing Agent. *Chem. Eur. J.* **2008**, *14*, 2310–2320.
47. (a) Kärkäs, M. D. Photochemical Generation of Nitrogen-Centered Amidyl, Hydrazonyl, and Imidyl Radicals: Methodology Developments and Catalytic Applications. *ACS Catal.* **2017**, *7*, 4999–5022. (b) Zard, S. Recent progress in the generation and use of nitrogen-centred radicals. *Chem. Soc.Rev.* **2008**, *37*, 1603–1618. (c) Chen, J.-R.; Hu, X.-Q.; Lu, L.-Q.; Xiao, W.-J. Visible light photoredox-controlled reactions of *N*-radicals and radical ions. *Chem. Soc. Rev.* **2016**, *45*, 2044–2056.
48. (a) Xiong, T.; Zhang, Q. New amination strategies based on nitrogen-centered radical chemistry. *Chem. Soc. Rev.* **2016**, *45*, 3069–3087. (b) Cosgrove, S. C.; Plane, J. M. C.; Marsden, S. P. Radical-mediated direct C–H amination of arenes with secondary amines. *Chem. Sci.* **2018**, *9*, 6647–6652. (c) Nagib, D. Nitrogen gets radical. *Nature Chem.* **2019,** *11*, 396–398.
49. (a) Bullock, R. M. Reaction: Earth-Abundant Metal Catalysts for Energy Conversions. *Chem* **2017**, *2*, 444–447. (b) Holland, P. L. Reaction: Opportunities for Sustainable Catalysts. *Chem*, **2017**, *2*, 443–444.
50. Olah, G. A.; Olah, J. A.; Overchuk, N. A. Aromatic Substitution. XXIII. Nitration of Pyridine with Nitonium and Nitrosonium Tetrafluoroborate. Isolation of *N*-Nitro- and *N*-Nitrosopyridinium Tetratfluoroborate. *J. Org. Chem.*, **1965**, *30*, 3373.
51. Kim, E. K.; Bockman, T. M.; Kochi, J. K. Electron-Transfer Mechanism for Aromatic Nitration via the Photoactivation of EDA Complexes. Direct Relationship to Eloectrophilic Aromatic Substitution. *J. Am. Chem. Soc.* **1993**, *115*, 3091–3104.

52. Boursalian, G. B.; Ham, W. S.; Mazzotti, A. R.; Ritter, T. Charge-transfer-directed radical substitution enables para-selective C–H functionalization. *Nature Chem.* **2016**, *8*, 810–815.
53. (a) Menschutkin. N. Beiträgen zur Kenntnis der Affinitätskoeffizienten der Alkylhaloide und der organischen Amine *Z. Phys. Chem.* **1890**, *5*, 589. (b) Menschutkin, N. Über die Affinitätskoeffizienten der Alkylhaloide und der Amine *Z. Phys. Chem.* **1890**, *6*, 41.

A P P E N D I X

General Considerations

Reagents and solvents were purchased at the highest commercial quality and used without purification. Yields refer to chromatographically and spectroscopically (^{1}H NMR, ^{13}C NMR, ^{19}F NMR) homogenous material, unless otherwise noted. The yields in the Supporting Information describe the result of a single experiment. Reactions were monitored by GCMS (Agilent Technologies 5975 Series MSD GCMS) and thin-layer chromatography using 0.25 mm E. Merck silica gel plates (60F-254) using UV light. NMR spectra were recorded on a Varian-INOVA 400 MHz or 500 MHz spectrometer and calibrated using residual undeuterated solvent as an internal reference ($CDCl_3$ – ^{1}H NMR: 7.26 ppm, ^{13}C NMR: 77.16 ppm; CD_3CN – ^{1}H NMR: 1.94 ppm, ^{13}C NMR: 1.32 ppm), whereas for ^{15}N spectra, a sealed capillary filled with nitromethane (0 ppm) was used as an internal standard, and for ^{19}F spectra, a sealed capillary filled with hexafluorobenzene (-164.90 ppm) was used. The following abbreviations were used to explain multiplicities (s – singlet, d – doublet, t – triplet, q – quartet, m – multiplet).

A P P E N D I X - A

Experimental Set Up: Benzylic C–H Radical Fluorination using Unprotected Amino Acids as Radical Precursors

General Reaction Procedures

General Procedure:

The threads of a 3 mL borosilicate scintillation vial were thoroughly taped with Teflon tape. To this vial containing a stir bar was added Selectflour (142 mg, 0.4 mmol, 2 equiv), glycine (30 mg, 0.4 mmol, 2 equiv), and arene (0.2 mmol, 1 equiv). Acetonitrile (1 mL) and H_2O (0.9 mL) were then added and stirred for about 1 min at room temperature. A solution of $AgNO_3$ (0.1 mL of a 0.4M solution in H_2O, 0.04 mmol) was added in one portion. The reaction vial was flushed with argon. The reaction was capped with a teflon screw cap and rubber septa (24/40). The reaction was heated to 35 °C until reaction was completed judged by GCMS (up to 24 hours).

Upon completion, the reaction was diluted with 1 mL ethyl acetate and transferred to a test tube containing saturated $NaHCO_3$ (3 mL). The aqueous phase was extracted with ethyl acetate (3 x 3 mL) and the combined organic layers were dried over $MgSO_4$, filtered and carefully concentrated *in vacuo* due to product volatility. The crude material was purified by silica gel chromatography (ethyl acetate:hexanes or ether:pentanes) to yield the desired fluorinated products.

NMR Yield Procedure:

For low-molecular weight and highly volatile products**,** the reaction was diluted with $CDCl_3$ (1 mL) and using a micro-syringe, trifluorotoluene (25 μL) was added as an internal standard. The reaction mixture was transferred into a test tube. The reaction vial was then rinsed with 1 mL of H_2O, transferred to same test tube and the layers were separated. The organic layer was dried over $MgSO_4$, filtered, and transferred to an NMR tube. NMR yields were then determined from ^{19}F NMR spectroscopic analysis. Spectroscopic parameters: 16-32 scans, 50 s relaxation delay between each scan, spectroscopic window set from -400 ppm to 200 ppm.

Cyclic Voltammetry Experiments

General Procedure:

In a borosilicate scintillation cell, 5 mL of tetrabutylammonium tetrafluoroborate (TBAF) supporting electrolyte solution was added (0.1 M in CH_3CN). The glassy carbon working electrode, platinum counter electrode, and platinum pseudo reference electrode were positioned in the cell with ~0.5 cm of the electrode tips submerged in the electrolyte solution. The additive (0.5 mmol) was added to the cell and stirred until the solution was homogenous. A CV spectrum was collected. $AgNO_3$ was then added (84.9 mg, 0.5 mmol) and the solution was stirred until the solution was homogenous. A CV spectrum was collected. All spectra were collected with Gamry Instruments Framework, version 6.25, build 3318. All spectral analyses were performed with Gamry Echem Analyst, version 6.25.

Cyclic Voltammetry Parameters:

$initial_E$ (V): 0.5 vs. E_{ref}
scan limit 1 (V): 3 vs. E_{ref}
scan limit 2 (V): 0.4 vs. E_{ref}
$final_E$ (V): 0.4 vs. E_{ref}
scan rate (mV/s): 200
electrode area (cm^2): 1
equil. Time (s): 0
I/E range mode: auto I/E range
max. current (mA): 5
cycles (#): 3
open circuit (V): 0
sampling mode: Noise reject

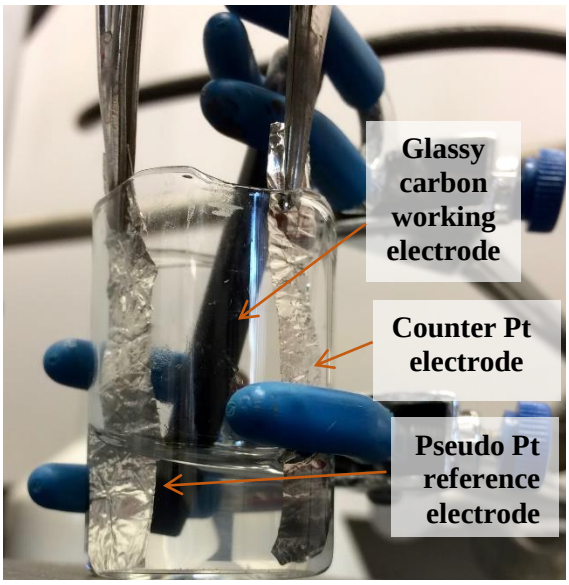

ReactIR Experiments

Experimental Procedure

In a 3 mL borosilicate scintillation vial containing a stir bar, Selectfluor (354 mg, 1.0 mmol, 5 equiv), and *p*-tolyl acetate (29 uL, 0.2 mmol, 1 equiv) were combined with 2 mL CH_3CN:H_2O (0.1 M, 1:1). The resulting mixture was stirred for approximately 1 minute at room temperature. A bored-through 14/20 rubber septum was fitted firmly over the opening of the vial. The ReactIR probe was inserted through the opening of the septum. The reaction was heated to 35 °C and stirred at 600 rpm. Data acquisition was initiated. After approximately 10 minutes, data acquisition was paused and solid $AgNO_3$ (169 mg, 1.0 mmol, 5 equiv) was added in one portion. Data were collected for an additional 10 minutes, during which time no appreciable reaction was observed. Data acquisition was paused, and solid glycine (75 mg, 1.0 mmol, 5 equiv) was added as a single portion. Data were collected until reaction was complete, as evidenced by consumption of Selectfluor. Data were acquired using a Mettler Toledo ReactIR 15 instrument and analyzed with the Mettler Toledo iC IR 7.0 software package. Graphical analysis was performed using Excel.

ReactIR Parameters:
Detector: MCT
Apodization: HappGenzel
Probe: DiComp (Diamond)
Interface: AgX 6 mm x 1.5 m fiber (Silver Halide)
Sampling: 3000 to 650 cm^{-1}
Resolution: 8
Scan Option: AutoSelect
Gain: 1x
Time Interval: Data collected every 2 minutes for first 5 hours; data collected every 5 minutes for remainder of experiment
Spectrum Math: Second Derivative
Baseline: Two-point baseline

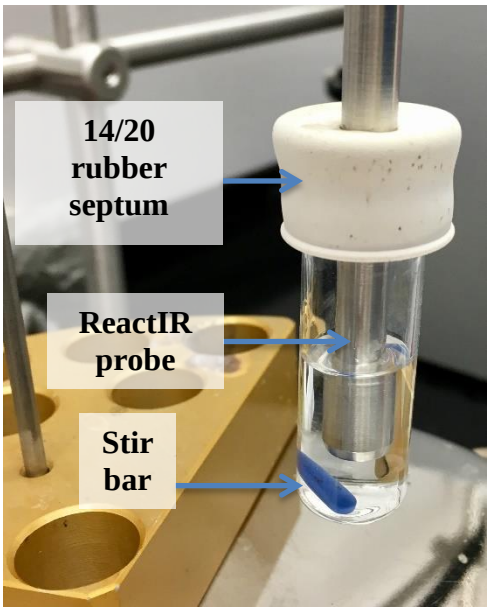

^{13}C NMR spectral evidence for the formation of methylamine

Exp*erimental Procedure*

In a 3 mL borosilicate scintillation vial with a stir bar was added Selectfluor® (177 mg, 0.5 mmol), glycine (38 mg, 0.5 mmol), and toluene-d_8 (10.6 uL, 0.1 mmol). CH_3CN (500 µL), H_2O (450 µL) were added and stirred for about 1 min at room temperature. The content of the reaction vial was then transferred into a screw-top NMR tube and was flushed with argon. The NMR tube was sealed with a Teflon cap with a septum. A solution of $AgNO_3$ (50 µL of a 0.4M solution in H_2O, 0.02 mmol) was injected into the sealed NMR tube in one portion. Spectroscopic data (^{13}C-NMR) was collected after 12 hours. Toluene-d_8 was used for the solvent lock.

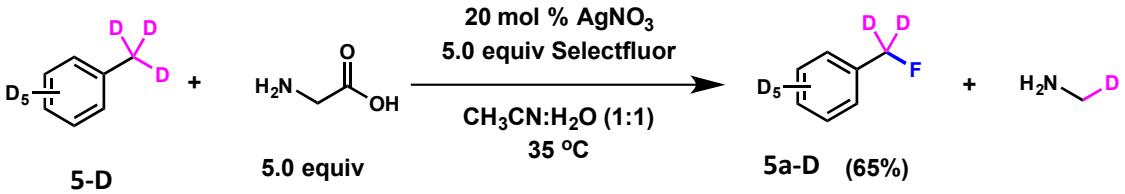

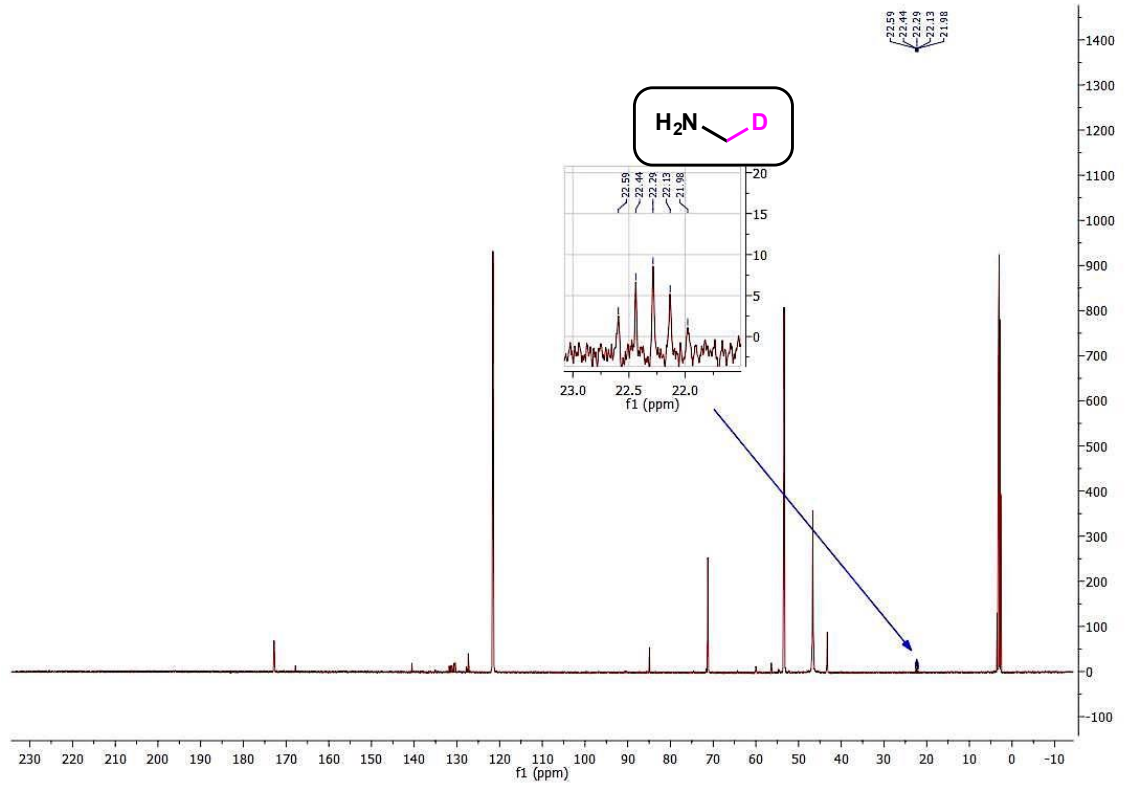

^{19}F NMR spectral evidence for the formation of fluoride anion

Experimental Procedures

In a 3 mL borosilicate scintillation vial with a stir bar was added Selectflour® (177 mg, 0.5 mmol), glycine (38 mg, 0.5 mmol), and toluene-d_8 (10.6 uL, 0.1 mmol). CH_3CN (500 μL), H_2O (450 μL) were added and stirred for about 1 min at room temperature. The content of the reaction vial was then transferred into a screw-top NMR tube and was flushed with argon. The NMR tube was sealed with a Teflon cap with a septum. ^{19}F-NMR spectroscopic data was collected at "time zero" prior to addition of the catalyst. A solution of $AgNO_3$ (50 μL of a 0.4M solution in H_2O, 0.02 mmol) was injected into the sealed NMR tube in one portion. Spectroscopic data were collected approximately every 15 minutes, over a course of 7 hours.

Experimental Procedures and Characterization Data

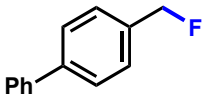

5, 3a

4-(fluoromethyl)-1,1'-biphenyl (3a): The general procedure was employed using 4-methyl-1,1'-biphenyl (33.7 mg, 0.2 mmol), Selectfluor® (141.7 mg, 0.4 mmol), and glycine (30 mg, 0.4 mmol). The reaction afforded **3a** (28.2 mg, 76% yield) as a white solid. The data matches those previously reported.[A1]

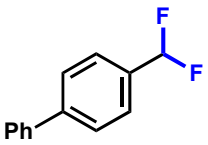

6, 3b

4-(difluoromethyl)-1,1'-biphenyl (3b): The general procedure was modified using 4-methyl-1,1'-biphenyl (33.7 mg, 0.2 mmol), Selectfluor® (354 mg, 1.0 mmol), and glycine (75 mg, 1.0 mmol). The reaction afforded **3b** (26.1 mg, 64% yield) as a white solid. The data matches those previously reported.[A1]

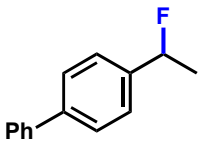

7a, 4a

4-(1-fluoroethyl)-1,1'-biphenyl (4a): The general procedure was employed using 4-ethyl-1,1'-biphenyl (36.5 mg, 0.2 mmol), Selectfluor® (141.7 mg, 0.4 mmol), and glycine (30

mg, 0.4 mmol). The reaction afforded **4a** (12.3 mg, 31% yield) as a white solid. The data matches those previously reported.[A1]

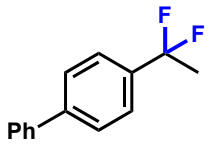

8 4b

4-(1,1-difluoroethyl)-1,1'-biphenyl (4b): The general procedure was modified using 4-ethyl-1,1'-biphenyl (36.5 mg, 0.2 mmol), Selectfluor® (354 mg, 1.0 mmol), and glycine (75 mg, 1.0 mmol). The reaction afforded **4b** (16.7 mg, 38% yield) as a white solid. The data matches those previously reported.[A1]

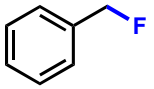

2 5a

Benzyl fluoride (5a): The general procedure was employed using toluene (21.3 μL, 0.2 mmol), Selectfluor® (354 mg, 1.0 mmol), and glycine (75 mg, 1.0 mmol). The reaction afforded **5a** (89% NMR yield). The data matches those previously reported.[A2]

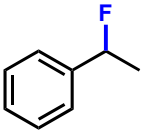

3 6a

(1-Fluoroethyl)-benzene (6a): The general procedure for volatile products was employed using ethyl benzene (24.5 μL, 0.2 mmol), Selectfluor® (354 mg, 1.0 mmol), and glycine (75 mg, 1.0 mmol). The reaction afforded **6a** (39% NMR yield). The data matches those previously reported.[A1]

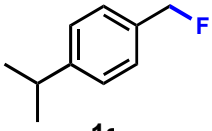

1 8a

1-(fluoromethyl)-4-isopropylbenzene (8a): The general procedure was employed using *p*-cymene (31.32 μL, 0.2 mmol), Selectfluor® (141.7 mg, 0.4 mmol), and glycine (30 mg, 0.4 mmol). The reaction afforded afforded **8a** (19.6 mg, 65% yield) as a colorless oil. The data matches those previously reported.[A3]

^{1}H NMR (400 MHz, $CDCl_3$): 7.33 (d, *J* = 1.8 Hz, 1H), 7.31(d, *J* = 1.9 Hz, 1H), 7.27–7.25 (m, 2H), 5.35 (d, *J* = 48.4 Hz, 2H), 2.98–2.88 (m, 1H), 1.27 (s, 3H), 1.26 (s, 3H)
^{13}C NMR (100 MHz, $CDCl_3$): 149.9, 128.1 (d, *J* = 5.5 Hz), 126.8 (d, *J* = 1.7 Hz), 84.8 (d, *J* = 165.0 Hz), 34.1, 24.1
^{19}F NMR (376.5 MHz, $CDCl_3$): -203.9 (t, *J* = 48.3 Hz)

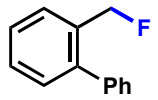

9a

2-(fluoromethyl)-1,1'-biphenyl (9a): The general procedure was employed using 2-methyl-1,1'-biphenyl (33.7 mg, 0.2 mmol), Selectfluor® (141.7 mg, 0.4 mmol), and glycine (30 mg, 0.4 mmol). The reaction afforded **9a** (22.3 mg, 60% yield) as a colorless oil. The data matches those previously reported.[A4]

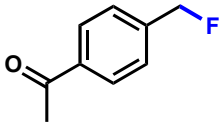

10a

1-(4-fluoromethyl)phenyl)ethan-1-one (10a): The general procedure was employed using acetophenone (26.7 μL, 0.2 mmol), Selectfluor (141.7 mg, 0.4 mmol), and glycine (30 mg, 0.4 mmol). The reaction afforded **10a** (9.1 mg, 30% NMR yield) as a colorless oil. The data matches those previously reported.[A5]

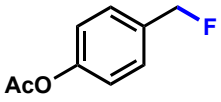

11a

4-(fluoromethyl)phenyl acetate (11a): The general procedure was employed using *p*-toluic acid (28.7 μL, 0.2 mmol), Selectfluor® (354 mg, 1.0 mmol), and glycine (75 mg, 1.0 mmol). The reaction afforded **11a** (26.1 mg, 70% yield) as a colorless oil. The data matches those previously reported.[A5]

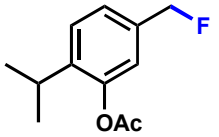

12a

5-(fluoromethyl)-2-isopropylphenyl acetate (12a): The general procedure was employed using 2-isopropyl-5-methylphenyl acetate (38.4 mg, 0.2 mmol), Selectfluor® (354 mg, 1.0 mmol), and glycine (75 mg, 1.0 mmol). The reaction afforded **12a** (31.4 mg, 75% yield) as a colorless oil.

^{1}H NMR (400 MHz, $CDCl_3$): 7.35 (d, *J* = 8.0 Hz, 1Hz), 7.23 (d, *J* = 7.9 Hz, 1H), 7.04 (s, 1H), 5.35 (d, *J* = 47.6 Hz, 2H), 3.09–2.99 (m, 1H), 2.34 (s, 3H), 1.22 (d, *J* = 6.8 Hz, 6H)
^{13}C NMR (100 MHz, $CDCl_3$): 169.7, 148.2, 140.9 (d, *J* = 2.9 Hz), 135.1 (d, *J* = 17.6 Hz), 127.2, 125.4 (d, *J* = 5.8 Hz), 121.5 (d, *J* = 6.1Hz), 83.9 (d, *J* = 166.9 Hz), 27.5, 23.0, 21.0
^{19}F NMR (376.5 MHz, $CDCl_3$): -207.6 (t, *J* = 50.8 Hz)

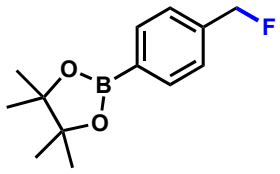

13a

2-(4-fluoromethyl)phenyl)-4,4,5,5-tetramethyl-1,3,2-dioxaborolane (13a): The general procedure was employed using 4-tolylboronic acid pinacol ester (44 mg, 0.2 mmol), Selectfluor® (141.7 mg, 0.4 mmol), and glycine (30 mg, 0.4 mmol). The reaction afforded **13a** (14.6 mg, 31% yield) as a light yellow oil.

^{1}H NMR (400 MHz, $CDCl_3$): 7.84 (d, *J* = 7.6 Hz, 2H), 7.38 (d, *J* = 7.0 Hz, 2H), 5.41 (d, *J* = 47.5 Hz, 2H), 1.35 (s, 12H)
^{13}C NMR (100 MHz, $CDCl_3$): 139.3 (d, *J* = 16.8 Hz), 135.1, 126.5 (d, *J* = 6.2 Hz), 84.5, 84.0, 83.3, 25.0
^{19}F NMR (376.5 MHz, $CDCl_3$): -209.9 (t, *J* = 47.5Hz)

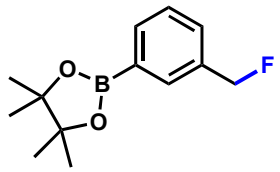

14a

2-[3-(fluoromethyl)phenyl]-4,4,5,5-tetramethyl-1,3,2-dioxaborolane (14a): The general procedure was modified using 4-tolylboronic acid pinacol ester (44 mg, 0.2 mmol), Selectfluor® (354 mg, 1.0 mmol), and glycine (75 mg, 1.0 mmol). The reaction afforded **14a** (21.0 mg, 45% yield) as a pale yellow oil.

^{1}H NMR (500 MHz, $CDCl_3$): 7.80–7.82 (m, 2H), 7.48–7.51 (m, 1H), 7.41 (t, *J* = 7.4 Hz, 1H), 5.38 (d, *J* = 47.9 Hz, 2H), 1.35 (s, 12H)
^{13}C NMR (100.56 MHz, $CDCl_3$): 135.3 (d, *J* = 3.1 Hz), 134.1 (d, *J* = 5.6 Hz), 130.6 (d, *J* = 5.6), 128.2 (d, *J* = 1.1 Hz), 85.6, 84.1 (d, *J* = 165.9 Hz), 29.9, 25.0, 24.7
^{19}F NMR (376.20 MHz, $CDCl_3$): -206.6 (t, *J* = 47.8 Hz)

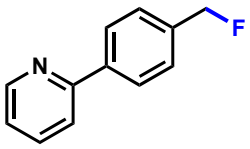

16a 15a

2-(4-fluoromethyl)phenyl)pyridine (15a): The general procedure was employed using 2-(p-tolyl)pyridine (33.8 mg, 0.2 mmol), Selectfluor® (354 mg, 1.0 mmol), and glycine (75 mg, 1.0 mmol). The reaction afforded **15a** (21.3 mg, 57% yield) as a colorless oil.

^{1}H NMR (400 MHz, $CDCl_3$): 8.71 (d, *J* = 4.7 Hz, 1H), 8.03 (d, *J* = 7.8 Hz, 2H), 7.76–X.XX (m, 2H), 7.49 (d, *J* = 6.9 Hz, 2H), 7.24–7.27 (m, 1H), 5.45 (d, *J* = 47.7 Hz, 2H)
^{13}C NMR (100 MHz, $CDCl_3$): 156.9, 149.8, 137.0, 137.0 (d, *J* = 6.0 Hz), 127.9 (d, *J* = 6.0 Hz), 127.3 (d, *J* = 1.0 Hz), 122.5, 120.8, 84.4 (d, *J* = 166.5), 29.9
^{19}F NMR (376.5 MHz, $CDCl_3$): -208.2 (t, *J* = 47.7Hz)

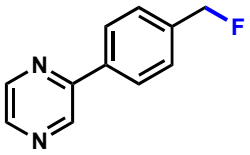

17 16a

2-(4-fluoromethyl)phenyl)pyrazine (16a): The general procedure was employed using 2-(p-tolyl)pyrazine (34 mg, 0.2 mmol), Selectfluor® (354 mg, 1.0 mmol), and glycine (75 mg, 1.0 mmol). The reaction afforded **16a** (23.2 mg, 62% yield) as an off-white solid.

^{1}H NMR (400 MHz, $CDCl_3$): 9.05 (s, 1H), 8.65 (s, 1H), 8.53 (s, 1H), 8.06 (d, *J* = 7.6 Hz, 2H), 7.52 (d, *J* = 9.1 Hz, 2H), 5.46 (d, *J* = 47.5 Hz, 2H)
^{13}C NMR (100 MHz, $CDCl_3$): 144.4, 143.2, 142.3, 138.1 (d, *J* = 17.1 Hz), 136.7 (d, *J* = 2.8 Hz), 130.2 (d, *J* = 50.0 Hz), 128.0 (d, *J* = 6.8 Hz), 127.2 (d, *J* = 56.7 Hz), 127.3 (d, *J* = 0.7 Hz), 84.2 (d, *J* = 167.3 Hz)
^{19}F NMR (376.5 MHz, $CDCl_3$): -209.7 (t, *J* = 47.5Hz)

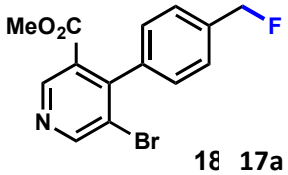

18 17a

Methyl 5-bromo-4-(4-(fluoromethyl)phenyl)nicotinate (17a): The general procedure was employed using methyl 5-bromo-4-(*p*-tolyl)nicotinate (37 mg, 0.12 mmol), Selectfluor® (214 mg, 0.61 mmol), and glycine (46 mg, 0.61 mmol). The reaction afforded **17a** (7.8 mg, 20% yield) as a colorless oil.

^{1}H NMR (400 MHz, $CDCl_3$): 8.97 (d, *J* = 19.8 Hz, 2H), 7.47 (d, *J* = 7.1, 2H), 7.23 (d, *J* = 7.8 Hz, 2H), 5.47 (d, *J* = 47.5 Hz, 2H), 3.66 (s, 3H)
^{13}C NMR (100 MHz, $CDCl_3$): 166.5, 154.4, 150.2, 149.1, 137.6 (d, *J* = 3.0 Hz), 136.9 (d, *J* = 17.3 Hz), 128.4, 127.2, 127.1, 84.3 (d, *J* = 167.6 Hz), 52.7, 29.9
^{19}F NMR (376.5 MHz, $CDCl_3$): -209.7 (t, *J* = 47.5Hz)

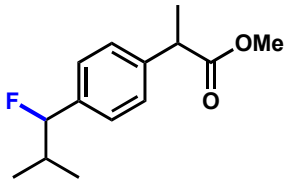

15 18a

methyl 2-[4-(1-fluoro-2-methylpropyl)phenyl]propanoate (18a): The general procedure was employed using (±)-ibuprofen methyl ester (44.1 mg, 0.2 mmol), Selectfluor® (354 mg, 1.0 mmol), and glycine (75 mg, 1.0 mmol). The reaction afforded **18a** (12.7 mg, 46% yield) as a white solid. The data matches those previously reported.[A6]

A P P E N D I X - B

Experimental Set Up: Benzylic C–H Radical Fluorination Facilitated by Halogen Bonding

General Reaction Procedures

General Procedure

The threads of a 3 mL borosilicate scintillation vial were thoroughly taped with Teflon tape. To this vial containing a stir bar was added Selectfluor (142 mg, 0.4 mmol, 2 equiv), and arene (0.2 mmol, 1 equiv). Acetonitrile (1 mL) and H_2O (0.9 mL) were then added and stirred for approximately 1 min at room temperature. A solution of $AgNO_3$ (0.1 mL of a 0.4 M solution in H_2O, 0.04 mmol) was added in one portion and stirred at 35 °C for approximately 10 minutes before the pyridine additive (0.2 mmol, 1 equiv) was added. The reaction was capped with a teflon screw cap and rubber septum (24/40). The reaction was heated to 35 °C until reaction was completed as judged by GCMS (up to 24 hours).

Upon completion, the reaction was diluted with ethyl acetate (1 mL) and transferred to a test tube containing saturated $NaHCO_3$ (3 mL). The aqueous phase was extracted with ethyl acetate (3 x 3 mL) and the combined organic layers were dried over $MgSO_4$, filtered and carefully concentrated *en vacuo* due to product volatility. The crude material was purified by silica gel chromatography (ethyl acetate:hexanes) to yield the desired fluorinated products.

NMR Yield Procedure

The reaction was diluted with ethyl acetate (1 mL) and transferred to a test tube containing saturated $NaHCO_3$ (3 mL) and 1,3,5-trimethoxybenzene (16.8 mg, 0.1 mmol) as an internal standard. The aqueous phase was extracted with ethyl acetate (3 x 3 mL) and the combined organic layers were dried over $MgSO_4$, filtered and carefully concentrated *en vacuo*. NMR yields were then determined from ^1H NMR spectroscopic analysis.

TEMPO Radical Trapping

General Procedure

In determining whether or not our reaction occurred via a radical pathway, (2,2,6,6-Tetramethylpiperidin-1-yl)oxyl (TEMPO, 32 mg, 0.2 mmol, 1 equiv) was added to reactions and observed how it affected the product yields. A reaction was run under standard conditions without TEMPO, and was quenched after 24 hours to give product yield of an unaltered reaction, (entry 1). NMR yield was obtained. Another reaction was run under standard conditions and globally quenched after five hours to determine the progress of a productive reaction up to that time point, (entry 2). NMR yield was then obtained. In a separate reaction run under standard conditions, TEMPO was added after five hours of productive reaction time and was stirred and heated for a total reaction time of 22 hours, (entry 3). An aliquot (~70 uL) of entry 3 was taken for HRMS analysis and then globally quenched to obtain NMR yield.

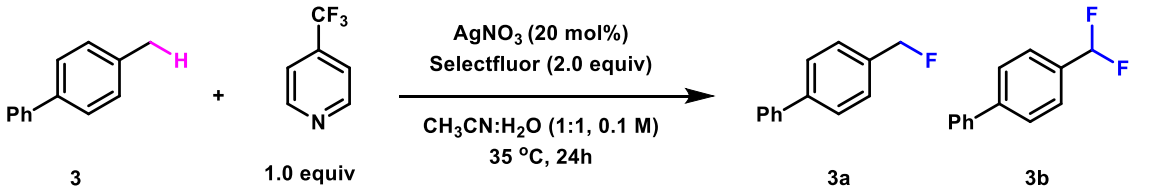

3 1.0 equiv 3a 3b

entry	deviation from standard conditions	time (h)	NMR yield (%)	
1	none	24	12	85
2	globally quenched after 5 hours	5	37	00
3	TEMPO (1.0 equiv) added after 5 hours	22	34	00

High Resolution Mass Spectroscopy (HRMS)

General Procedure

An aliquot (~70 uL) of the reaction mixture was diluted with HPLC grade CH_3CN/H_2O (1:1) to approximately 2 mL. The resulting solution was then filtered and injected onto the HRMS. Data collection was done using factory default parameters for positive ion ESI-MS.

Cyclic Voltammetry Experiments

General Procedure

In a borosilicate scintillation cell, tetrabutylammonium tetrafluoroborate supporting electrolyte solution was added (5ml, 0.1 M in CH_3CN). The glassy carbon working electrode, platinum counter electrode, and platinum pseudo reference electrode were positioned in the cell with ~0.5 cm of the electrode tips submerged in the electrolyte solution. All chemical components of CV experiments used were added in at 0.1 M (0.5 mmol), unless otherwise noted. All spectra were collected with Gamry Instruments Framework, version 6.25, build 3318. All spectral analyses were performed with Gamry Echem Analyst, version 6.25. Experiment set-up is shown in Figure S1.

Cyclic Voltammetry Parameters

initial$_E$ (V): 0 vs. E_{ref}
scan limit 1 (V): -3 vs. E_{ref}
scan limit 2 (V): 3 vs. E_{ref}
final$_E$ (V): 0 vs. E_{ref}
scan rate (mV/s): 200
electrode area (cm^2): 1
equil. Time (s): 0
I/E range mode: auto I/E rang
max. current (mA): 5
cycles (#): 3
open circuit (V): 0
sampling mode: Noise reject

CV experiment set up.

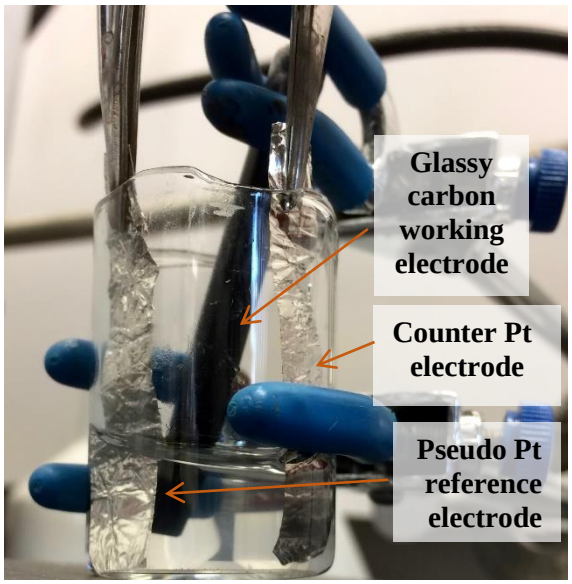

ReactIR Experiments

Experimental Procedure

In a 3 mL borosilicate scintillation vial containing a stir bar, Selectfluor (142 mg, 0.4 mmol, 2 equiv), *p*-tolyl acetate (29 uL, 0.2 mmol, 1 equiv), and 2 mL CH_3CN:H_2O (0.1 M, 1:1). The resulting mixture was stirred for approximately 1 minute at room temperature. A bored-through 14/20 rubber septum was fitted firmly over the opening of the vial. The ReactIR probe was inserted through the opening of the septum. A solution of $AgNO_3$ (0.1 mL of a 0.4 M solution in H_2O, 0.04 mmol) was added in one portion. The reaction mixture was stirred at 35 °C for approximately 10 minutes before the pyridine additive (0.2 mmol, 1 equiv) was added. Data acquisition was initiated. Data was collected for approximately 24 hours or until reaction was complete, as evidenced by consumption of Selectfluor. Data was acquired using a Mettler Toledo ReactIR 15 instrument and analyzed with the Mettler Toledo iC IR 7.0 software package. Graphical analysis was performed using Excel.

ReactIR Parameters
Detector: MCT
Apodization: HappGenzel
Probe: DiComp (Diamond)
Interface: AgX 6 mm x 1.5 m fiber (Silver Halide)
Sampling: 3000 to 650 cm^{-1}
Resolution: 8
Scan Option: AutoSelect
Gain: 1x
Time Interval: Data collected every 2 minutes for the entire duration of experiment
Spectrum Math: Second Derivative
Baseline: One-point baseline

ReactIR set up.

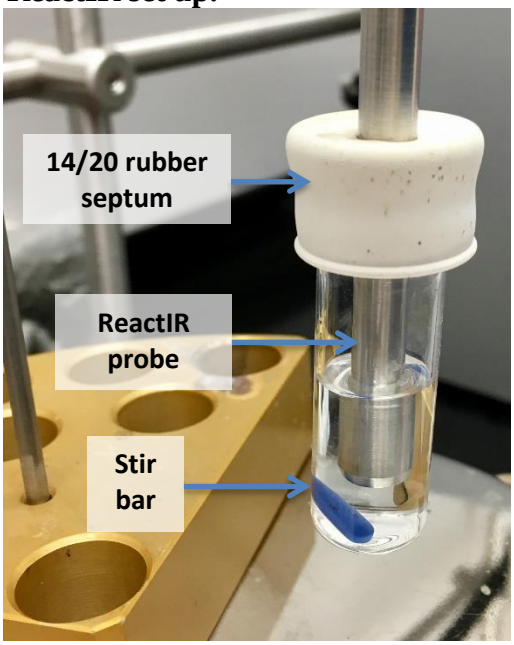

^{19}F NMR Experiment

General Procedure

In each ^{19}F NMR experiment, 0.4 mmol of Selectfluor and 0.4 mmol of 4-R-pyridine (R= CF_3, CO_2Et, H, OCH_3) was used. To an NMR tube, Selectfluor and 1.00 mL of CD_3CN was added, then inverted several times until Selectfluor was dissolved, then a sealed capillary of hexafluorobenzene as an internal standard was placed in the NMR tube. An NMR of the Selectfluor with the standard was taken, immediately following 0.4 mmol of the 4-R-pyridine additive was added. The NMR tube was then gently inverted several times and an ^{19}F NMR was immediately taken.

^{1}H/^{15}N HMBC Experiment

General Procedure

In each HMBC experiment, 0.1 mmol of 4-R-pyridine (R = OCH_3, H, CO_2Et, CF_3) and 0.1 mmol of Selectfluor (when applicable) was used. To a test tube, the compound(s) under investigation was added and diluted with 700 uL of CD_3CN, vigorously stirred, and transferred to an NMR tube containing a sealed capillary of nitromethane. Experimental parameters were adjusted from the default settings for ^{1}H/^{13}C HMBC found in VnmrJ (version 4.2 Revision A). The multiple bond coupling constant (*multiple bond jnxh*) was left at the default value of 8 Hz for all experiments except for the mixture of pyridine and Selectfluor. When *multiple bond jnxh* = 8 Hz, no correlation signals were detected for ^{1}H/^{15}N of pyridine upon interaction with Selectfluor. It was critical to set *multiple bond jnxh* = 12 Hz. For the HMBC studies that showed ^{1}H/^{15}N correlation when *multiple bond*

jnxh = 8 Hz, the coupling constants were calculated to be at least 10 Hz, which is on the higher end of the instrument's limitations when the protocol is looking for bonds with coupling constants around 8 Hz. HMBC spectral data processing was done using MestReNova. It should be noted that the *default* processing method varies between the software versions for Mac and Windows PC.

HMBC Parameters

f1 Nucelus: N15
N15 spec width: -400 to 400 ppm
t1 increments: 200
2-step J1xh x filter: No
Scans: 4 (up to 32)
Multiple bond jnxh: 8 Hz (12 Hz for pyridine + Selectfluor mixture)

HMBC Spectral Data Processing Method Parameters

Mac *(MestReNova version 10.0.2-15465)*

f2 - Time Domain
- FID Shift: not selected
- Truncate: not selected
- Apodization: not selected
- Zero Filling and LP
  - Spectrum Size: 2048 (2K)
    - Backward LP: not selected
    - Forward LP: not selected
  - LP Options
    - Method: Zhu-Bax
    - Basis Points: 1191
    - Coefficients: 10
- Fourier Transform
  - Protocol: none
  - Swap Halves: on
  - Mirror Image: on

f2 - Frequency Domain
- Phase Correction: selected
  - Method: Magnitude
- Baseline Correction: not selected
- Smoothing: not selected
- Reverse: not selected
- Cuts: not selected

f1 - Time Domain
- Truncate: not selected
- Apodization: selected
  - Gaussian: 39.33 GB(Hz)
- Zero Filling and LP
  - Spectrum Size: 2048 (2K)
    - Backward LP: not selected
    - Forward LP: not selected
  - LP Options
    - Method: Zhu-Bax
    - Basis Points: 189
    - Coefficients: 10

f1 - Frequency Domain
- Phase Correction: selected
  - Method: NoPC
- Baseline Correction: not selected
- Smoothing: not selected
- Reverse: not selected
- Cuts: not selected

Fourier Transform
Protocol: Echo-Antiecho
Swap Halves: on
Mirror Image: on

Windows PC *(MestReNova version 6.0.2-5475)*

f2 - Time Domain
FID Shift: not selected
Truncate: not selected
Apodization: selected
Sine Bell: 90.00 Deg
Zero Filling and LP
Spectrum Size: 2048 (2K)
Backward LP: not selected
Forward LP: not selected
LP Options
Method: Toeplitz
Basis Points: 1177
Coefficients: 24
Fourier Transform
Protocol: none
Swap Halves: on
Mirror Image: on

f2 - Frequency Domain
Phase Correction: selected
Method: Manual
PH0: 171.34 PH1: 0.00
Baseline Correction: not selected
Smoothing: not selected
Reverse: not selected
Cuts: not selected

f1 - Time Domain
Truncate: not selected
Apodization: selected
Sine Square: 90.00 Deg
First Point: 0.50
Zero Filling and LP
Spectrum Size: 2048 (2K)
Backward LP: not selected
Forward LP: not selected
LP Options
Method: Toeplitz
Basis Points: 187
Coefficients: 12
Fourier Transform
Protocol: Echo-Antiecho
Swap Halves: on
Mirror Image: on

f1 - Frequency Domain
Phase Correction: not selected
Baseline Correction: not selected
Smoothing: not selected
Reverse: not selected
Cuts: not selected

Experimental Procedures and Characterization Data

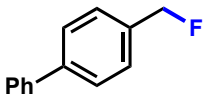

1i 3a

4-(fluoromethyl)-1,1'-biphenyl (3a): The general procedure was employed using 4-methyl-1,1'-biphenyl (33.7 mg, 0.2 mmol), Selectfluor (141.7 mg, 0.4 mmol), and 4-(trifluoromethyl)pyridine (23.2 μL, 0.2 mmol) in acetonitrile and water, (1:1, 2 mL each, 0.05 M). The reaction afforded quantitative amounts of **3a** (NMR yield). The data matches those previously reported.[A1]

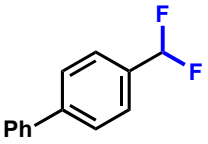

1l 3b

4-(difluoromethyl)-1,1'-biphenyl (3b): The general procedure was employed using 4-methyl-1,1'-biphenyl (33.7 mg, 0.2 mmol), Selectfluor (141.7 mg, 0.4 mmol), and 4-(trifluoromethyl)pyridine (23.2 μL, 0.2 mmol). The reaction afforded **3b** (85%, NMR yield). The data matches those previously reported.[A1]

Appendix References

[A1] Xia, J.; Zhu, C.; Chen, C. *J. Am. Chem. Soc.* **2013**, *135*, 17494–17500.
[A2] Mąkoza, M.; Bujok, R. *J. Fluorine Chem.* **2005**, *126*, 209–216.
[A3] Bloom, S.; Pitts, C. R.; Woltornist, R.; Griswold, A.; Holl, M. G.; Lectka, T. *Org. Lett.* **2013**, *15*, 1722–1724.
[A4] Ma, J.; Yi, W.; Lu, G.; Cai, C. *Org. Biomol. Chem.* **2015**, *13*, 2890–2894.
[A5] Champagne, P. A.; Benhassine, Y.; Dessroches, J.; Paquin, J. *Angew. Chem. Int. Ed.* **2014**, *53*, 13835–13839.
[A6] Bloom, S.; McCann, M.; Lectka, T. *Org. Lett.* **2014**, *16*, 6338–6341.